1975

Ultimate load tests of modified Parker type high truss bridge

Leonard William Timm
Iowa State University

Ultimate load tests

of a

modified Parker type high truss bridge

by

Leonard William Timm

A Thesis Submitted to the

Graduate Faculty in Partial Fulfillment of

The Requirements for the Degree of

MASTER OF SCIENCE

Department: Civil Engineering
Major: Structural Engineering

Approved:

_____
In Charge of Major Work

_____
For the Major Department

_____
For the Graduate College

Iowa State University
Ames, Iowa

1975

TABLE OF CONTENTS

LIST OF FIGURES

LIST OF TABLES

CHAPTER 1. INTRODUCTION

As a result of the construction of the Saylorville Dam and Reservoir on the Des Moines River, six highway bridges crossing the river were scheduled for removal. Five of these were old pin-connected, high-truss, single-lane bridges typical of many built in Iowa and throughout the country around the turn of the century. Since these five bridges were built about 1900, information on their design and construction is limited. Because of the increasing need to determine strength and behavior characteristics of all bridges, as indicated later, the removal of these bridges created an excellent opportunity for studying the behavior of bridges by testing actual prototype bridges rather than physical or mathematical models. The purpose of the ultimate load tests was to relate design and rating procedures presently used in bridge design to the field behavior of this type of truss bridge.

The determination of the feasibility of conducting these load tests was the purpose of a study[1] conducted several years ago by Iowa State University. The findings of the study included a recommendation to conduct a broad range of programs on several of the truss bridges included in the removal program. One of the replacement bridges was available early in the development of the entire project, because of the construction schedule. Therefore, the truss bridge to be replaced was available for testing during the summer of 1974. A research program to conduct a number of these recommended tests was, therefore, developed and undertaken by Iowa State University.

Objectives

Highway bridges in the United States are designed and rated using criteria in the specifications and manuals adopted by the American Association of State Highway Officials (AASHO)[2,3]. These criteria are based on rational structural analysis, actual experimental investigations, and engineering judgment. The criteria also attempt to take into account actual bridge behavior to assure safe and serviceable structures. However, as a result of the catastrophic collapses of several old bridges in the last 10 years, considerable interest has been generated in the actual load carrying capacity of bridges. This capacity of newer bridges can generally be obtained from plans and specifications that are supplemented by field examinations and actual field tests. However, for these old pin-connected, high-truss bridges, there are generally no technical data available and there is also a complete lack of field test data up to ultimate capacity. The general objective of this phase of the program was to provide data on the behavior of this bridge type in the overload range up to collapse.

As engineers undertake the analysis and rating of these bridges, many questions arise. These include the condition of pins, the corrosion in the joints, the strength of the eyes (including forgings) in the tension bars, and the behavior of the floorbeams and deck. Although the results reported herein are limited to a single bridge, they should provide an indication of possible answers to these questions.

The specific objectives of this load test program are to:

1. Relate appropriate AASHO criteria to the actual bridge behavior as determined from tests on the available truss bridge.

2. Determine the behavior and capacity of timber bridge decks used in this bridge under simulated truck loads.

3. Indicate the accuracy of load rating estimation techniques by providing the relation between the rating and actual capacity of the test bridge.

The results of the research will provide a better understanding of the actual strength of the hundreds of old high-truss bridges existing throughout Iowa and the rest of the nation.

Field Testing

In recent years a considerable number of field tests[4] on bridges have been conducted. Nearly all of these were conducted at or near design loads.

The approval of load factor design for steel bridges by the American Association of State Highway Officials (AASHO)[2,5] and, as indicated earlier, the requirement nationwide for rating of highway bridges[3] have generated considerable interest in tests of actual bridges to failure. However, only a very limited number of tests[1] have been conducted at substantial overloads or up to the ultimate capacity. Most of these were performed either on laboratory models or on specially designed bridges, as in the AASHO Road Tests[6,7]. The exceptions are a 1960 test of the Glatt Bridge in Switzerland[8] and four tests recently completed in Tennessee[9-12]. In addition, a special test

is planned for the summer of 1975 on a bridge in southeast Missouri[13].

The tests conducted as a part of the AASHO Road Tests[6,7] were made on eighteen 50-foot, simple-span, single-lane, beam-and-slab bridges. These bridges, which consisted of slabs supported by reinforced concrete, prestressed concrete or steel beams, were specifically designed for the test program. The bridge tested in Switzerland[8] was a prestressed concrete rigid frame bridge and is not typical of current design practice in this country. The University of Tennessee[9-12], in conjunction with a research study for the Tennessee Department of Highways and Federal Highway Administration, tested four deck girder highway bridges. Two of the bridges were continuous span with steel rolled beams, one of them composite in the positive moment regions and the other noncomposite. The third bridge was simple span composite with prestressed concrete beams. The fourth was composed of simple span reinforced concrete T-beams of monolithic construction. They were first tested dynamically using a standard AASHO design truck, an overloaded highway truck, and an Army tank transporter. In addition, the four bridges were tested to failure using simulated truck loads.

Although there is also information available on the overload and ultimate behavior of component parts of bridges, most of the information available on overload and ultimate behavior of the total bridge is limited to beam-and-slab type bridges. No information is available on the behavior of the old high-truss bridges typical of those found in Iowa and throughout other parts of the country. Therefore, this load

test program is intended to provide information on the ultimate load carrying capability through the testing of a typical old truss bridge.

General Test Program

The test program finally conducted consisted of ultimate load testing of one span of the bridge, ultimate load testing of two I-shaped floorbeams, and ultimate load testing of two panels of the timber deck. The truss span was tested in an "as is" condition with loads simulating actual truck loading. After initial failure, the truss was damaged and retested in this condition. The floorbeams were tested with loads to simulate an axle loading. One of the floorbeams had some initial crookedness, while the other was essentially straight. The loads were applied using hydraulic jacks and dead weights in both the truss test and the floorbeam tests. One of the timber deck tests was performed with loads, simulating a truck, centered on the deck panel and the other with loads placed 3 feet off center to simulate a truck on the edge of the deck panel.

The original test program[1,14] consisted, in part, of the load testing to failure of two spans of the bridge. One of the spans was to be tested in its "as is" condition with the other one tested after a major member had been damaged to simulate the effect of vehicular impact. However, the main thrust (member damage) of the proposed second truss test was accomplished while testing the first truss, thus the ultimate load testing of the second truss was modified. The

testing program was changed to include ultimate load tests of the floor-beams at panel points 4 and 5.

The field work began shortly after the bridge was closed to vehicular traffic in late May 1974. All field testing was performed during that summer and completed by mid-August.

CHAPTER 2. THE TEST BRIDGE

The highway bridge selected for testing is located on the Des Moines River northwest of Des Moines, Iowa, in an area which will be included in the Saylorville Reservoir. The prime function of the reservoir will be to store floodwaters of the Des Moines River. As a result there can be a considerable fluctuation in the reservoir level. The differential between the conservation and flood pools is about 57 feet. Therefore, the bridge selected for testing would have been inundated during a flood. The high-truss bridge selected was the Hubby Bridge (Figs. 1 and 2), located in southern Boone County about 5 miles northeast of Woodward and built in 1909. It was composed of four modified Parker type high-truss simple-spans, each 165 feet long.

Truss Description

The trusses of the bridge consisted of tension eye-bars of both square and rectangular cross sections, built-up laced channels for the end posts and upper chord compression members, and laced channels for the other compression members. Square tension eye-bars ranged in size from 3/4 in. to 1-1/8 in. and were used for truss hangers and diagonals. Rectangular tension eye-bars ranged in size from 5/8 in. X 3 in. to 13/16 in. X 4 in. and were used for the truss lower chords and diagonals. The eyes for these two types of eye-bars were formed by bending the end of the bar around to form a tear-shaped eye. The end of the bar was forged to form a permanent connection with the rest of the bar. The channels ranged in size from 4 in. to 9 in. deep and were used for

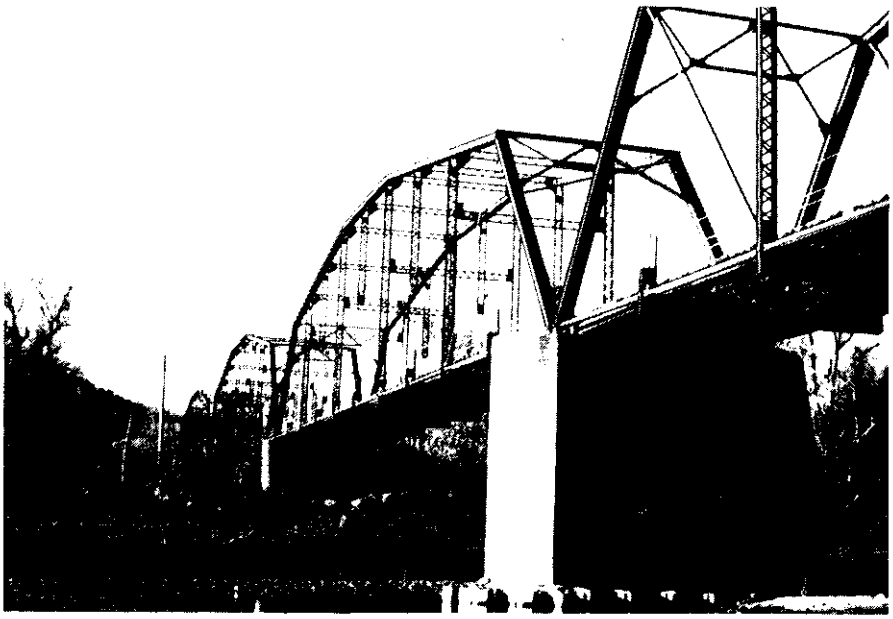

Fig. 1. Photographs of the Hubby Bridge.

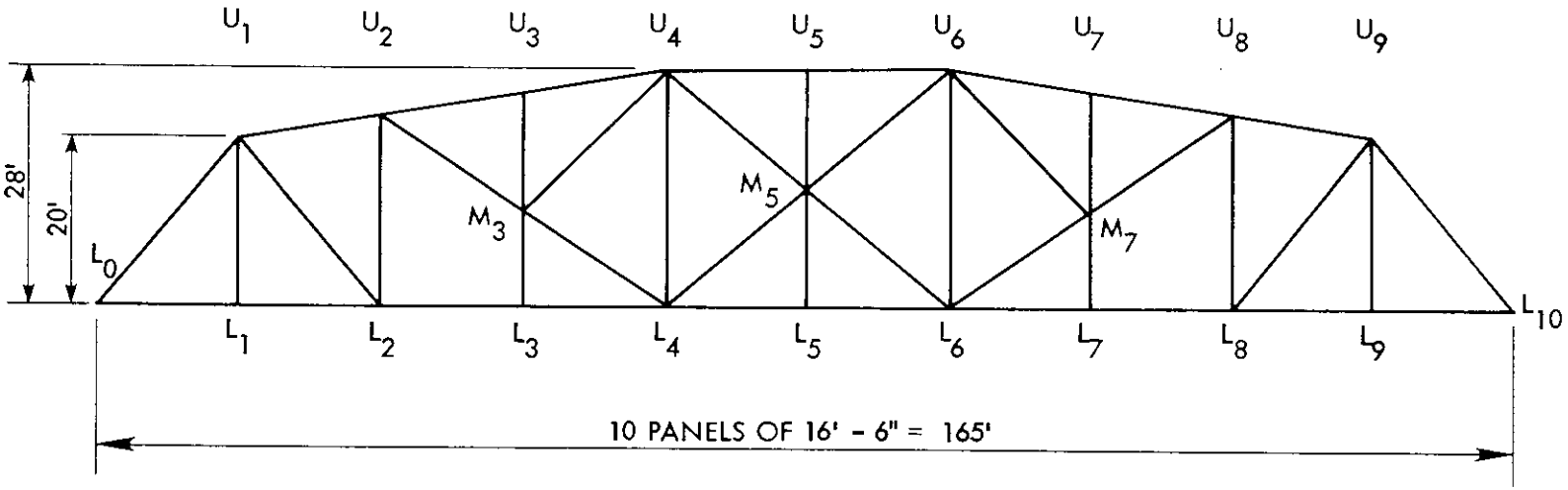

a. Member layout.

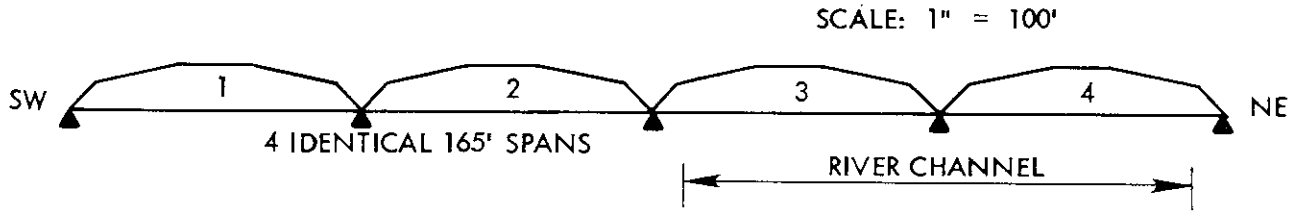

b. General layout.

Fig. 2. Details of the Hubby Bridge.

truss compression members. The deck was built of timber stringers, timber crossbeams, and timber floor planks. The stringers in the west two spans (which were load tested) were creosote treated, while the stringers in the east spans were not. The stringers stood on edge and were simply supported between rolled I-shaped floorbeams. Stringers were positioned, approximately one foot apart, with their longest dimension parallel to the length of the bridge. Crossbeams, spaced approximately 2 feet on center, were placed flat on top of the stringers and were positioned with their longest dimension perpendicular to the length of the bridge. The floor planks were placed flat on top of the crossbeams and were positioned with their longest dimension parallel to the length of the bridge. All of the timber members were 3 in. X 12 in. and approximately 17 feet long. A typical panel of deck consisted of 15 stringers, eight crossbeams, and 16 floor planks as shown in Fig. 3. The floorbeam was a standard I-section, 12 in. deep and weighing 30.6 pounds per foot of length, and was connected to the truss by means of clip angles and 1/2 in. bolts as shown in Figs. 4 and 5. These two figures also show the pins which were used to connect the eye-bars at each joint. The floorbeam tests were conducted in span 1, while the timber deck tests and the truss test were conducted in span 2.

Material Properties

Based on chemical analysis and physical property tests, the tension eye-bars were determined to be made of wrought iron and the other members of steel. The results of the chemical analysis are shown in Table 1.

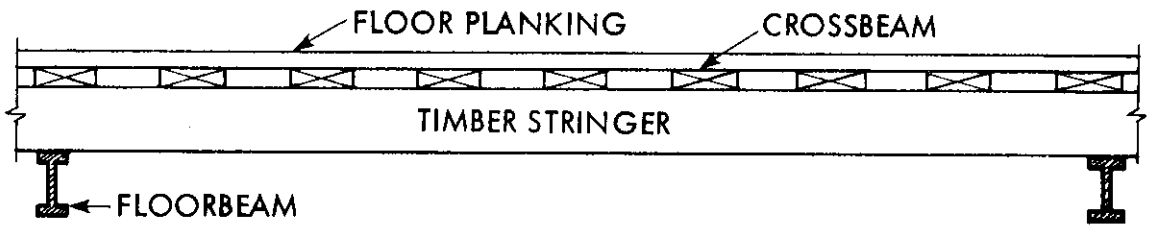

SCALE: 1" = 3'

a. Elevation view.

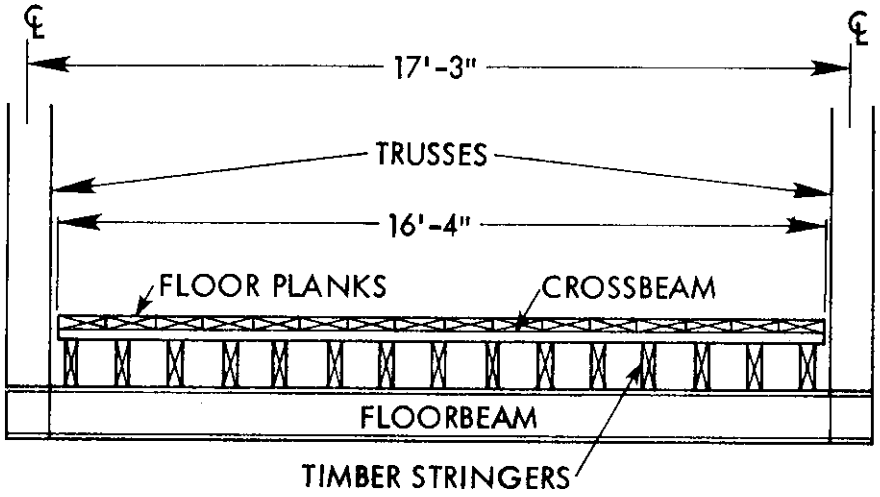

SCALE: 1" = 4'

b. End view.

Fig. 3. Timber deck layout.

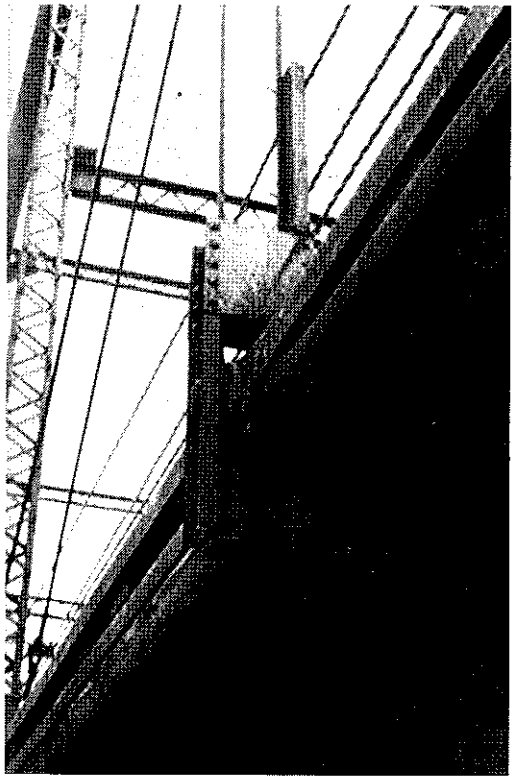

Fig. 4. Photograph of typical connection of floorbeam to truss at hanger member.

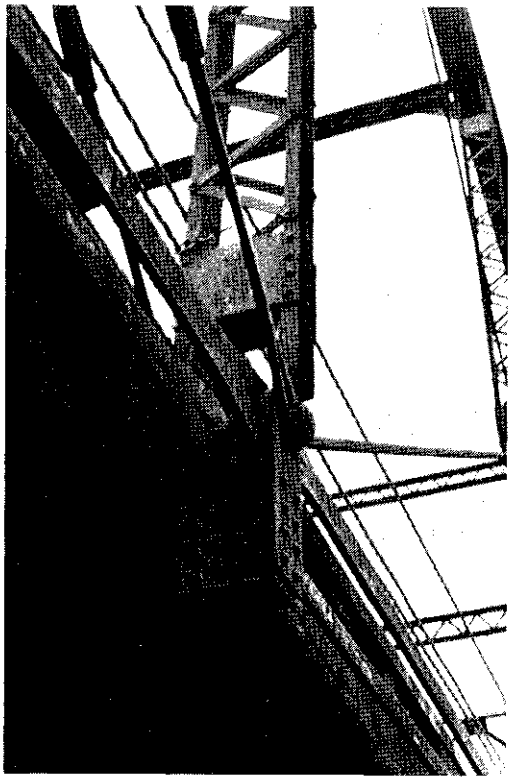

Fig. 5. Photograph of typical connection of floorbeam to truss at vertical laced channel member.

Table 1. Chemical properties

Element	Percentage in wrought iron	Percentage in steel
Carbon	< 0.03	0.19
Manganese	< 0.05	0.40
Phosphorus	0.29	0.012
Sulfur	0.042	0.029
Nickel	< 0.05	< 0.05
Chromium	< 0.05	< 0.05
Molybdenum	< 0.03	< 0.03
Copper	< 0.03	0.03
Aluminum	0.03	–
Vanadium	< 0.01	–
Silicon	0.22	< 0.05
Cobalt	0.02	–

Tensile tests were conducted on coupons from typical members of both wrought iron and steel to obtain material properties. Six tests were conducted on coupons from wrought iron specimens. Three coupons were from a square eye-bar (typical of truss hangers and some diagonals) and measured approximately 1-1/4 in. x 1/2 in. Three tests were conducted on coupons from two steel channels (typical of truss compression members) and measured approximately 1-1/8 in. x 1/8 in. All of the coupons had a gage length of 8 in. The results of the tensile tests

are shown in Table 2 with typical stress-strain curves for wrought iron and steel shown in Fig. 6.

Table 2. Physical properties

Material	σ_y (ksi)	σ_{ult} (ksi)	E (ksi)
Wrought iron	35.5	49.1	28,000
Steel	42.0	58.7	30,900
Timber	–	4.02	1,150

The results shown in Tables 1 and 2 indicate that the steel satisfies the requirements for ASTM A36 steel even though the steel was manufactured around the turn of the century. The wrought iron also conforms to ASTM specifications (A207).

The timber members were made from Douglas Fir which had been sized and pressure treated with creosote in accordance with Iowa State Highway Commission Standards. Flexure tests, using two equal loads placed equidistant from mid-span to develop a pure moment region, were conducted on typical timbers in both the flat and on edge positions to determine material properties. The modulus of elasticity for the timber was determined from the load-deflection curves of the specimens tested. A typical load-deflection curve is shown in Fig. 7. The results of these tests are also shown in Table 2.

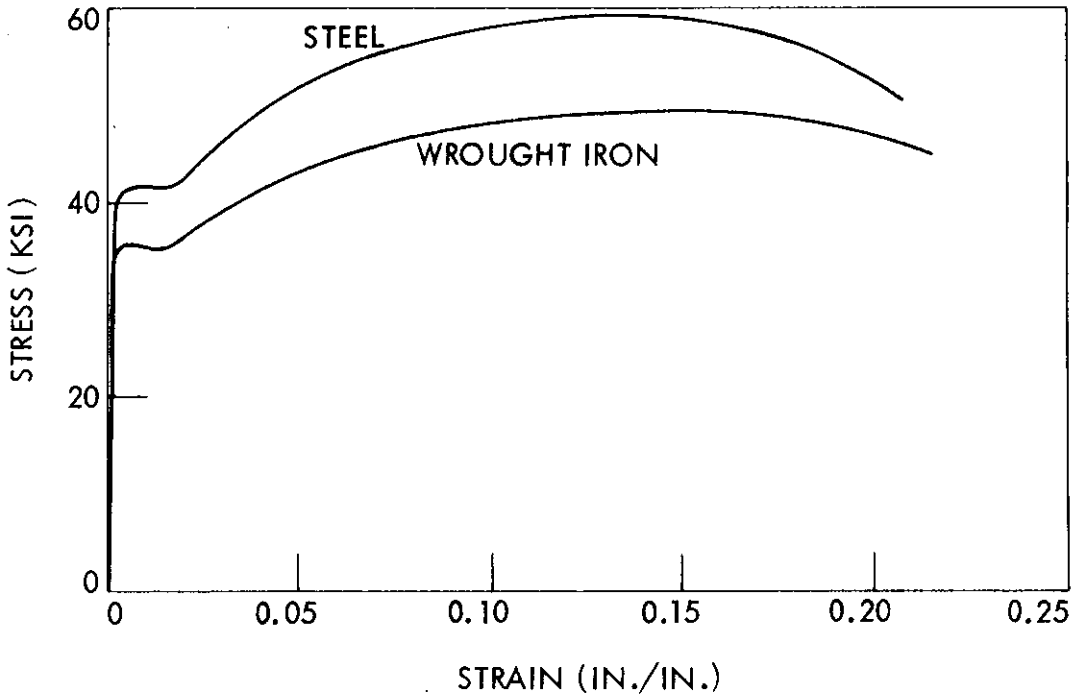

Fig. 6. Typical stress-strain curves for wrought iron and steel.

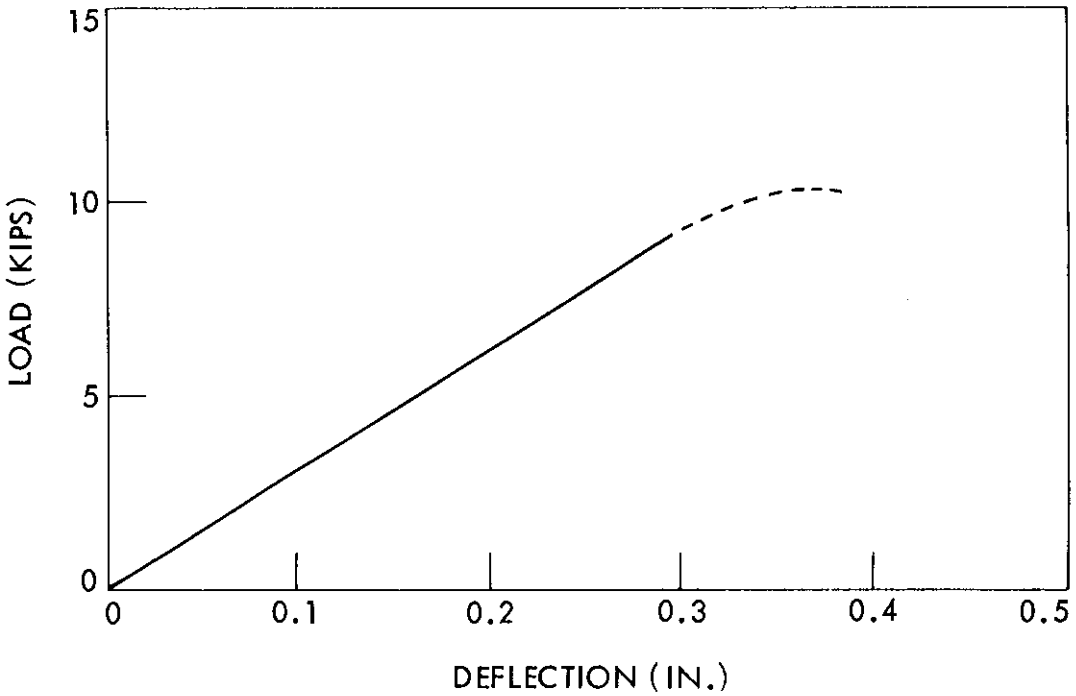

Fig. 7. Typical load-deflection curve timber flexure test.

CHAPTER 3. TESTS AND TEST PROCEDURE

This section outlines the details of the specific tests and the events which occurred during each of the tests. Each test (i.e. timber deck test, truss test, and floorbeam test) will be discussed separately. In this section only the occurrences will be discussed as the analysis of the behavior will be presented in Chapter 4.

The test procedure for each test was to

1. Apply the first load increment,
2. Hold the load until the appropriate instrumentation readings could be taken,
3. Record any behavioral indications,
4. Increase this load by the pre-established increment, and
5. Repeat steps 2-4 until failure occurs.

Timber Deck Test

The timber deck in two different panels on span 2 was the first part of the bridge to be tested. Each of the panels was tested to failure using a simulated axle load which was applied by hydraulic jacks.

The first test was conducted on the panel between L_8 and L_9 with the loads centered on the panel as shown in Figs. 8 and 9. The second test was conducted on the panel between L_2 and L_3 with the loads eccentrically placed so that the center of the axle was 3 feet from the center of the panel (edge wheel 2 feet from edge of the roadway)

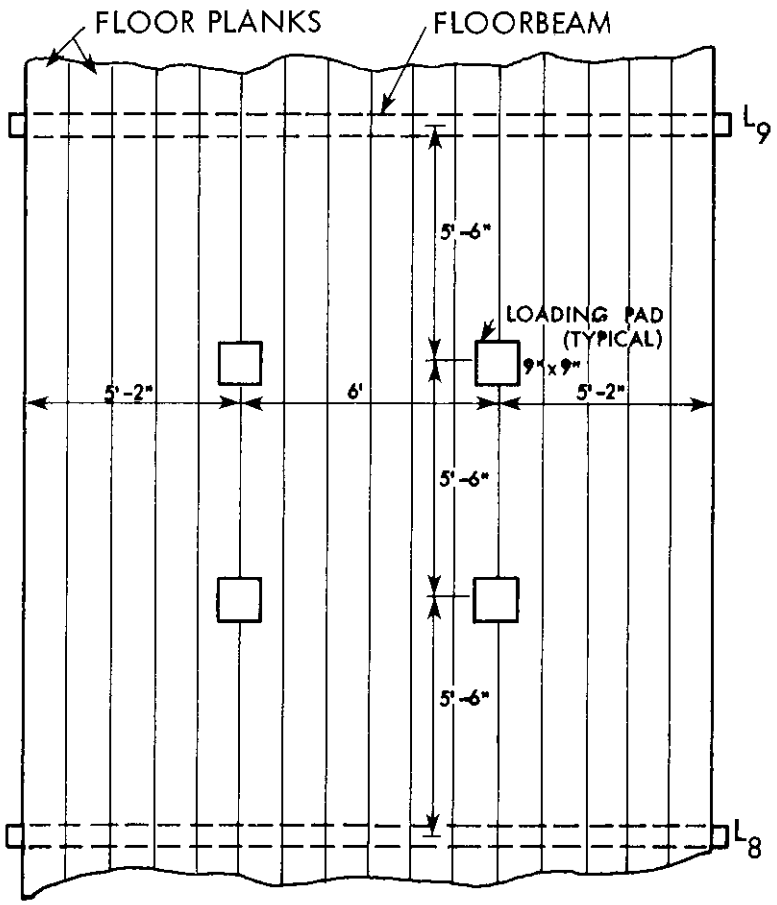

Fig. 8. Load location for deck test 1 (plan view).

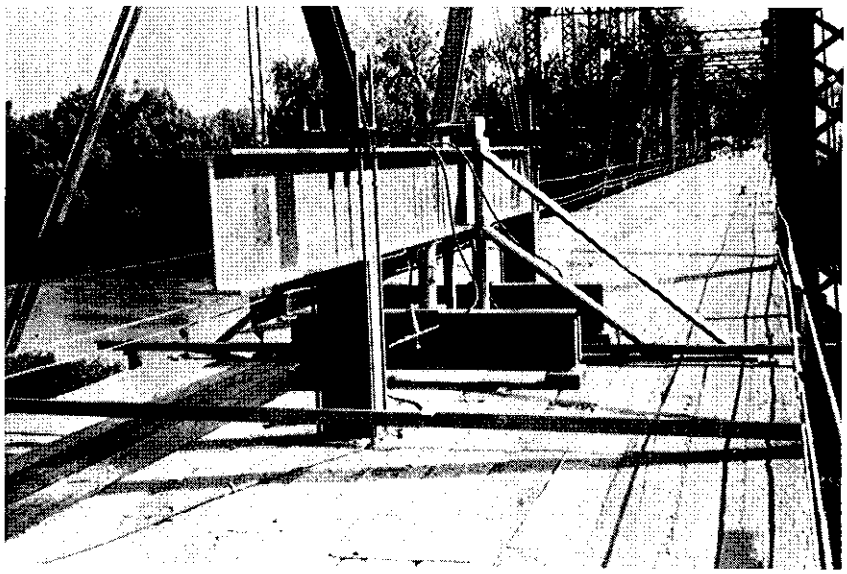

Fig. 9. Photograph of deck test 1 setup.

as shown in Figs. 10 and 11. The load placement longitudinally along the panel is shown in Fig. 12, and the position of load in relation to the stringers is given in Fig. 13. The tests were conducted using a self-contained system with the floorbeams acting as reactions as seen in Fig. 12.

Instrumentation on the timber deck tests was limited to deflection dials placed across the panel mid-span between panel points (Fig. 14). Six deflection dials were used in the first deck test, while seven were used in the second test (Figs. 15 and 16).

The load was first applied in increments of 10 kips, but as the loading progressed to higher levels, the load increments were reduced to 5 kips until failure was reached. Loading proceeded as planned on the first test at loads up to 65 kips, when the fifth stringer from the left broke. As the load was increased up to the maximum load of 101.5 kips, stringers split and failed. The behavior of the deck at loads above 65 kips can be seen in Fig. 17 and the failure order of the stringers in Fig. 13. At each failure there was a sudden drop in load. However, upon reloading there was usually a recovery of load and a further increase in load. After the failure of 10 stringers the test was terminated because the deck was unable to sustain any additional load. Figure 18 shows the top of the deck at a load near failure. The failed stringers are shown in Fig. 19.

The second test went according to test procedure plans up to a loading of 50 kips. For loads greater than 50 kips the behavior of the deck can readily be seen in Fig. 20. As the load was increased up to the maximum load of 77.4 kips, stringers split and failed. The failure

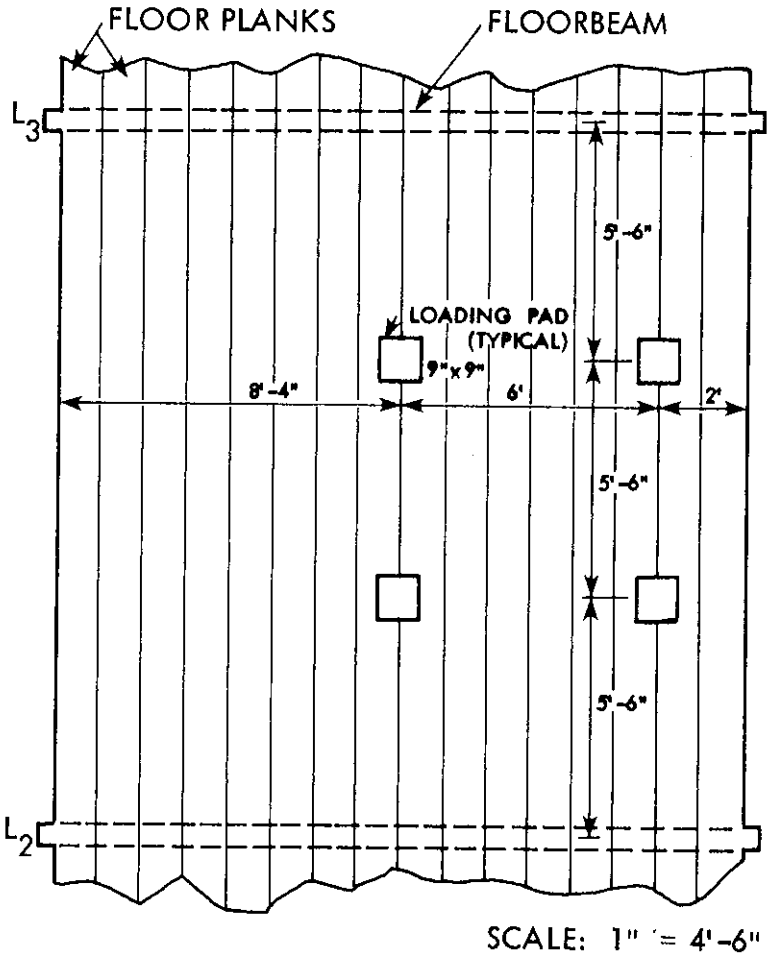

Fig. 10. Load location for deck test 2 (plan view).

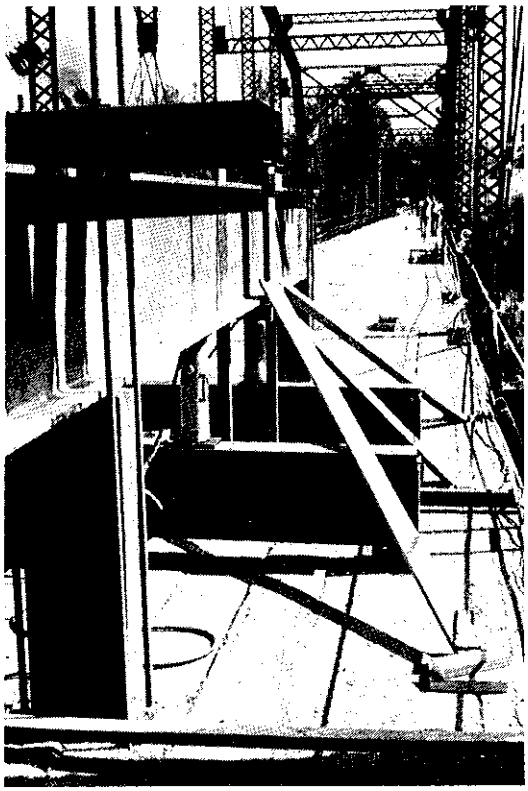

Fig. 11. Photograph of deck test 2 setup.

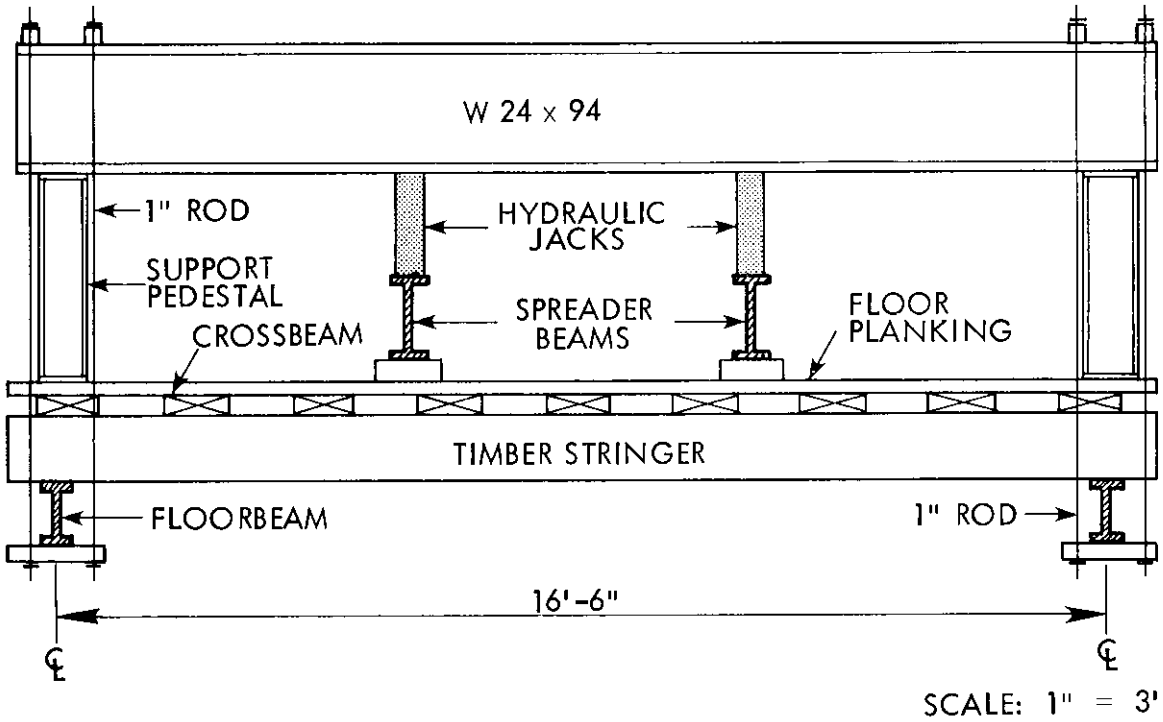

Fig. 12. Deck test setup (elevation view).

DECK TEST 1

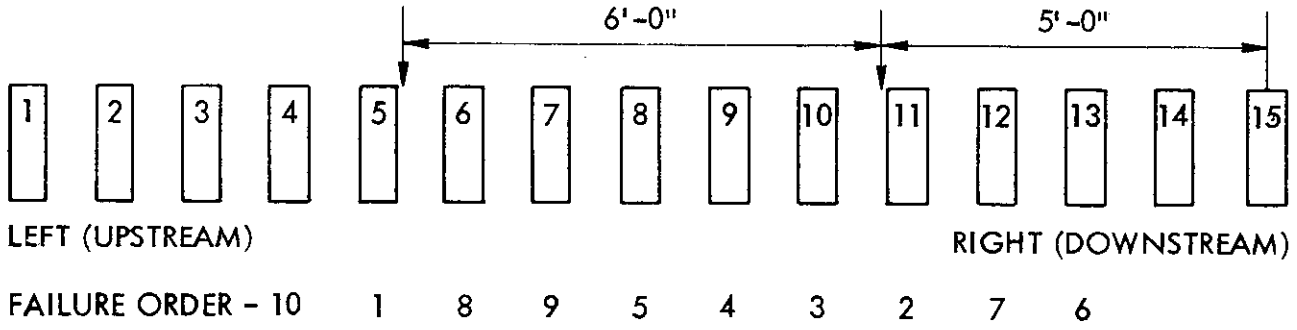

DECK TEST 2

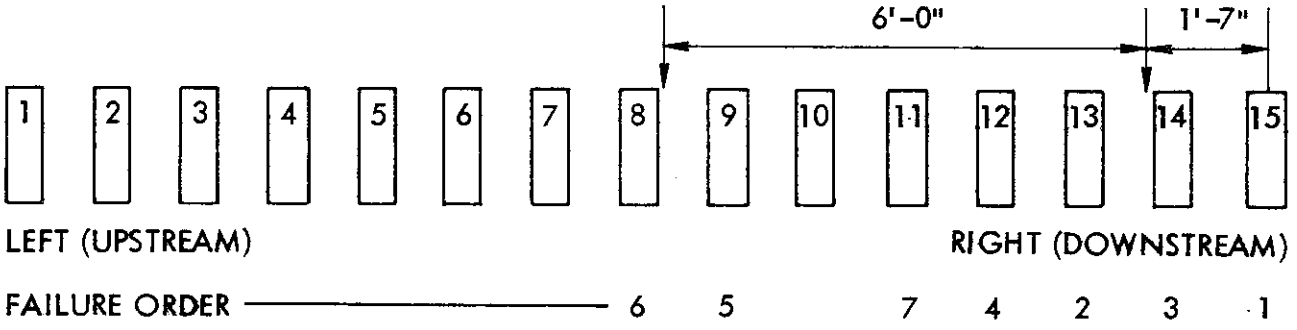

Fig. 13. Numbering system and failure order of stringers for deck tests 1 and 2.

SCALE: 1" = 20"

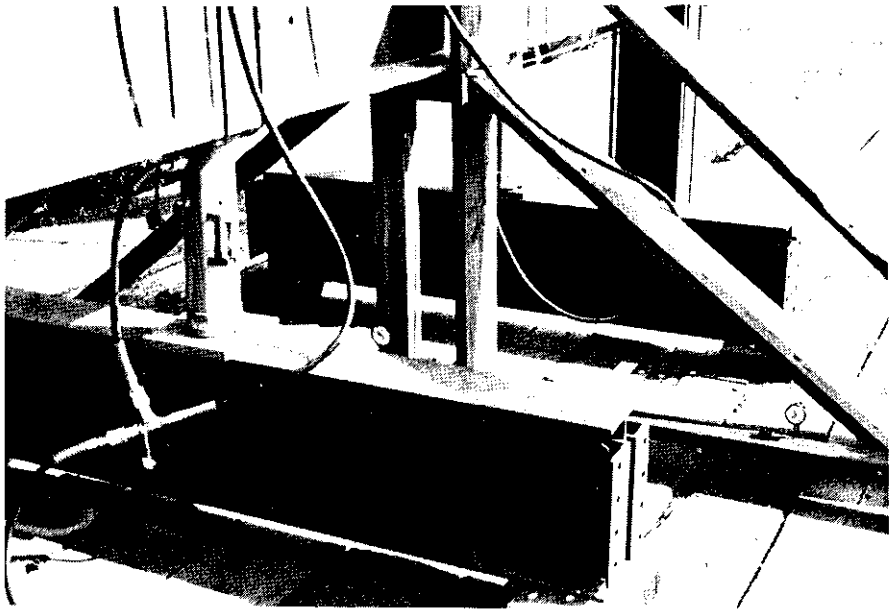

Fig. 14. Photograph of deck test 1 setup showing deflection dials.

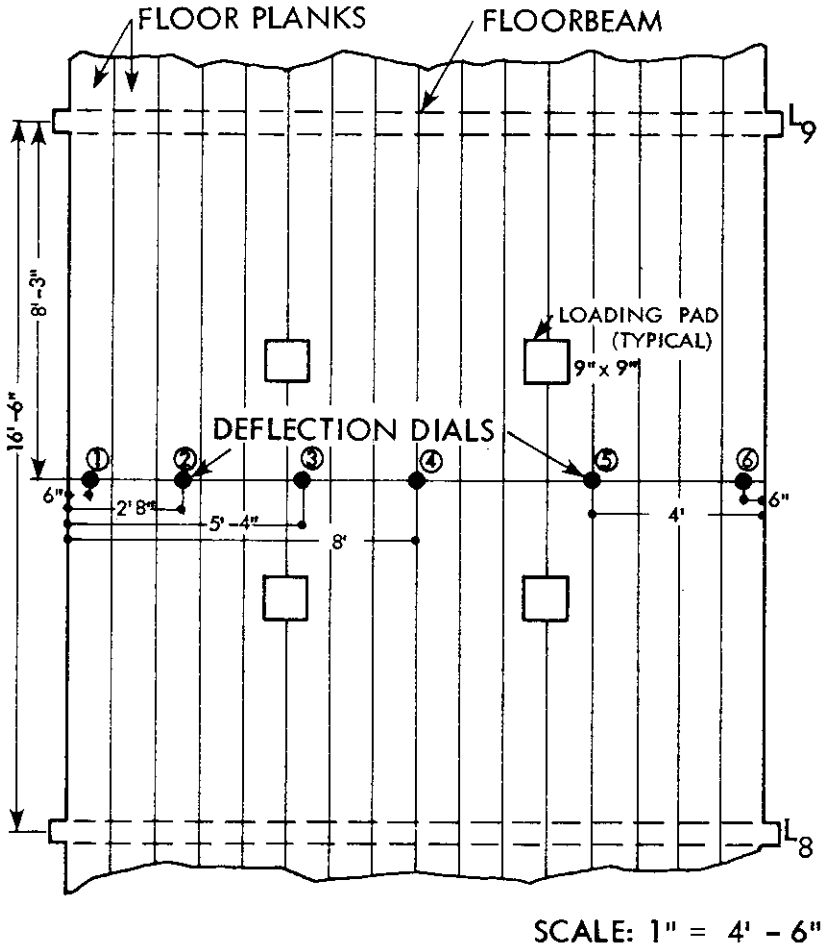

Fig. 15. Location of deflection dials for deck test 1.

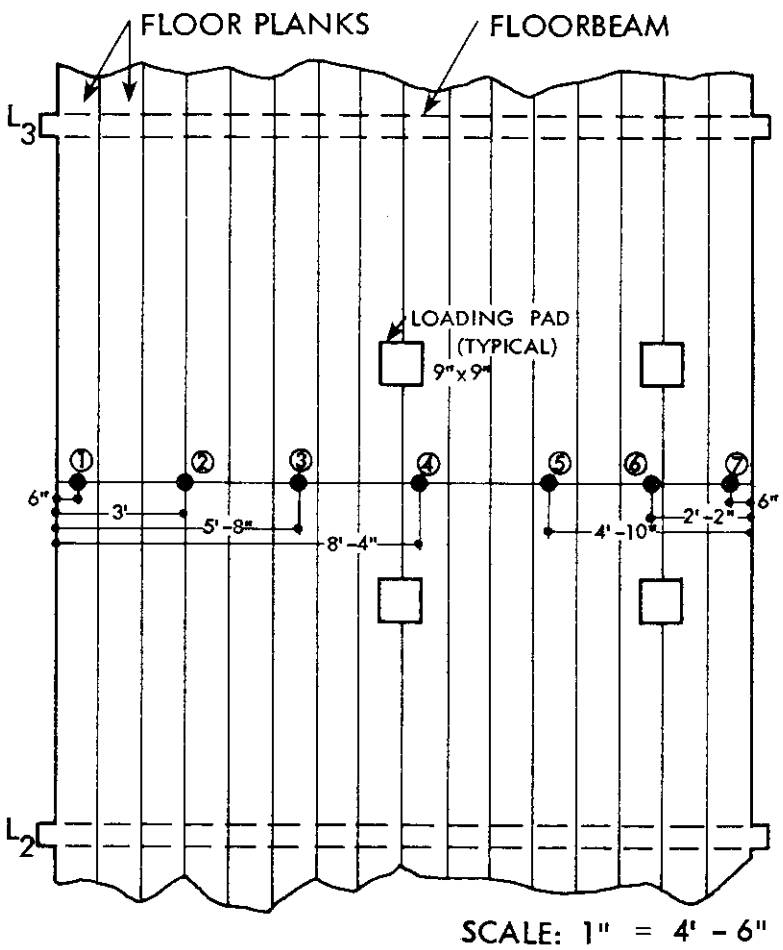

Fig. 16. Location of deflection dials for deck test 2.

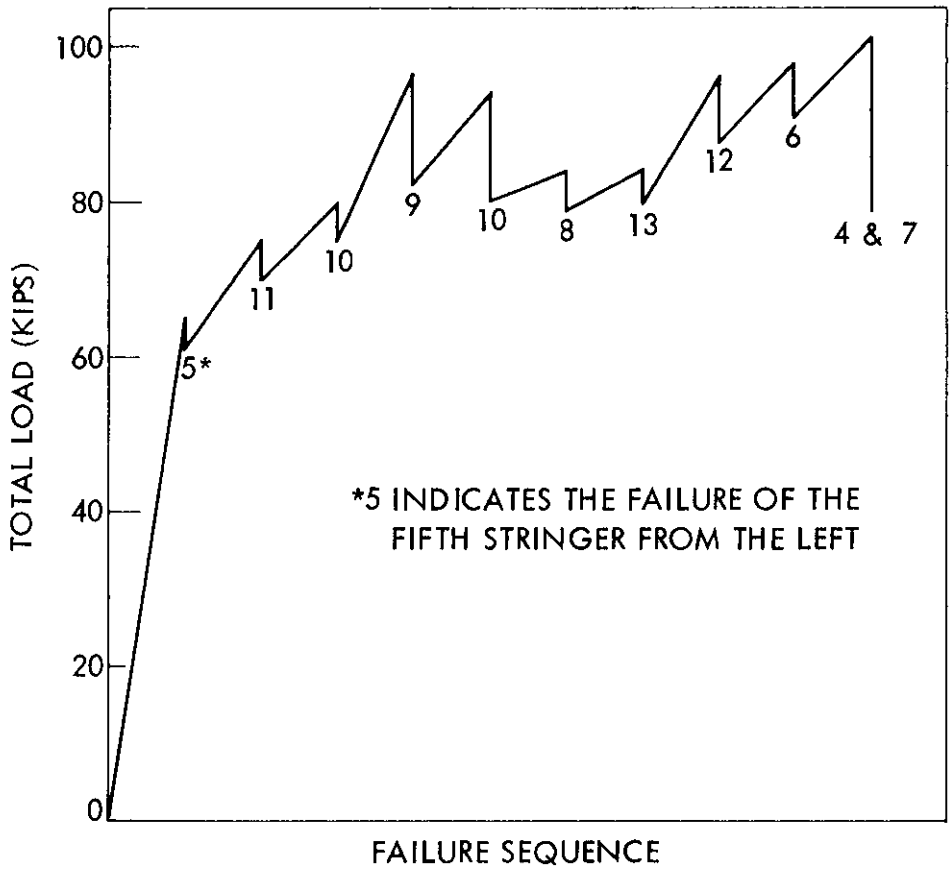

Fig. 17. Load history for deck test 1.

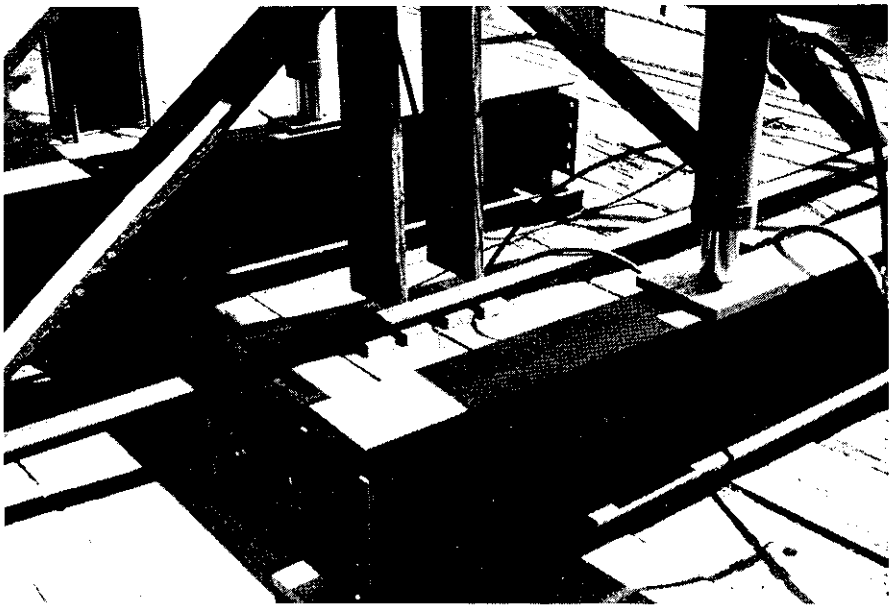

Fig. 18. Photograph of deck test 1 near ultimate load.

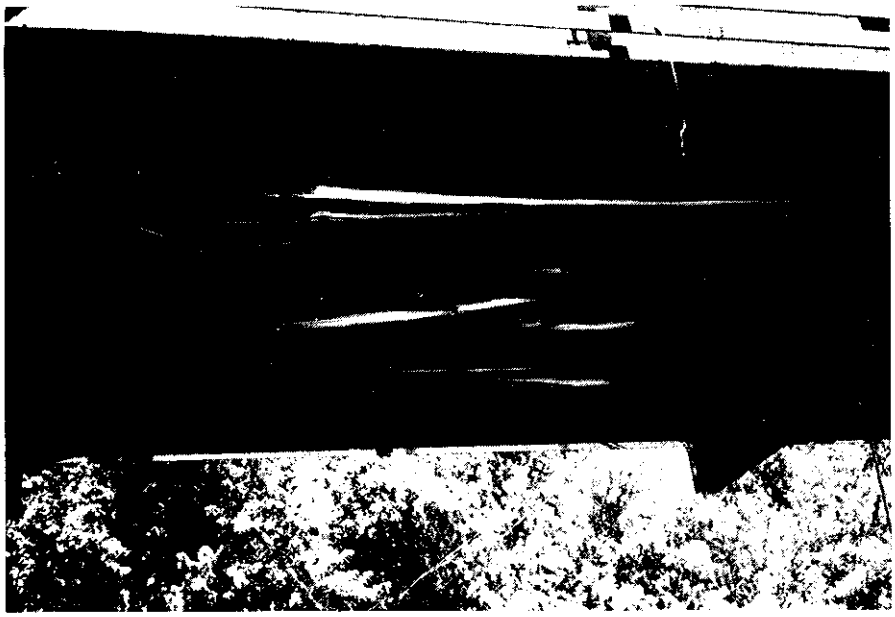

Fig. 19. Photograph of failed stringers from deck test 1.

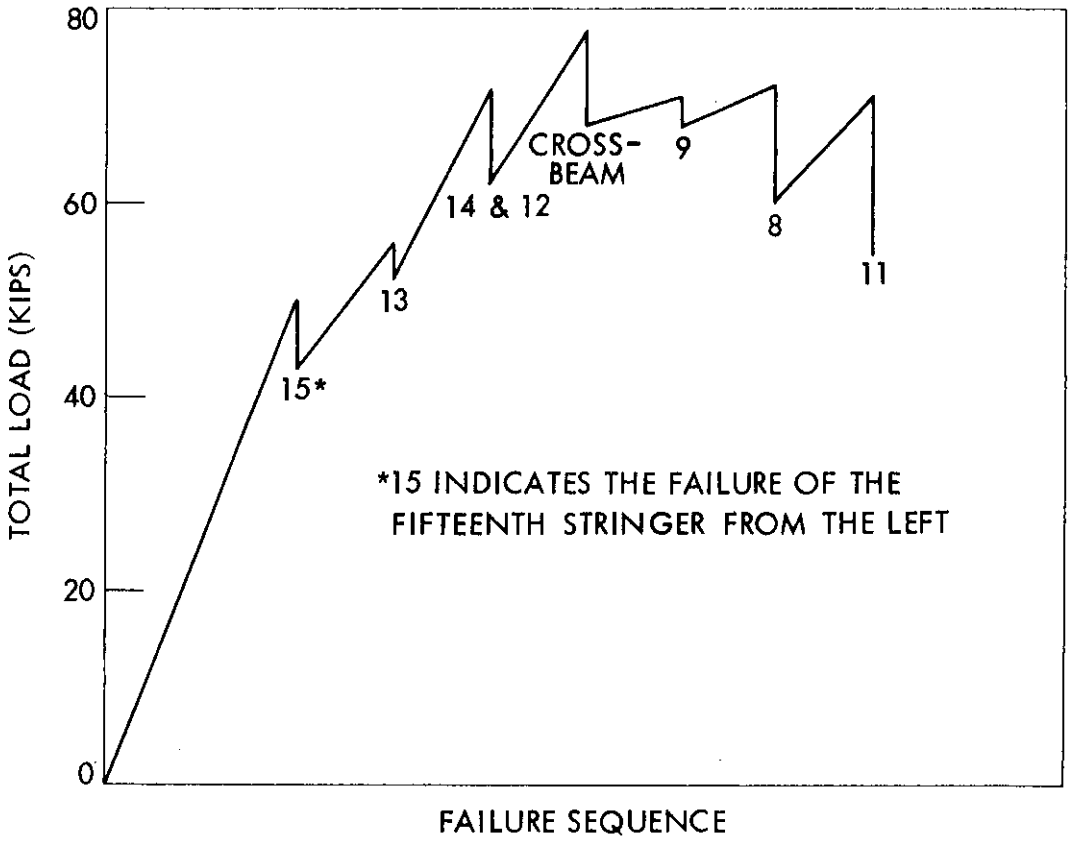

Fig. 20. Load history for deck test 2.

order of the stringers for this test is also given in Fig. 13. At each failure there was a sudden drop in load. However, upon reloading there was usually a recovery of load and a further increase in load. After the failure of seven stringers, the test was terminated due to the transverse load beam resting on the floor planking of the bridge, as shown in Fig. 21. Figure 22 shows the failed stringers near the loaded edge of the deck.

Truss Test

The second part of the bridge to be tested was the trusses of span 2. The test was performed using simulated axle loads applied at joints L_4 and L_5 in the ratio of 1 to 4, with the greater load being applied at L_5. This ratio was used because it represented the relationship between the axles on an AASHO H 15 truck. Although the load spacing in the truss test was 16.5 feet (limited by floorbeam spacing and panel length), the effect of this difference from the actual 14-foot specified axle spacing will not significantly affect the results. The effect of the difference is minimized because of the large load ratio differential.

The loads were applied using hydraulic jacks connected to large dead weights. Four large reinforced concrete mats, which were used to supply the needed dead weights, were formed using prefabricated steel forms for the sides and lumber for the bracing (Fig. 23). Considerable delays in the construction of the mats were encountered due to extremely heavy rains and two periods of flooding on the Des Moines River. The

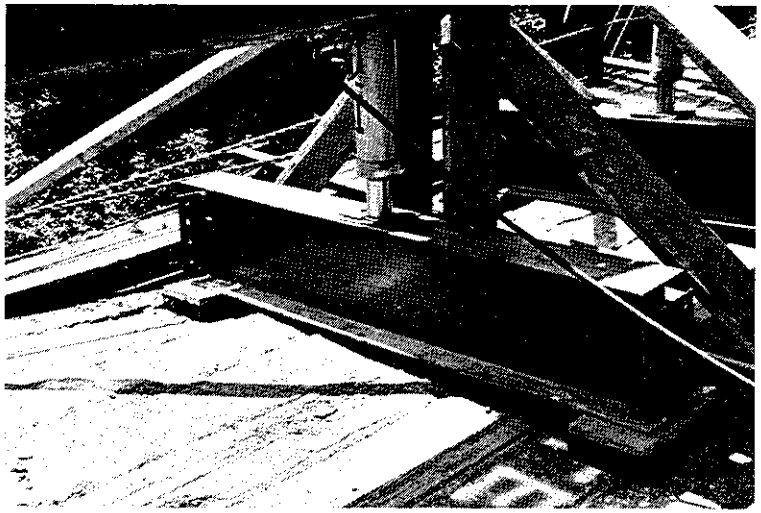

Fig. 21. Photograph of deck test 2 near ultimate load.

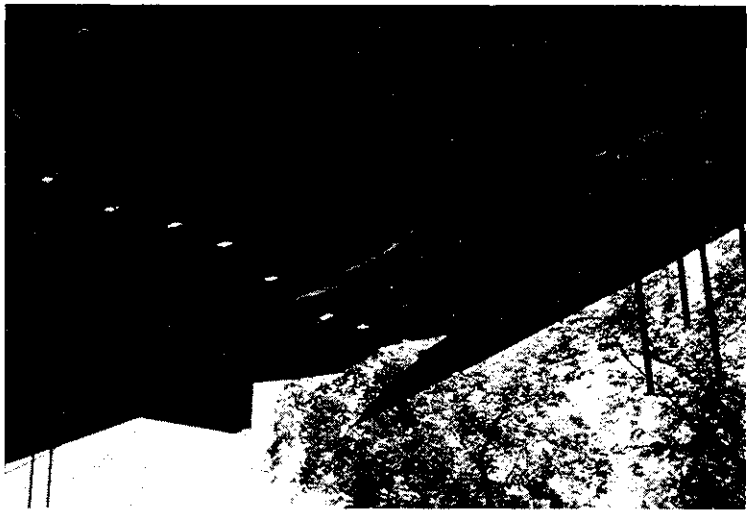

Fig. 22. Photograph of failed stringers from deck test 2.

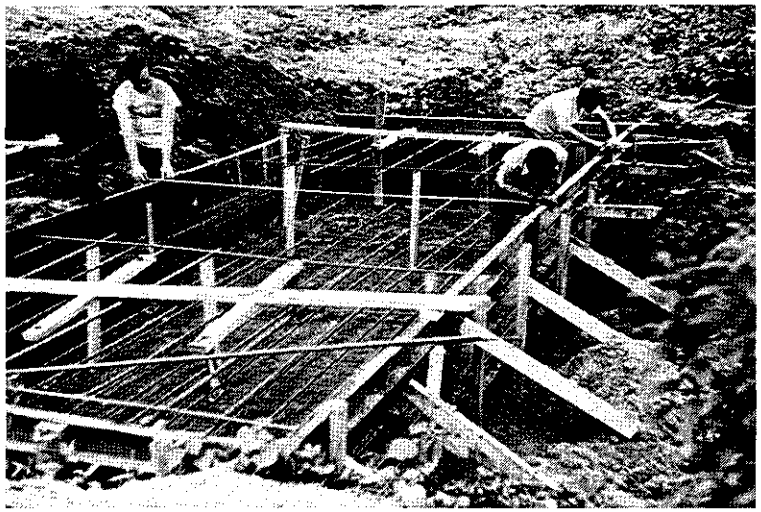

Fig. 23. Photograph of formwork for concrete mat showing formwork, concrete inserts, and reinforcing steel.

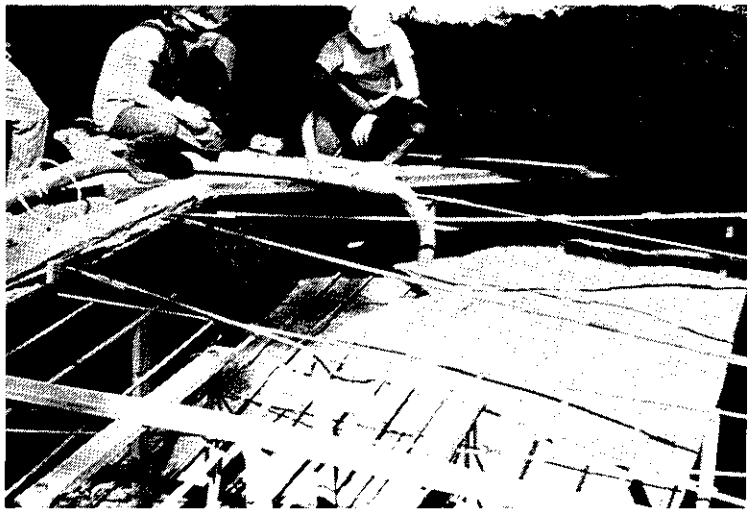

Fig. 24. Photograph of the concrete pour.

four mats were poured (Fig. 24) using a concrete pumping system in which the concrete was pumped from the southwest end of the bridge to the locations of the forms for the mats. The sizes of the concrete mats varied from 1.5 ft X 6 ft X 25 ft to 3 ft X 10 ft X 25 ft. The weights of these mats ranged from 34 kips to 112 kips. Soil was piled on top of each of the concrete mats to increase its weight, as illustrated in Fig. 25. Two of these mats, cast under span 2, were used for the truss test. The other two, under span 1, were used for the subsequent floorbeam tests.

One-inch diameter rods were attached to the concrete mats using concrete inserts and a system of structural tubes (Fig. 26). The hydraulic jacks were connected to the rods through a similar system of structural tubes so the loads could be applied to the truss (Fig. 27). Sketches of the loading system are shown in Figs. 28-30.

The instrumentation on the truss test consisted mainly of strain gages on the truss members as shown in Fig. 31. The strain gages were series CEA and self-temperature compensated for steel manufactured by Micro-Measurements Inc. of Romulus, Michigan. The strain gages were installed in the normal manner with M-Bond 200 adhesive after the surface rust was removed. Lead wires were soldered to the strain gages and connected to strain indicators. A three-wire lead was used to minimize the effect of the long lead wires and any temperature changes. The strain gages on the truss members in span 2 were coated with successive waterproofing coats of polyurethane, nitrile rubber, acrylic lacquer, and polysulfide epoxy. The strain gages on the truss members in span 1 were coated only with polyurethane, because

Fig. 25. Photograph of concrete mat with soil.

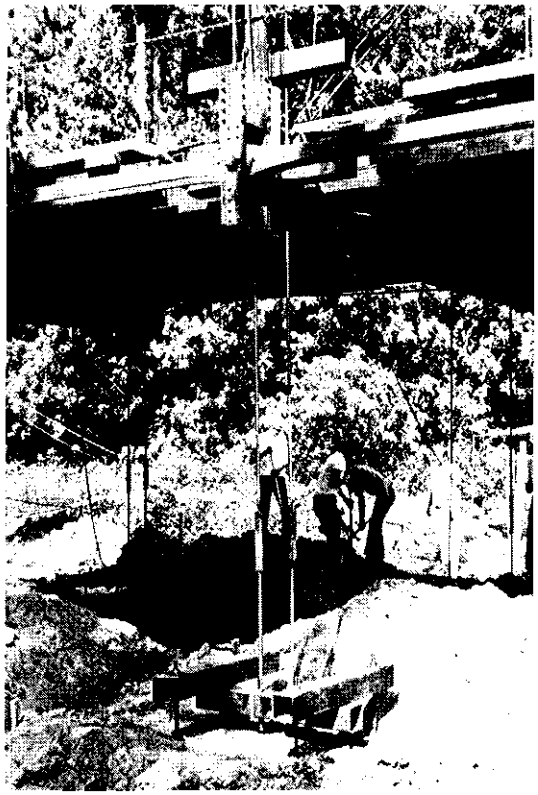

Fig. 26. Photograph showing system used to attach steel rods to concrete mats.

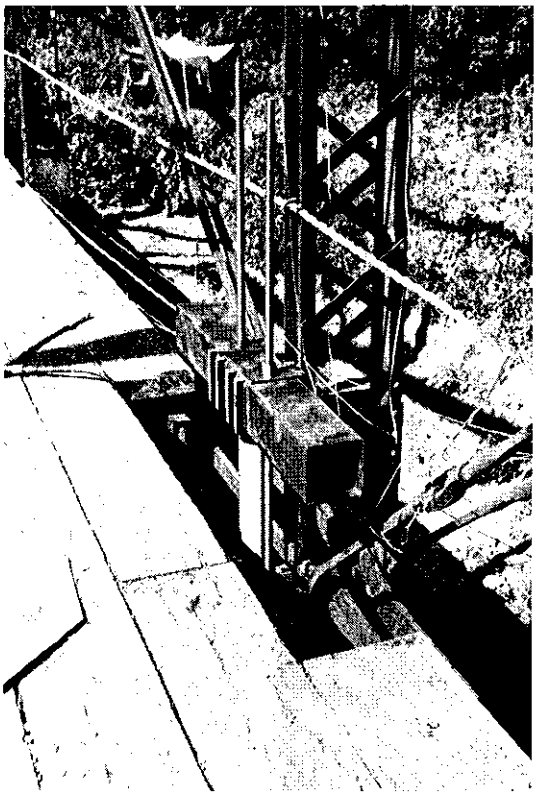

Fig. 27. Photograph showing hydraulic jack and structural tube arrangement.

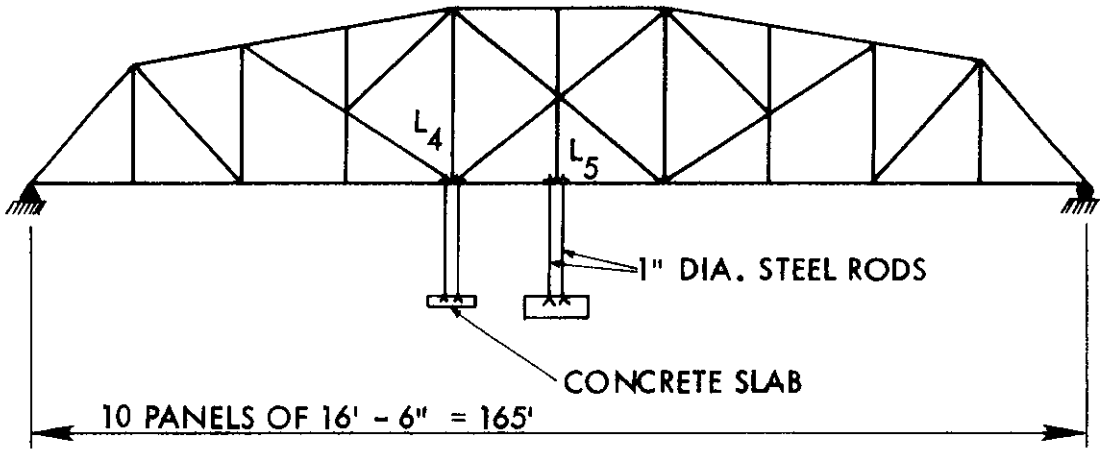

Fig. 28. General truss view showing loading system.

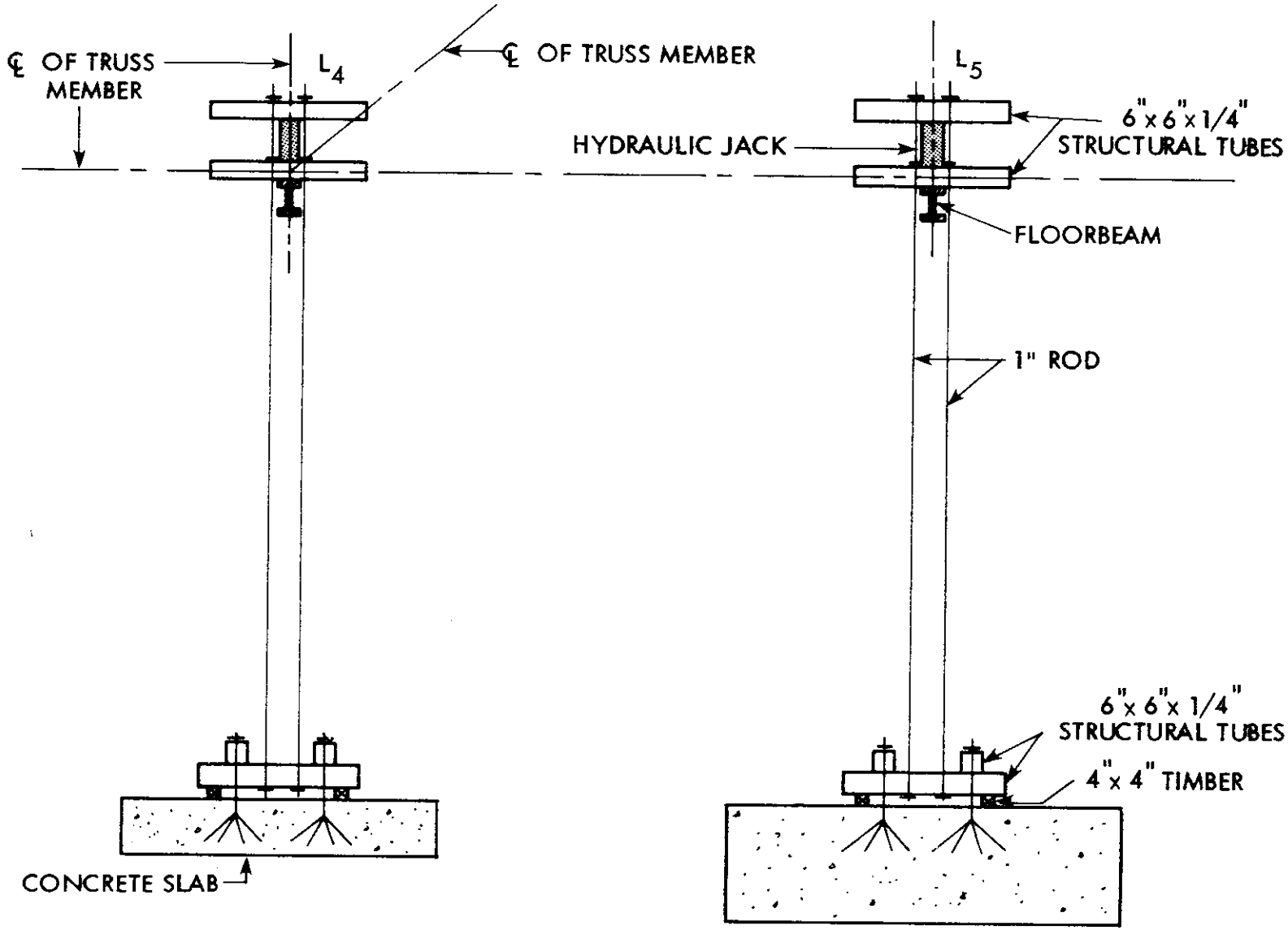

Fig. 29. Loading system details (elevation view).

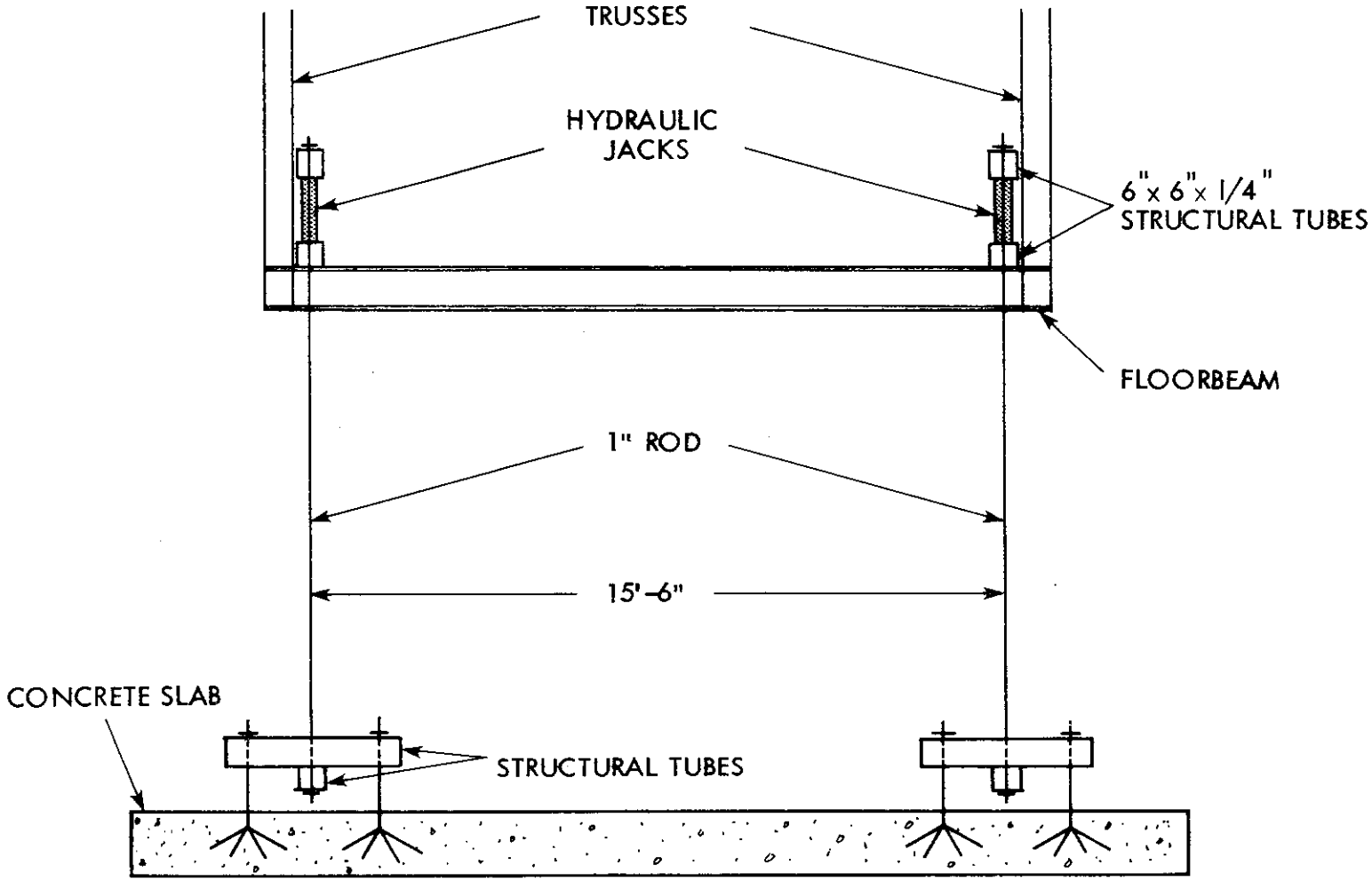

Fig. 30. Loading system details (end view). SCALE: 1" = 4'

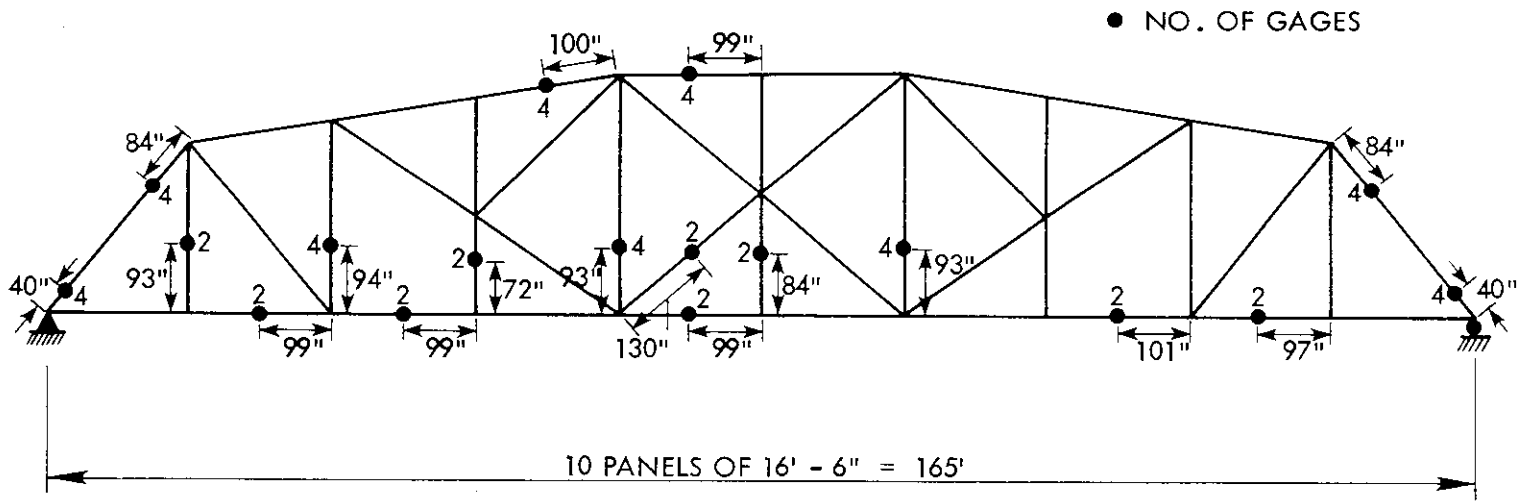

Fig. 31. Location of strain gages on span 2 (truss test).

the lead wires, which were being used in span 2, could not be installed until after testing was completed on span 2. Members which had two strain gages on them were tension eye-bars. One strain gage was mounted on each of the two bars of the members, as shown in Fig. 32. Members which had four strain gages were composed of two laced channels or two built-up laced channels. The gages were mounted near the four corners of the member to allow the computation of the bending moment in both directions as well as the axial force for the member from the strain gage data. Vertical and horizontal deflection readings were taken at mid-span and at the three-tenths points on both sides of the truss. The deflections were read from scales attached to the bridge using a transit and a level set up at the end of the bridge, as illustrated in Fig. 33. For the truss test, a total of nine deflection readings were taken, and 108 strain gages were used on the truss members.

The load was first applied in increments of 10 kips (8 kips at L_5 and 2 kips at L_4), and as the loading progressed to higher levels, the load increments were reduced to 5 kips (4 kips at L_5 and 1 kip at L_4) until failure was reached. The truss test proceeded as planned up to a total load of 80 kips. While increasing the load to 90 kips the observation was made that yielding was taking place in one of the hangers at L_5 on the downstream side. The yielding made it extremely difficult to hold and increase loads. During the load increment to 110 kips, there was considerable yielding at L_5. At a total load of 110 kips, a snapping sound was heard, and the load dropped several kips, however, no visible sign of failure was evident. Loading proceeded

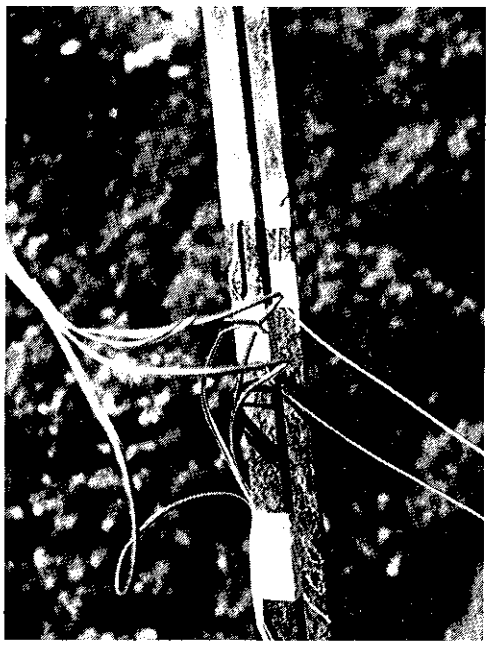

Fig. 32. Photograph of typical strain gage installation on eye-bar members.

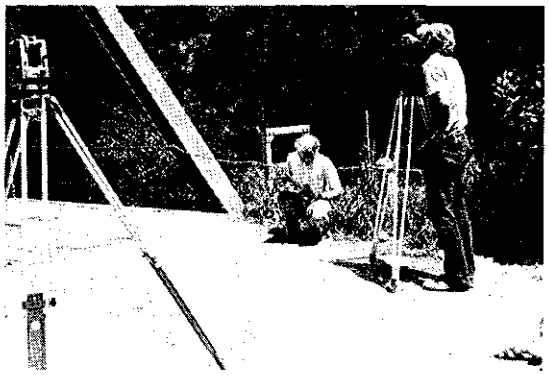

Fig. 33. Photograph of transit and level for taking deflection readings.

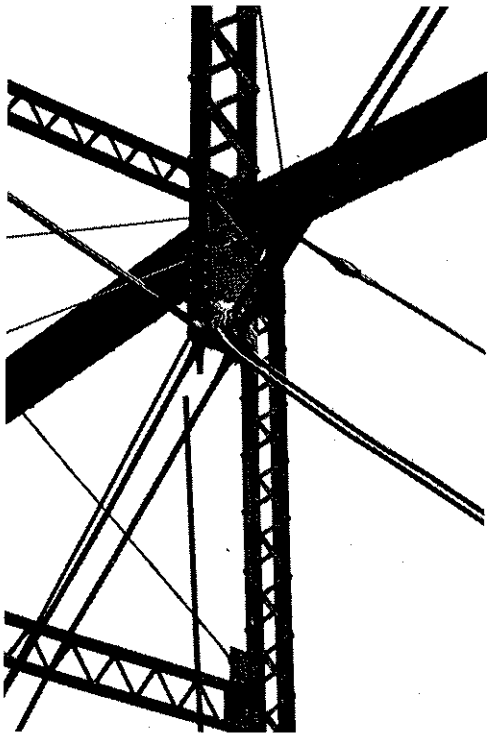

Fig. 34. Photograph showing location of failure of member L_5M_5.

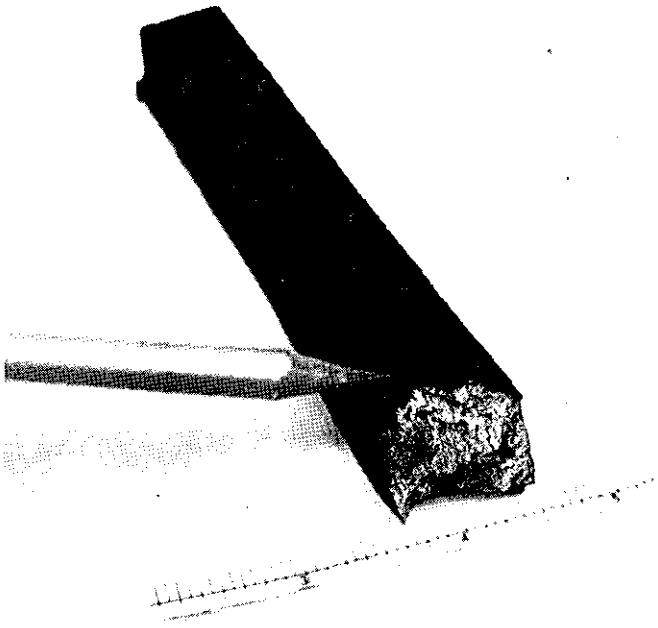

Fig. 35. Photograph of fracture.

with the same difficulty to a load of 130 kips. At this load the flaking of the rust on the hangers at L_5 (upstream side) was very noticeable.

At a total load of 133 kips (106 kips at L_5 and 27 kips at L_4), one of the hangers at L_5 (upstream side) failed. The location of the failure and a close-up of the fracture are shown in Figs. 34 and 35. When the failure occurred, a portion of the load transferred from L_5 to L_4 resulting in a load of 63 kips at L_5 and 38 kips at L_4 (resulting in a loading ratio of 1.66 to 1). The decision was made to apply all additional load at L_5, rather than at both L_4 and L_5, to try to restore the original load ratio (4:1) and increase the loading at critical L_5. The load at L_5 was increased to 68 kips when the jack stroke limit was reached. The structural tubes were repositioned at this point to allow the application of additional load. During reloading, the diagonal member near L_5 (member L_4M_5 – shown in Fig. 2a) started to buckle. The observation was made that the truss deflection was large enough that there was a 4-in. gap between the timber stringers and the floorbeam at L_5. This occurred because of the continuity of the floor system and the lack of a positive tie between the timber floor and floorbeams. The hanger at L_5 (the one that did not fail on the upstream side) had buckled as shown in Fig. 36, due to the unloading for the repositioning of the jacks. The member buckled because it had been elongated under load and thus, under the reduced load, the member was too long for the distance between L_5 and M_5. After repositioning of the structural tubes was completed, the load was reapplied. The load was increased to 125 kips (90 kips at L_5 and 35 kips at L_4), and instrumentation readings were taken. The load continued to be

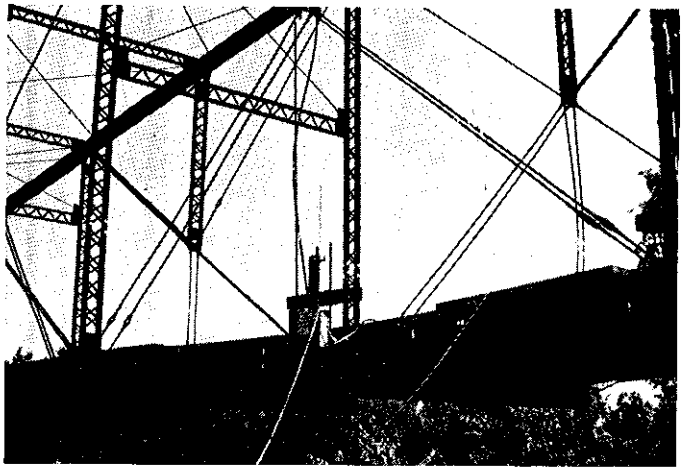

Fig. 36. Photograph of hangers buckling at L_5.

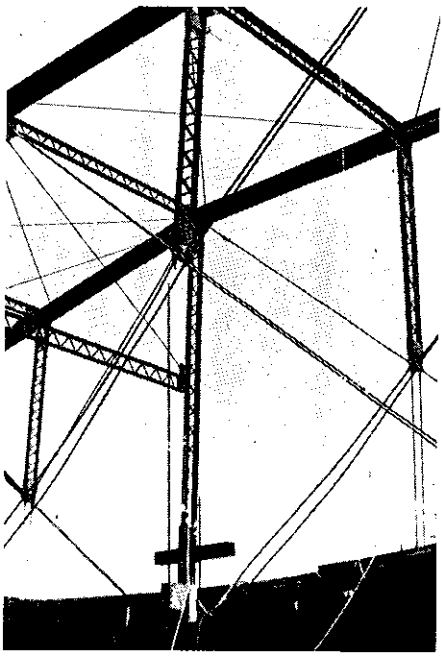

Fig. 37. Photograph of distortion of lower chord at L_5.

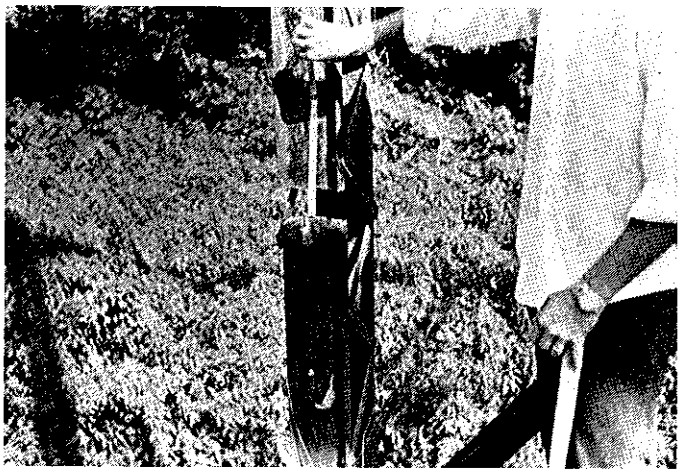

Fig. 38. Photograph of damaged member (one channel cut).

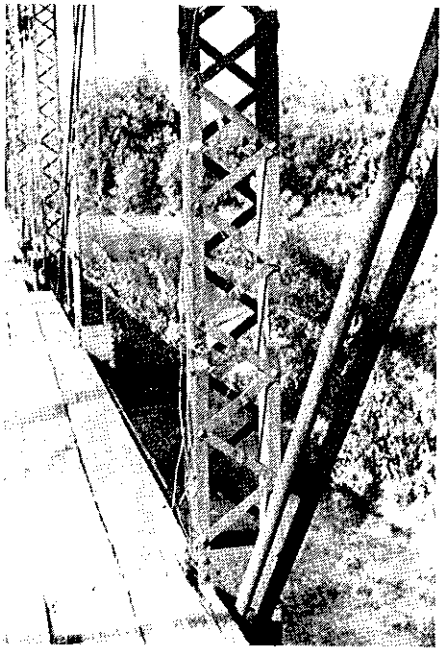

Fig. 39. Photograph of damaged member with only web of outside channel remaining.

increased until it was 112 kips at L_5 and 28 kips at L_4. At this load a significant distortion of the bridge was visible, as shown in Fig. 37, but the remaining hanger at L_5 on the upstream side had not failed.

After readings were taken at this load, the load was removed from L_5, because any further increase in load would only have caused more distortion of the lower chord at L_5. During the attempt to remove the load from L_5, the bridge came down on the nuts on the tube on the downstream side. Increasing the load at L_5 was necessary to relieve these nuts. After the load had been removed from L_5, the load at L_4 had increased to 45.5 kips. Instrumentation readings were taken at this load. The load was increased at L_4, with instrumentation readings being taken at intermediate levels. The capacity of the loading system was reached at a load of 78.5 kips. Instrumentation readings were taken and the load removed.

It was decided that further testing of the trusses would not provide additional meaningful information. The decision was then made to pursue the objectives of the second truss test by "damaging" one of the key members and reloading. To simulate the damage, member L_2U_2 was cut with an acetylene torch. This member was damaged because it is representative of laced channel compression members. Secondly, severely damaging an end post would result in an immediate catastrophic failure. Finally, the forces required to sufficiently damage an end post would require the use of an elaborate loading system. The cut (Fig. 38) was made 46 in. from the center line of the pin and 32 in. from the timber deck, with only one of the two channels comprising the member being cut. Initial instrumentation readings were taken and reloading at L_4 began. The

load was increased to 70 kips with sets of instrumentation readings taken at periodic intervals. After the load of 70 kips was reached without any signs of additional distress, the decision was made to cut the other channel comprising member L_2U_2 to obtain a failure of the truss. The member was cut so as to leave only the web of one channel remaining intact (Fig. 39). The load at L_4 was again increased to 70 kips without any signs of distress. The load was again removed from the bridge, and one bar of member L_2U_1 was cut. The truss was again loaded at L_4 to a load of 72 kips with no apparent signs of distress. The load was removed, and the decision was made to cut member L_2U_2 completely through (Fig. 40). The load was again applied at L_4, with the load reaching 39 kips before the member collapsed upon itself (forming a complete but shorter member) at the cut location (Fig. 41). This resulted in a slight drop in load. The load was then increased to 72 kips with no further distress of the truss. The load was removed and all testing terminated because of the potential danger of collapse during any additional member damage.

Floorbeam Test

The final portion of the ultimate test program was the testing of two floorbeams in span 1. They were both tested to failure using a load applied by hydraulic jacks and simulating a truck axle. The first test was conducted on the floorbeam at L_5. Initially, the compression flange of this floorbeam was approximately 13/16 in. out of line horizontally at mid-span. The second test was conducted on the

Fig. 40. Photograph of damaged member cut completely through.

Fig. 41. Photograph of damaged member after collapsing upon itself.

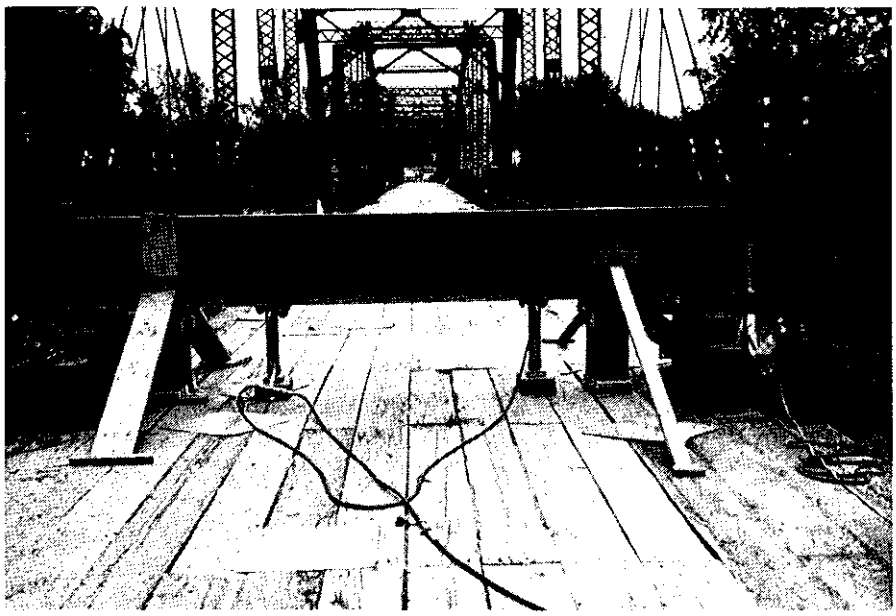

Fig. 42. Photograph of floorbeam test setup.

floorbeam at L_4. The compression flange of this beam was initially straight (within allowable tolerances). The test setup and load placement on the floorbeam are shown in Figs. 42 and 43. As can be seen from these two figures, each floorbeam was loaded using a system similar to that employed for the truss test.

Instrumentation for the floorbeam tests consisted of deflection dials on the floorbeam being tested (Fig. 44) and strain gages on selected truss members (Fig. 45) and on four adjacent floorbeams. The deflection dials were located at the centerline, quarter points, and near the ends of the floorbeam being tested (Fig. 46). The strain gages on the floorbeams were mounted on the inside surface of both the compression and tension flanges of the floorbeams and located at the centerline, third points, and near the ends of floorbeams 4 and 5 (test beams). The strain gages on floorbeams 3 and 6 (adjacent to test beams) were located at the centerline and near the ends of the beam (Fig. 47).

Five deflection dials, 10 strain gages on each of floorbeams 4 and 5, six strain gages on each of floorbeams 3 and 6, and 76 strain gages on the truss members were used for the floorbeam test at L_5. For the floorbeam test at L_4, the same number of deflection dials and strain gages on the floorbeams were used, but 84 strain gages were used on the truss members. The eight additional strain gages used on the floorbeam test at L_4 were mounted on the lower portion of member L_4U_4 on each truss near the connection to the floorbeam to detect any measurable rotation of the joint.

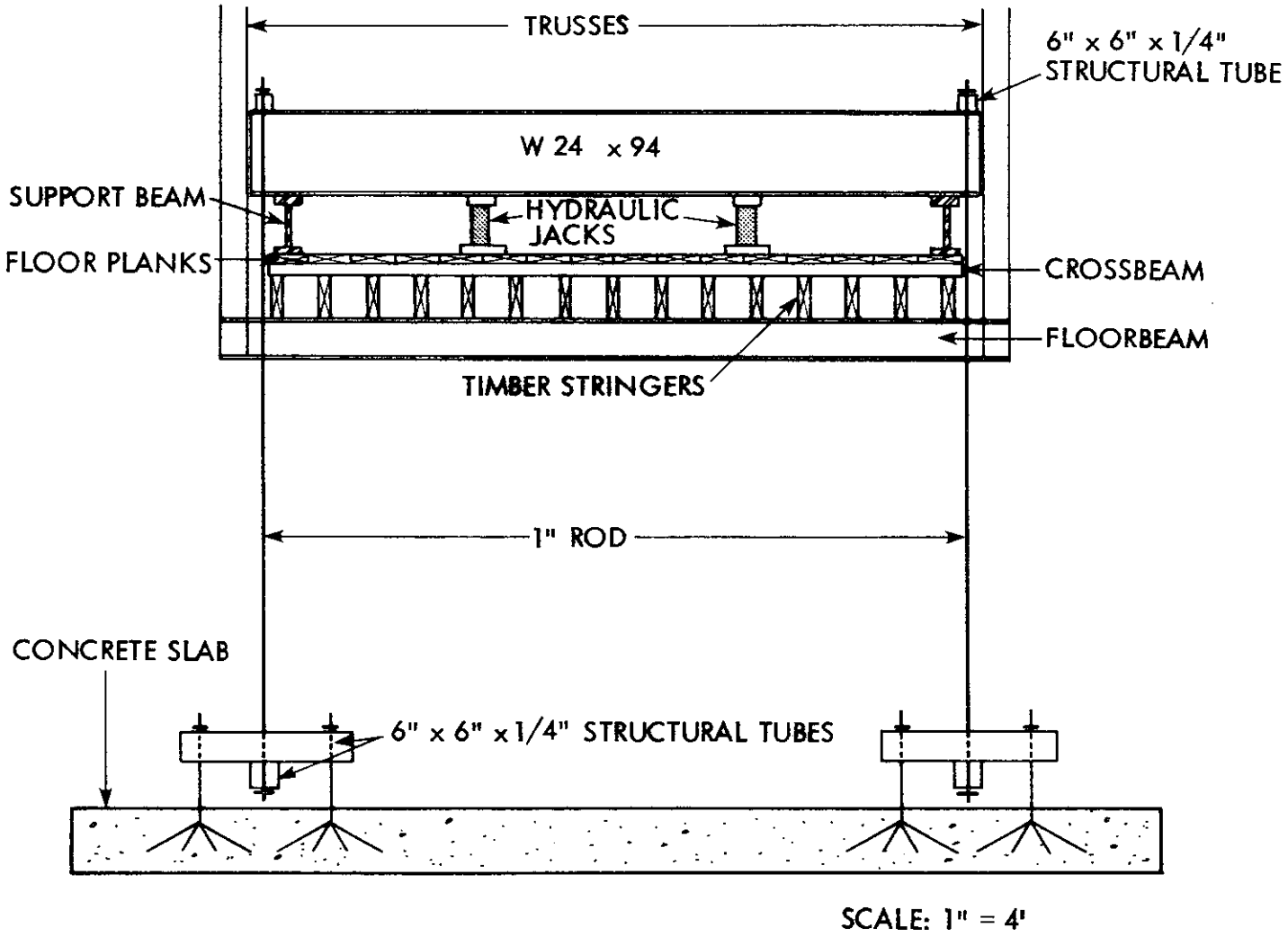

Fig. 43. Floorbeam test setup (elevation view).

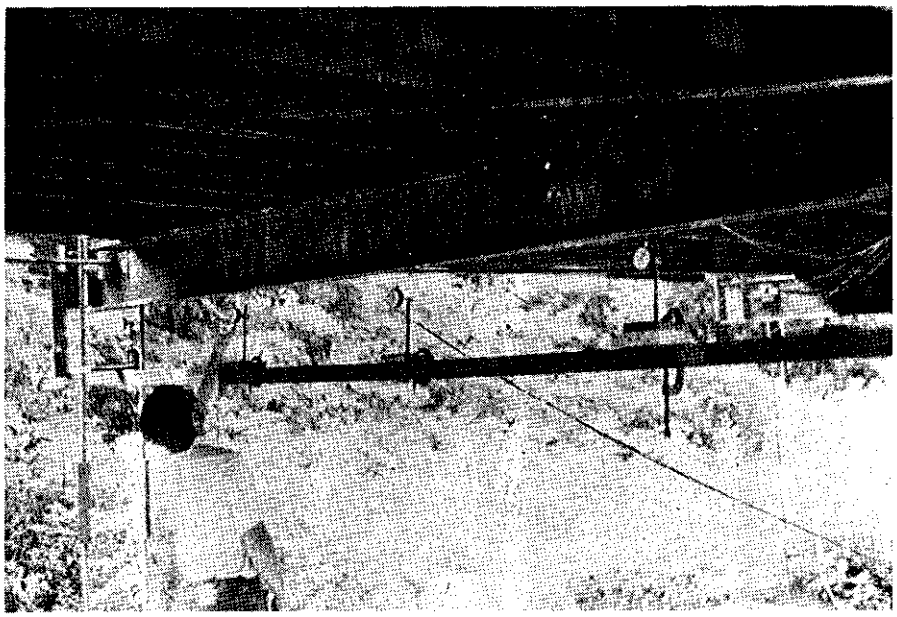

Fig. 44. Photograph of deflection dial placement for floorbeam test.

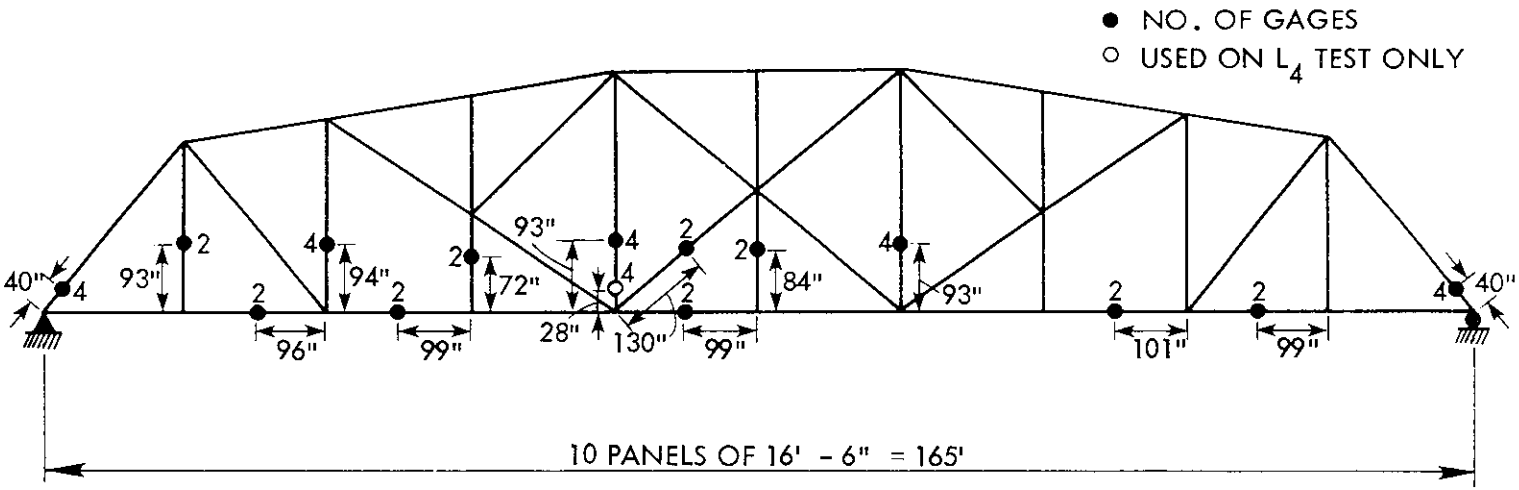

Fig. 45. Location of strain gages of span 1 (floorbeam test).

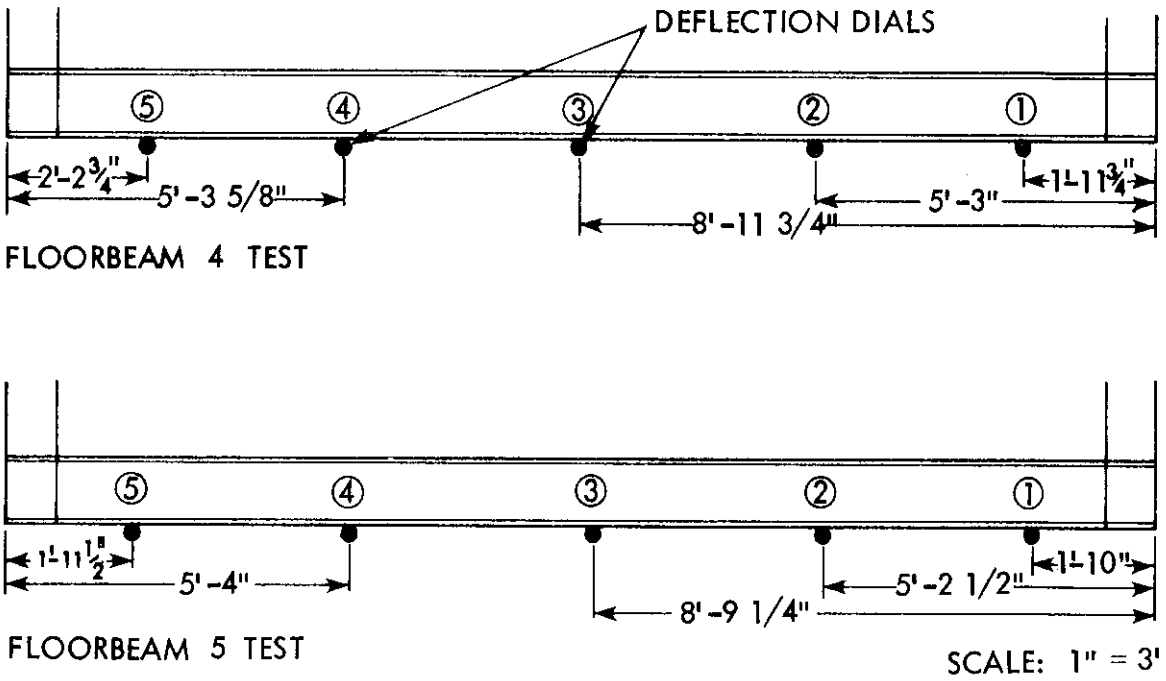

Fig. 46. Location of deflection dials for each floorbeam test.

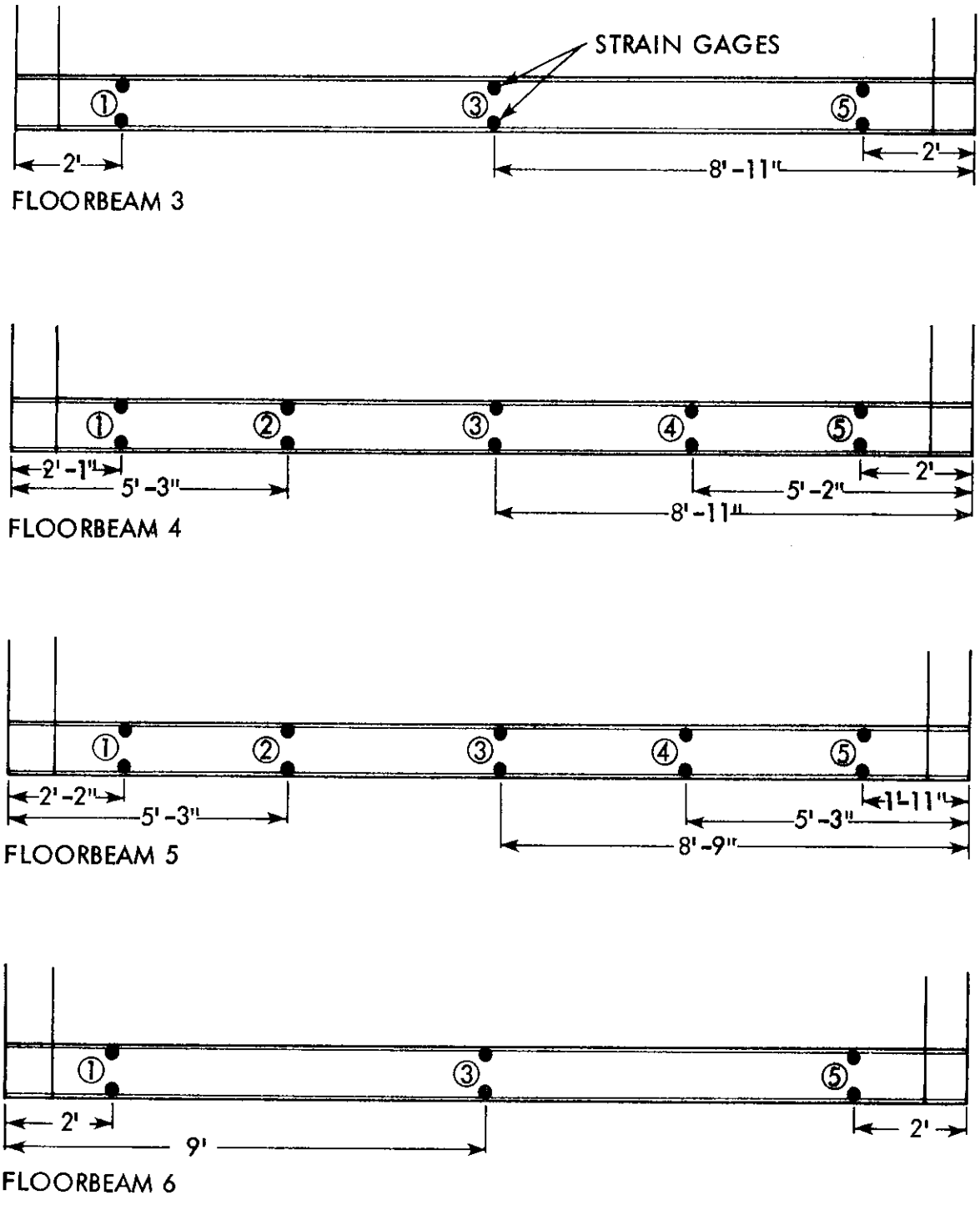

Fig. 47. Location of strain gages on floorbeams.

The load was first applied in increments of 10 kips, but as the loading progressed to higher levels the load increment was reduced to 5 kips until failure was reached. The test on floorbeam 5 proceeded as planned up to a load of 40 kips. At this load the floorbeam had started to buckle laterally between load points as well as to pull away from the timber stringers. As the load reached 45 kips the floorbeam continued to buckle laterally and pull away from the stringers. The load was then increased to 50 kips, at which point the lateral deflection due to buckling was approximately 1 in. beyond the initial crookedness of the floorbeam at its centerline. The observation was made that a vertical channel, which was part of the connection to the floorbeam, shown in Fig. 4, on the downstream end of the floorbeam was resting against one of the hangers. Readings were taken on the deflection dials and strain gages before the load was removed. The vertical channel was cut, and the floorbeam was reloaded to 49 kips. At this load there was excessive lateral displacement of the top flange of the floorbeam as shown in Fig. 48. Termination of the test occurred when the floorbeam was unable to sustain any increase in load.

Wedges (Fig. 49) were inserted between floorbeam 5 and the timber stringers to assure deck continuity for the floorbeam 4 test. The purpose was to provide, in effect, a new floorbeam at L_5 so as not to affect the test of floorbeam 4.

The test of floorbeam 4 proceeded without any lateral distortion or excessive end distress up to a load of 50 kips. The observation was made at this load that the plate connecting the floorbeam to the truss was bent considerably. Loading continued up to 65 kips. After

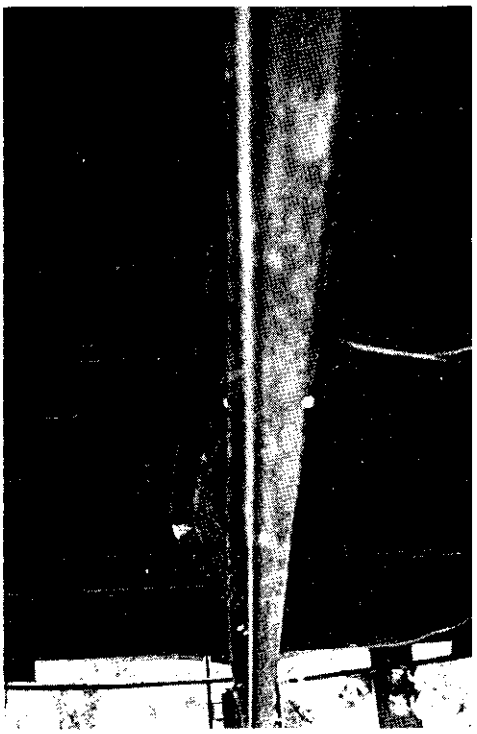

Fig. 48. Photograph of buckling of compression flange of floorbeam 5.

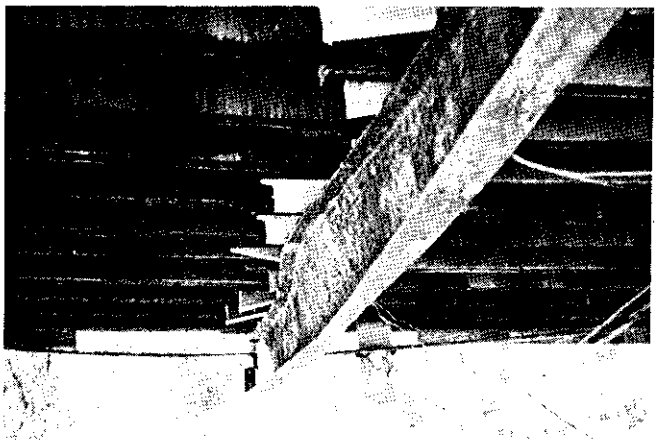

Fig. 49. Photograph of wedges inserted to assure deck continuity.

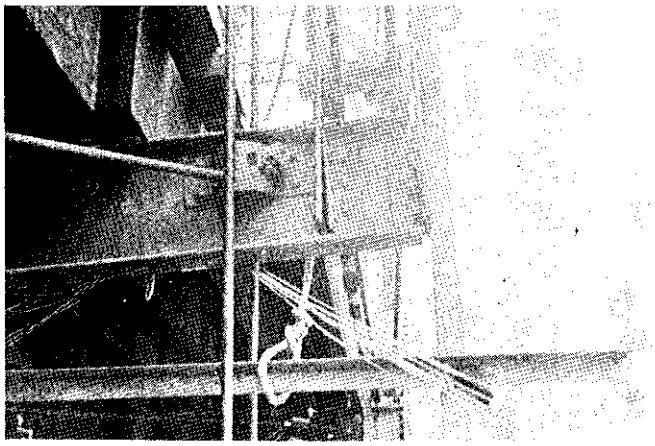

Fig. 50. Photograph showing where first three bolts broke.

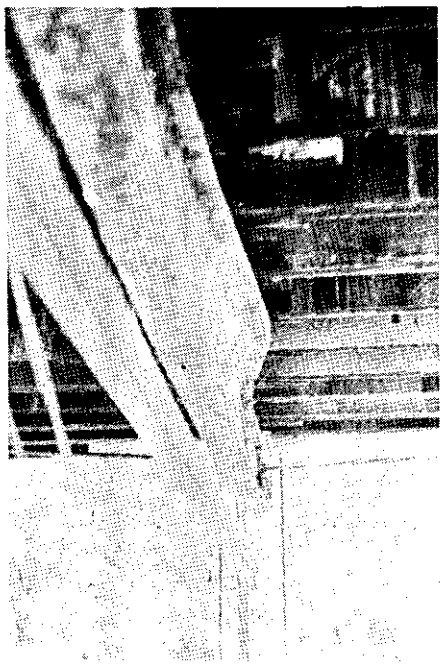

Fig. 51. Photograph of lateral buckling of floorbeam 4.

reaching this load, three bolts broke on the upstream end connection of the floorbeam to the truss, and the load dropped to 61 kips. These bolts were located on one side of the interior part of the connection of the floorbeam to the verticals (Fig. 50). At this time the floorbeam was approximately 3/8 in. out of line at its centerline. The floorbeam had buckled laterally (Fig. 51) only between the load points, indicating that the load points provided lateral bracing. The floorbeam was reloaded to 66 kips, when four bolts broke on the upstream connection of the floorbeam to the truss, causing the load to drop to 54 kips. These bolts were located on the other side of the interior part of the connection of the floorbeam to the verticals (Fig. 52). An attempt was made to increase the load, but it could only be increased to 55 kips due to extensive lateral buckling of the beam, thus terminating the test.

Fig. 52. Photograph showing where last four bolts broke.

CHAPTER 4. TEST RESULTS AND ANALYSIS

In Chapter 3, the details of the test program and the actual events which occurred during each test were indicated. In subsequent paragraphs in this chapter, the results of each test will be summarized and an analysis of their significance presented. Each test will be discussed separately.

Timber Deck Test

The ultimate load and equivalent H truck for each of the tests are shown in Table 3. The equivalent H truck for the deck tests was determined by placing the rear axle of the truck at mid-span of the panel. The total ultimate load for deck test 1 (load centered on

Table 3. Ultimate loads

Test	Ult. load (kips)	Equiv. H truck[a]
Timber deck		
Centered load	101.5	H 42
Edge load	77.4	H 32
Truss		
General loading	140	H 70[b]
Initial failure	133	—
Maximum load at L_4	78.5	—
Floorbeam		
At L_4	66.0	H 40
At L_5	50.0	H 30

[a]Standard AASHO H truck providing same total static moment as provided by ultimate load.

[b]H 66.5 at initial fracture of L_5M_5.

roadway) was 101.5 kips, and for deck test 2 (load placed eccentrically) it was 77.4 kips. For deck test 1 this is equivalent to a load of 25.4 kips at each of the load points, with the corresponding maximum moment on the total deck panel at 279.4 ft-kips or 17.5 ft-kips per foot of width of the deck panel. For deck test 2 the equivalent load and moments are 19.4 kips, 212.8 ft-kips, and 13.3 ft-kips per foot of width, respectively. Although the loads were applied transversely at 6-foot centers (wheel track spacing), there were two equal loads spaced longitudinally at the third-points. However, these loads can be related to other behavior by determining the equivalent AASHO truck. For deck test 1 (centered load) failure occurred at an equivalent H 42 truck and for test 2 (eccentric load) at an H 32 truck.

The primary behavioral indicator for the deck tests was the deflection readings taken across the width of the panel at mid-span of the panel. The load-deflection curves of the two deck tests at various points transversely across the section are shown in Figs. 53 and 54. These curves, along with the ultimate load data, indicate the behavior of the deck throughout the test to failure.

The behavior of deck test 1 was typical of that expected. The load-deflection curves for that test (Fig. 53) indicate that the behavior of the deck up to a total load of 60 kips (H 25 truck) was linear. Beyond 60 kips the influence of stringers breaking can easily be seen in Fig. 53. Figure 53c indicates that a nonlinear increase in deflection occurred between 60 and 65 kips of load at the deflection dial located at approximately the one-third point of the roadway (near one of the load points). This increase in deflection

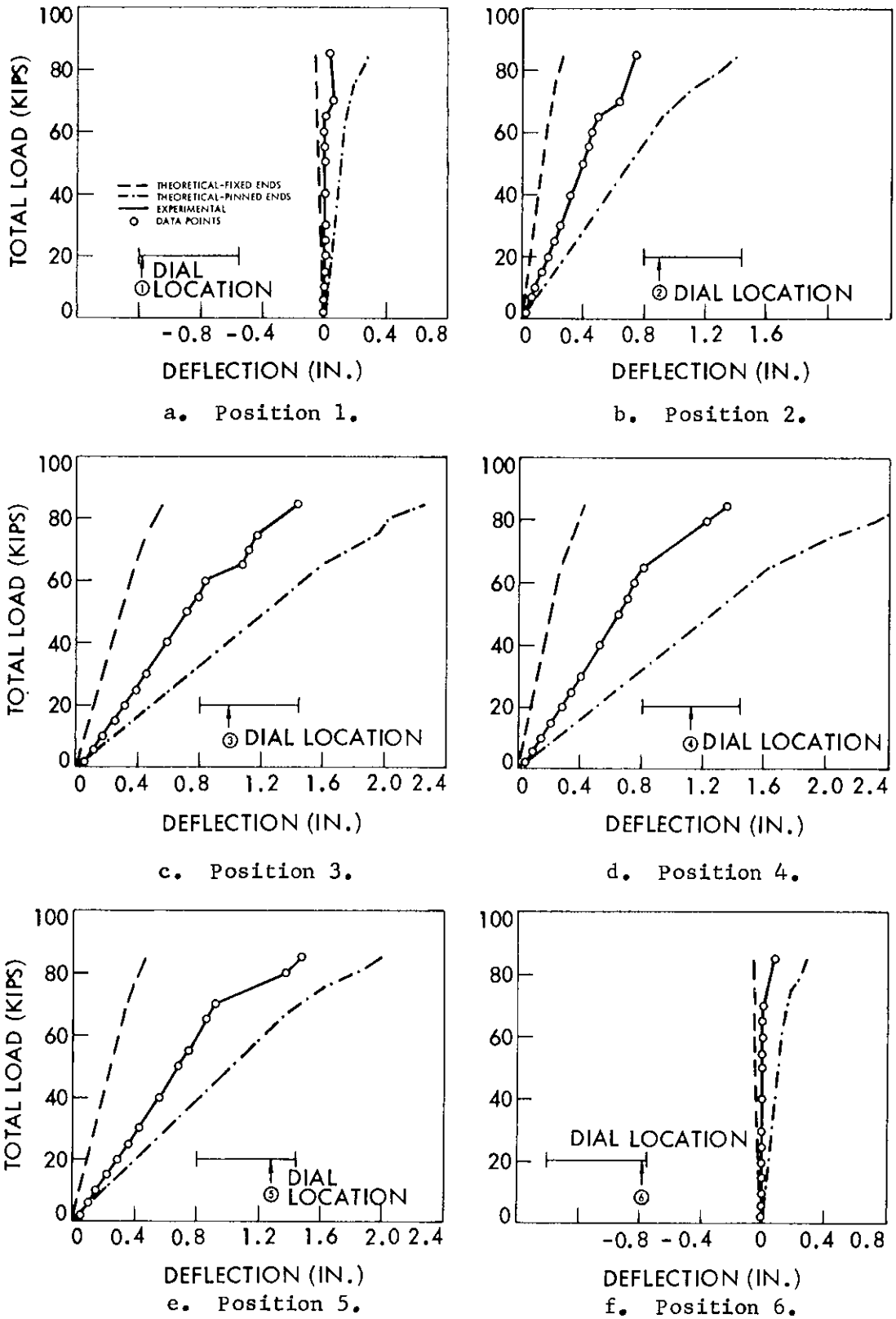

Fig. 53. Load-deflection for deck test 1.

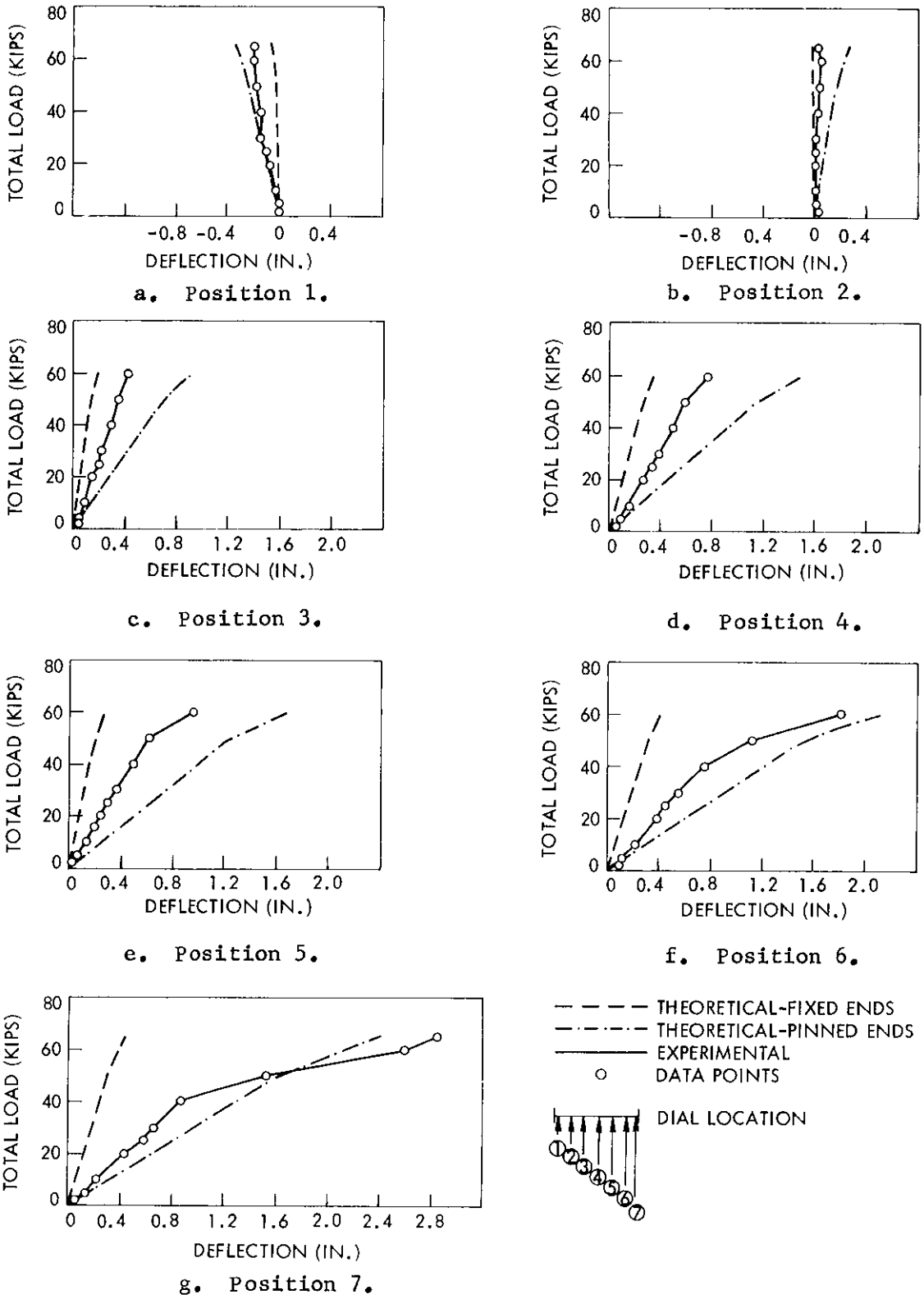

Fig. 54. Load-deflection for deck test 2.

can be attributed to the failure of stringer 5 which was approximately 5 feet from the upstream edge of the deck. The same behavior occurs in Figs. 53a and 53b between 65 and 70 kips of load. The increase in deflection at these points also can be attributed to the failure of the same stringer.

A similar behavior can be seen in Figs. 53d and 53e between 65 and 80 kips of load. This behavior is due to the failure at 75 kips of stringer 11 which was about 5 feet from the downstream edge of the deck. The decrease in deflection in Fig. 53a and the increase in deflection in Fig. 53f between 70 and 85 kips can be attributed to the increase in deflection at the center and downstream side of the panel. This increase in deflection at the center and downstream side of the panel is caused by the failure of several stringers in this area. The increase in deflection in this area results in an uplift near the edge of the deck on the upstream side and an increase in deflection near the edge of the deck on the downstream side.

Another indication of behavior can be seen in Fig. 53b between 70 and 85 kips, in Fig. 53c between 65 and 75 kips and in Fig. 53e between 80 and 85 kips. In these instances the slope of the load-deflection curve increases, indicating that the unfailed portions of the deck are carrying a greater portion of the total load than they had previously carried. These unfailed portions of the deck must carry more load because the failed portions of the deck are unable to sustain the additional load.

The deflection readings in Fig. 53 can be combined to form a deflection cross section at various load levels (Fig. 55). This figure

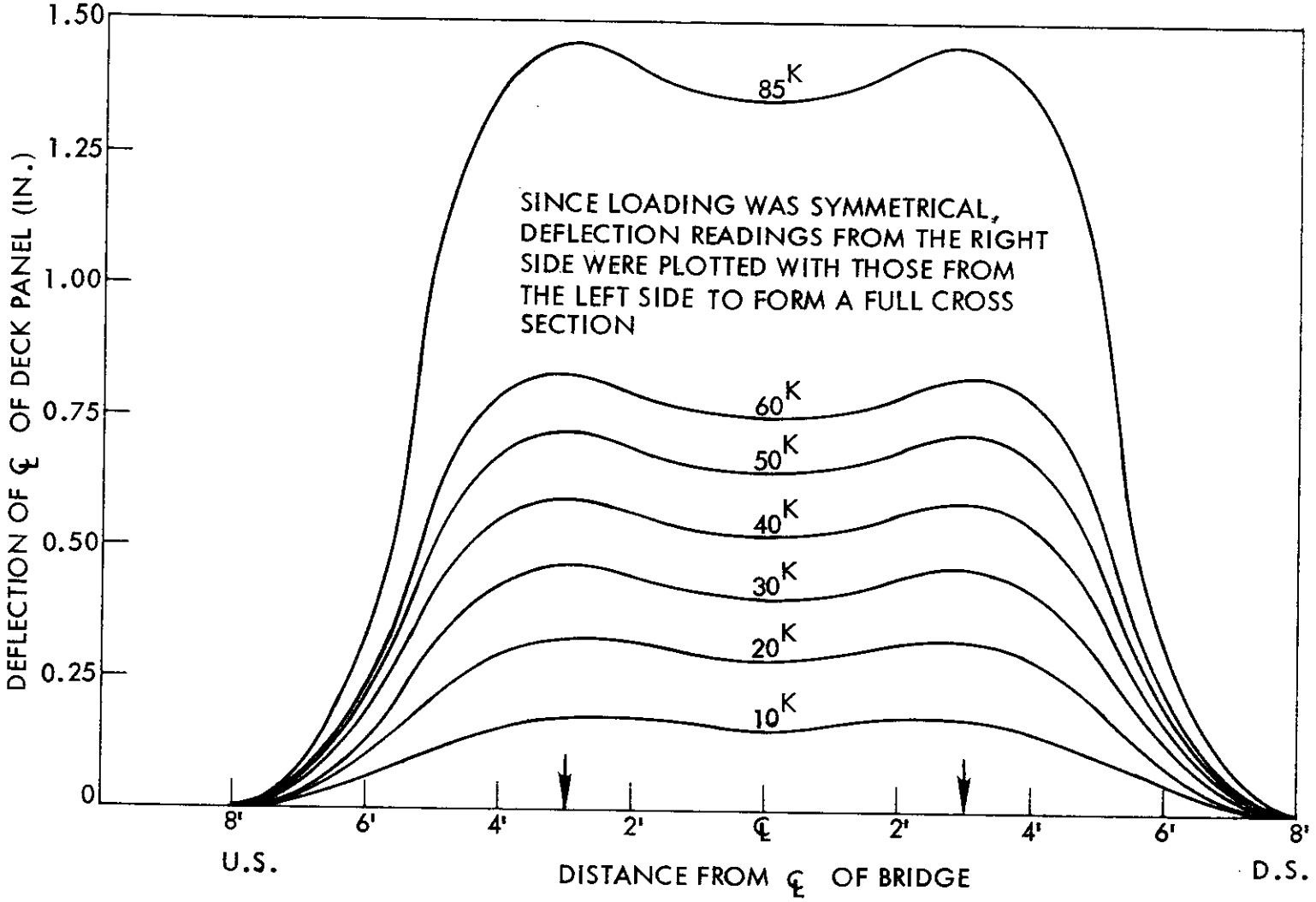

Fig. 55. Deflection cross section at mid-span of deck panel for deck test 1 at various loads.

gives an indication of the distribution of the load to each of the stringers. From these deflections, the amount of load distributed to each of the stringers can be calculated. The figure shows that the greatest part of the load is being carried by the stringers around and between the load points. It also indicates that the deflection increases linearly until the first stringer fails.

The percentage of the total load carried by the most heavily loaded stringer can then be compared to the distribution as determined from the AASHO Specifications[2]. The AASHO distribution is given as S/4 wheels in Article 1.3.1, where S is the average stringer spacing in feet. For deck test 1 the percentage of the total load distributed to the most heavily loaded stringer is, according to the Specifications, 14%.

Table 4 shows the experimental percentage of the load distributed to the most heavily loaded stringer and the equivalent distribution factor at loads below the load which caused the first stringer to fail. The load distribution characteristics remain the same in this case (up to stringer cracking).

Table 4 shows that the experimental percentages of the load distributed to the most heavily loaded stringers are less than predicted from the AASHO Specifications. Although this loading represents the usual load case (centered loading), eccentric loading (truck near roadway edge) case is more critical and will result in the edge stringers receiving more load. The centered load case (deck test 1) would be conservative because the Specifications cover the most critical case.

Table 4. Experimental percentage of the load distributed to the most heavily loaded stringer and the equivalent distribution factor for deck test 1

Load (kips)	Percentage of the load distributed to the most heavily loaded stringer	Equivalent distribution factor[a]
10	10.5	5.33
20	10.2	5.49
30	10.4	5.38
40	10.2	5.49
50	10.2	5.49
60	10.1	5.54

[a]AASHO = 4 from S/4 (Article 1.3.1)[(2)].

The theoretical capacity of the deck for deck test 1 was determined, using data from tests of stringers removed from the bridge, to be 104.7 kips. Thus the actual capacity of the deck (101.5 kips) is very close to the theoretical capacity.

Figure 13 shows the order in which the stringers failed for each of the two deck tests. The first two stringers to fail in deck test 1 were near the applied loads. The third through seventh stringers to fail were mainly under the influence of the loads on the right side of the panel. This behavior indicates either that more of the load was applied to the right side of the panel than to the left side of the panel or that the right side of the panel was not as strong as the left side of the panel. The last three stringers to fail were under the influence of the loads on the left side of the panel.

The behavior of deck test 2 was also typical of that expected. The load-deflection curves for that test (Fig. 54) indicate that the behavior of the deck was linear up to a total load of 40 kips (H 17 truck). The behavior of the deck shown by Figs. 54a and 54b is not really indicative of behavior of the entire deck because these two deflection dials were near the edge of the panel opposite the loading. This portion of the deck underwent only uplift and very small deflections.

At loads greater than 40 kips the influence of high stress levels in the stringers and the failure of stringers can be seen in Figs. 54d-54g. Figures 54f and 54g indicate that a nonlinear increase in deflection occurred between 40 and 50 kips of load at these two deflection dial locations near the edge of the deck. This nonlinear increase in deflection was caused by the high stress levels in this portion of the deck. Figures 54d-54g indicate a similar behavior between 50 and 60 kips of load at these deflection dial locations. This increase in deflection can be attributed to the failure of stringers 13 and 15. A different type of behavior is shown in Fig. 54g between the loads of 60 and 65 kips. The slope of the load-deflection curve increases, indicating that other portions of the deck are taking a greater portion of the load than they had previously taken.

The deflection readings in Fig. 54 are combined in the same manner as Fig. 53 to form a deflection cross section at various loads (Fig. 56). Figure 56 gives an indication of the distribution of the load to each of the stringers. This figure also indicates that the major portion of the load is being carried by the stringers on the loaded side of the

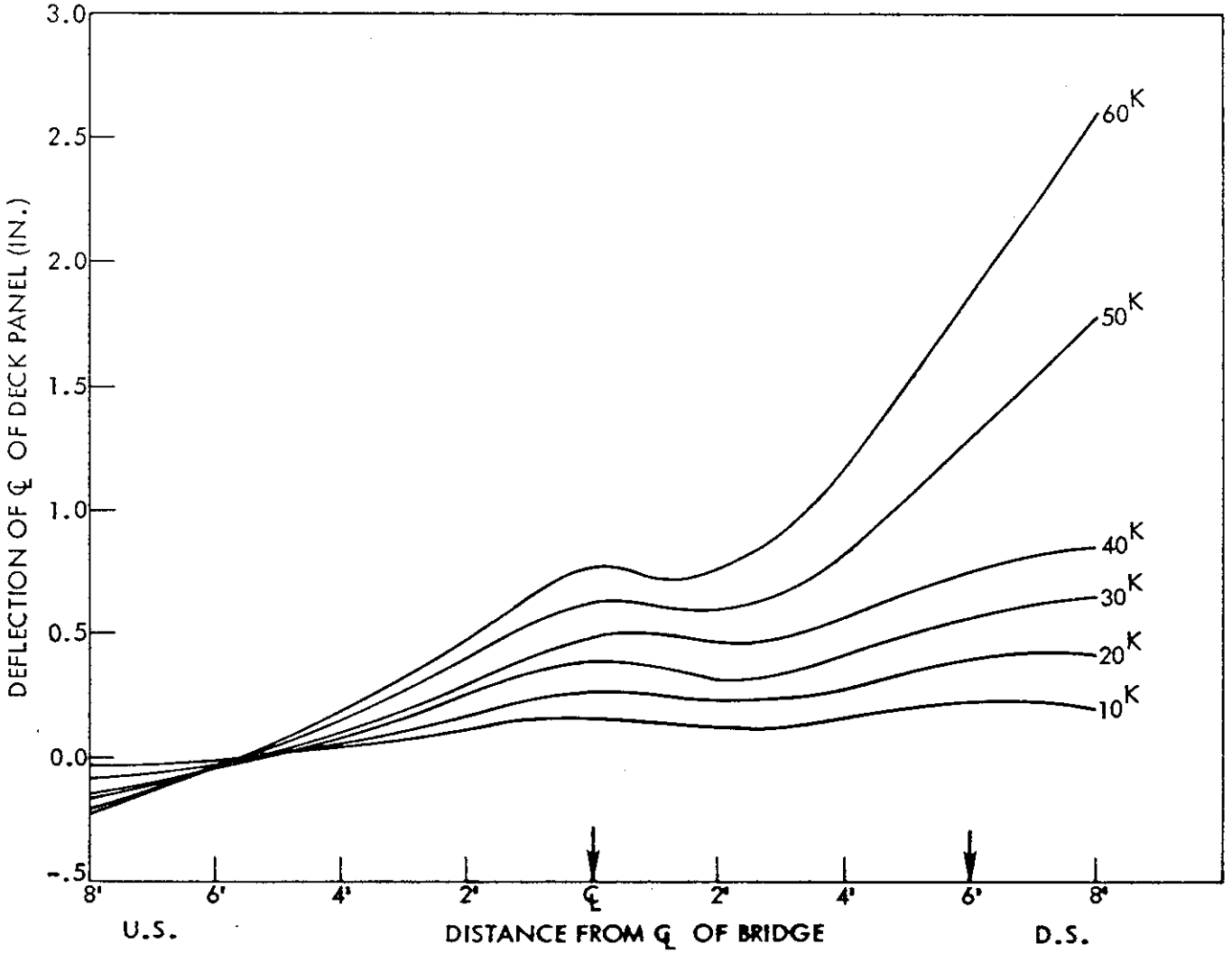

Fig. 56. Deflection cross section at mid-span of deck panel for deck test 2 at various loads.

panel and that the deflection increases linearly up to a total load of 40 kips.

As in deck test 1 the percentage of the total load carried by the most heavily loaded stringer can be compared to the distribution as determined by the Specifications[2]. For deck test 2 the percentage of the total load distributed to the most heavily loaded stringer is about 15% at the equivalent of an H 15 truck. Table 5 shows the experimental percentage of the load distributed to the most heavily loaded stringer and the equivalent distribution factor at loads below the load which caused the first stringer to fail.

Table 5. Experimental percentage of the load distributed to the most heavily loaded stringer and the equivalent distribution factor for deck test 2

Load (kips)	Percentage of the load distributed to the most heavily loaded stringer	Equivalent distribution factor[a]
10	13.7	4.00
20	14.9	3.69
30	15.8	3.48
40	15.2	3.62

[a]AASHO = 4 from S/4 (Article 1.3.1)[2].

Table 5 indicates that the experimental percentages of the load distributed to the most heavily loaded stringer are equal to or slightly greater than those predicted by the AASHO Specifications[2] (13.7%). The critical stringer (at edge) carried a higher percentage

of the load for this more severe eccentric case than in the centered case (test 1).

Table 5 also indicates that the distribution did change slightly as the load increased. This could be attributed to a very high moment gradient in the weaker transverse planking, which is the major distributing agent.

The theoretical capacity of the deck for deck test 2 was determined to be 78.5 kips. This is extremely close to the actual capacity of the deck (77.4 kips).

The results from both deck tests indicate a high degree of validity for both the distribution procedure indicated by AASHO[2] and the calculations for deck capacity. However, the timber deck used in the bridge consisted of heavy transverse planks to assist in the distribution of load. Distribution characteristics could vary significantly for other deck types. Although there is a good comparison in this case, the need exists for the consideration of various deck configurations in distribution determination.

The first four stringers to fail in deck test 2 were located near the load that was applied toward the edge of the panel. These stringers failed first because there were fewer stringers available to take the load that was applied toward the edge of the panel. The next two stringers to fail were under the load applied near the center of the panel. The final stringer to fail was located midway between the loads. This stringer failed as a result of the unfailed stringers trying to carry the load that had been carried by the previously failed stringers.

Theoretical deflections of the timber deck were obtained by modeling the timber deck as a beam on an elastic foundation. The beam was composed of the eight timber members that make up the crossbeams (on top of the stringers) in each panel of timber deck. The elastic foundation was composed of the 15 stringers and 16 floor planks in each panel of deck. A stringer would be eliminated from the foundation stiffness if it became incapable of taking further load during the course of a test. The loss in stiffness was distributed along the entire length of the beam. The stiffness of the elastic foundation was computed based on the fact that the stringers and floor planks had either the condition of simple or fixed supports. These conditions generated two theoretical curves. The actual support conditions for the stringers and floor planks lie somewhere between simple and fixed supports. Therefore, the two theoretical curves will give only extremes within which the actual deflections should fall. The solution for the deflection based on foundation stiffness, loading, and load placement is based on the method presented by Hetenyi[15].

Figures 53 and 54 show that the experimental deflection does, in most cases, fall about midway between the theoretical deflections based on simple and fixed ends. Deck test 1, in which the loads were applied symmetrically, exemplifies this behavior. In deck test 2 the loads were applied to one side of the panel causing a departure from this behavior. This behavior can be seen most clearly in Figs. 54f and 54g. The main reason for this behavior is the fact that when a stringer was unable to continue carrying load the foundation stiffness contributed by that stringer was eliminated. The method in which the loss of stiffness was

distributed allowed the side of the panel of deck on which the stringers had failed to have a greater stiffness than actually existed. Therefore, the theoretical deflection was less than the experimental deflection. Thus for the case of eccentric loading the more conservative simple support condition should be used in theoretical deflection calculations.

The final failure configuration of deck test 1 indicates that all of the failed stringers were interior stringers. Ten of the original 15 stringers were failed. The five remaining stringers appeared to be in excellent condition.

The failure of deck test 2 indicates that all of the failed stringers were on the loaded side of the panel. The failed stringers were clustered around the load points. Seven of the original 15 stringers were failed. The remaining unfailed stringers appeared to be in excellent condition.

Truss Test

The initial failure of the truss took place at a load of 133 kips. This failure was the breaking of one of the hangers which made up member L_5M_5. The applied loading was 106 kips and 27 kips at L_5 and L_4, respectively. Additional load was applied in an attempt to get additional members to fail. A large distortion of the lower chord of the truss near the load at L_5 occurred under this higher loading without any additional failure. The maximum load under this general loading

was 140 kips (112 kips at L_5 and 28 kips at L_4). The maximum vertical deflection at L_5 at this time was 15 in.

After adjustment of the loading system, all load was applied at L_4 with the maximum load being 78.5 kips. The test program then included damaging a member. After member L_2U_2 was cut completely through, a load of 39 kips produced a failure of the truss. This resulted in a vertical displacement of the member at the cut location.

The behavioral indicators for the truss test were the deflection readings at mid-span and at the three-tenths points and the forces in the truss members as computed from the strain gage readings taken during the test. The experimental strains were converted to stresses assuming that both the wrought iron and steel were elastic-perfectly plastic materials. The materials were assumed elastic up to the yield strain computed from appropriate values of yield stress and modulus of elasticity in Table 2 and assuming no increase in stress beyond the yield strain. The areas of each individual member were used to convert the stresses to forces in the individual members. Figure 57, the theoretical and experimental load-deflection curves for the vertical deflection at mid-span, indicates that yielding began to occur in member L_5M_5 at a total load of approximately 80 kips. The curve was relatively linear at loads less than 80 kips and above 80 kips the slope of the curve decreases indicating yielding of member L_5M_5. The small nonlinearities at loads below 80 kips are indicative of the effect that rusting of the members and pins and the distorted shape of some members had on the behavior of the truss. Figure 58, the theoretical and experimental load-deflection curves for the vertical deflection at

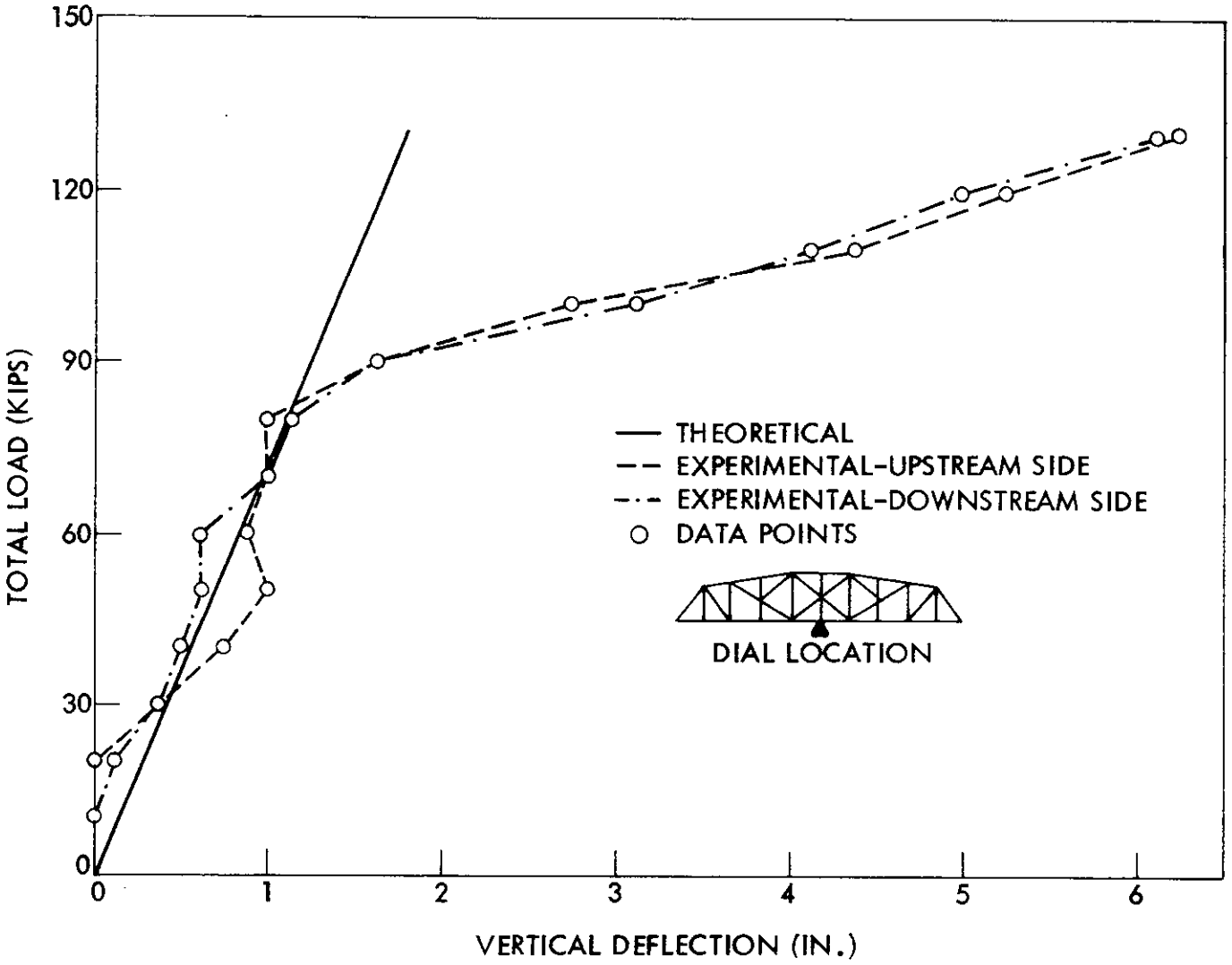

Fig. 57. Total load-vertical deflection at L_5 for truss test.

L_3 and L_7. Figure 58 shows that both of the three-tenths points had fairly linear behavior. Although there is some agreement between the two sides of the truss, the small magnitude of the deflections and the apparent effect of the rusted condition of the truss make it difficult to determine if this agreement is valid. The horizontal deflections of the truss were negligible.

Figure 59, the total load-force in truss member L_5M_5 curve, indicates, for this truss, approximately the same behavior as the total load-vertical deflection curve at L_5 (Fig. 57). Figures 60-70, curves for other total load-force in truss member, indicate linear behavior up to the maximum load at which readings were taken.

The theoretical forces used in Figs. 59-70 were obtained from a structural analysis of the truss assuming that all of the members were held together by pins at the joints. Most of the experimental forces determined from strain gage readings agree quite closely with the theoretical forces determined from analysis. Some of the experimental data for the vertical members is quite erratic, as can be seen in Figs. 59, 62, and 63. Other experimental data differs considerably in magnitude from the theoretical curve, but the slope of the curve is very similar to that of the theoretical curve. This trend can be seen in Figs. 64, 67, and 68 and occurs in lower chord tension members only. This behavior is due to the lack of rotational capability ("frozen" condition) of the member resulting from the rusted members and pins. Data for members L_1L_2, L_3M_3, L_4U_4, L_4M_5, L_4L_5 and L_6U_6 is not shown because of an electrical malfunction in the strain gage indicator monitoring the gages on these members. The remaining experimental

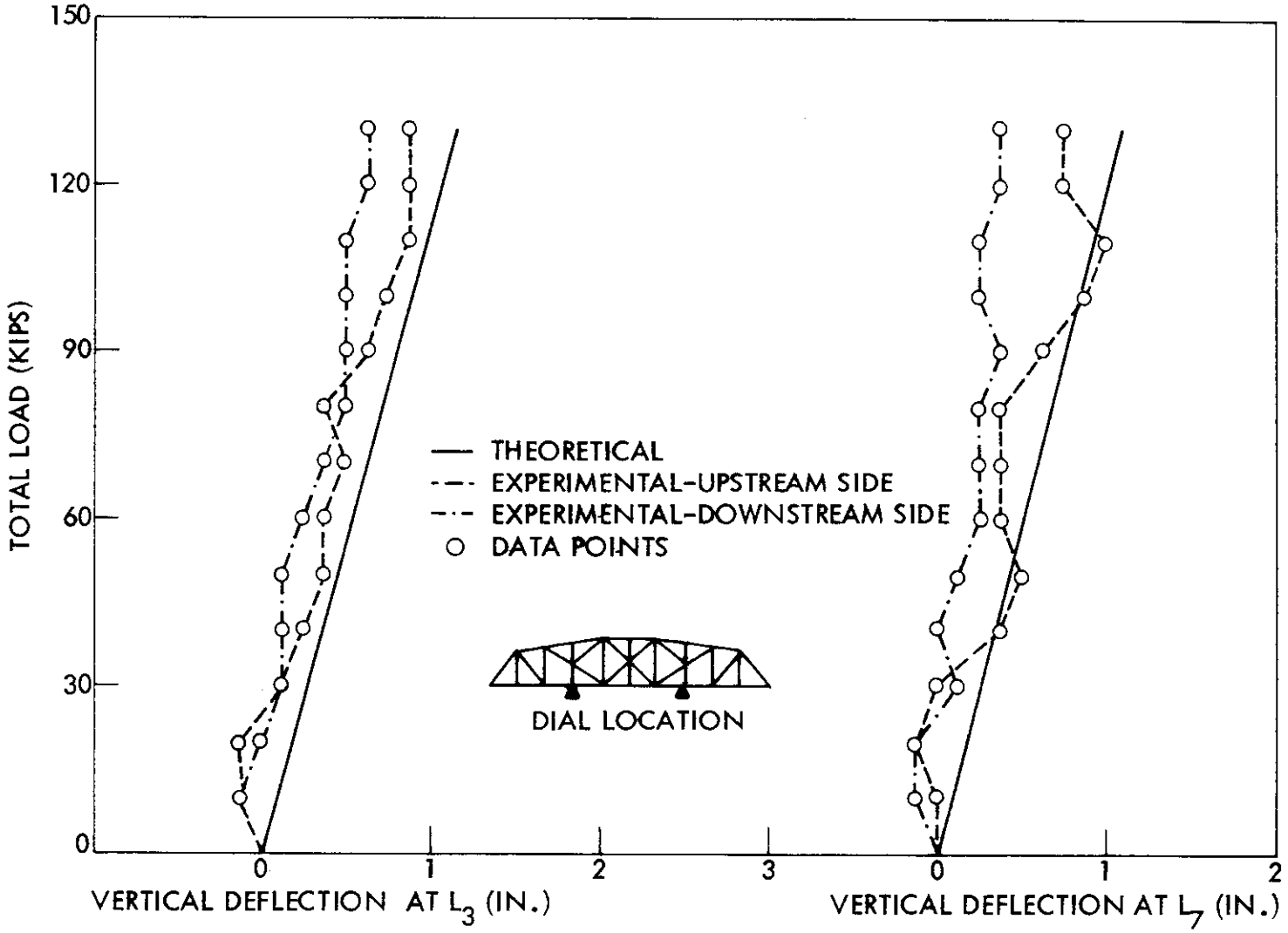

Fig. 58. Total load-vertical deflection at L_3 and L_7 for truss test.

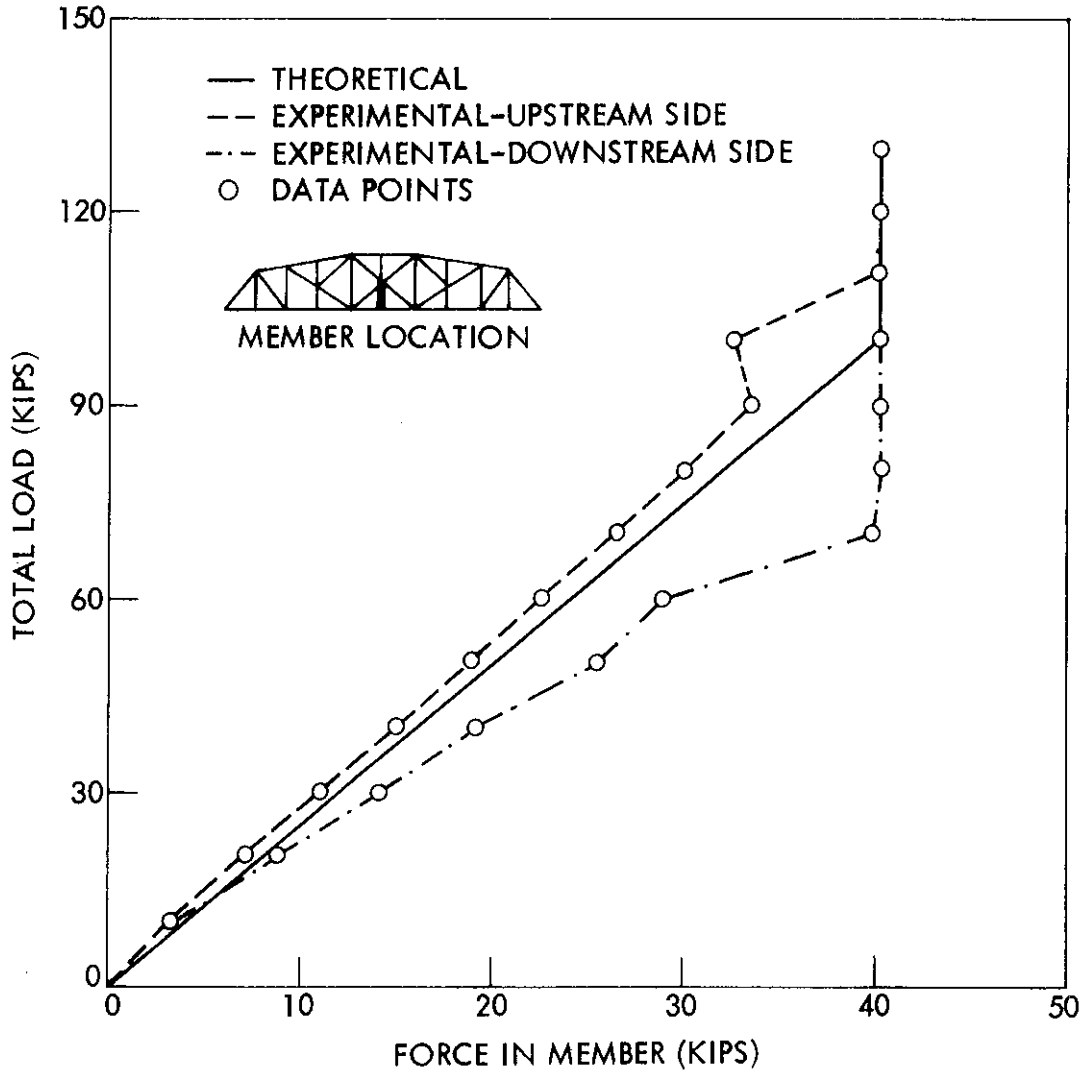

Fig. 59. Total load-force in member L_5M_5.

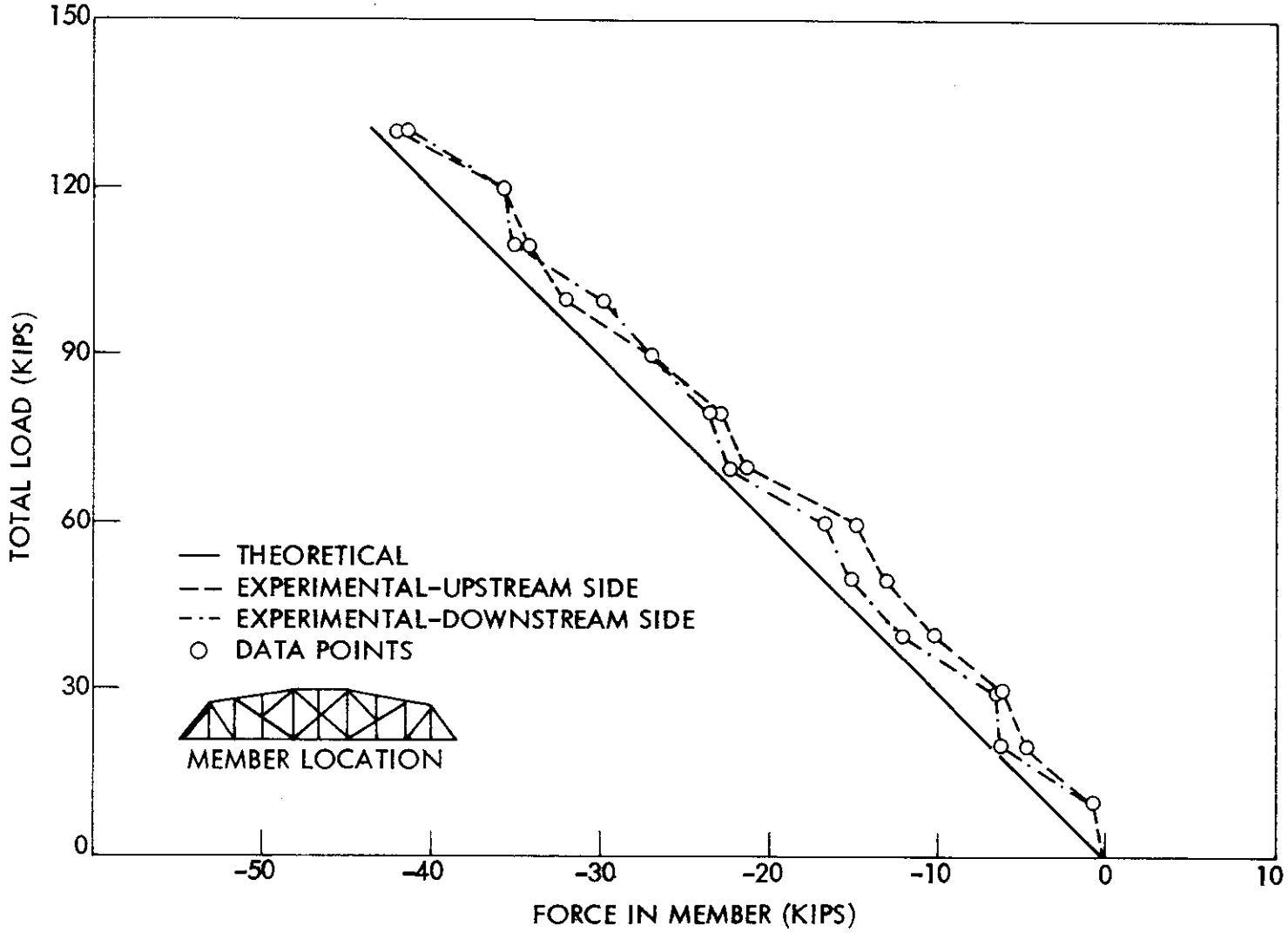

Fig. 60. Total load-force in member L_0U_1 (upper gages).

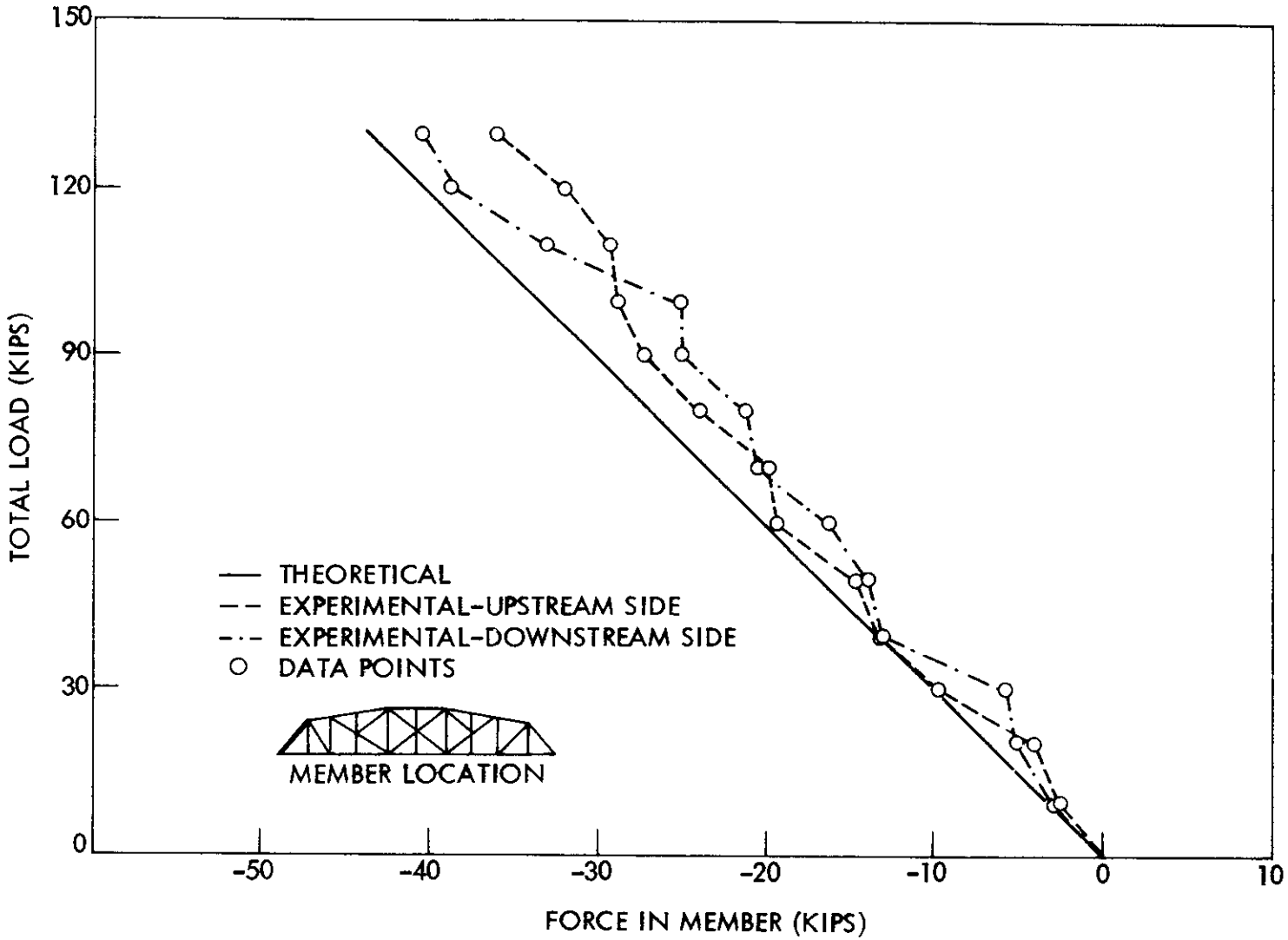

Fig. 61. Total load-force in member L_0U_1 (lower gages).

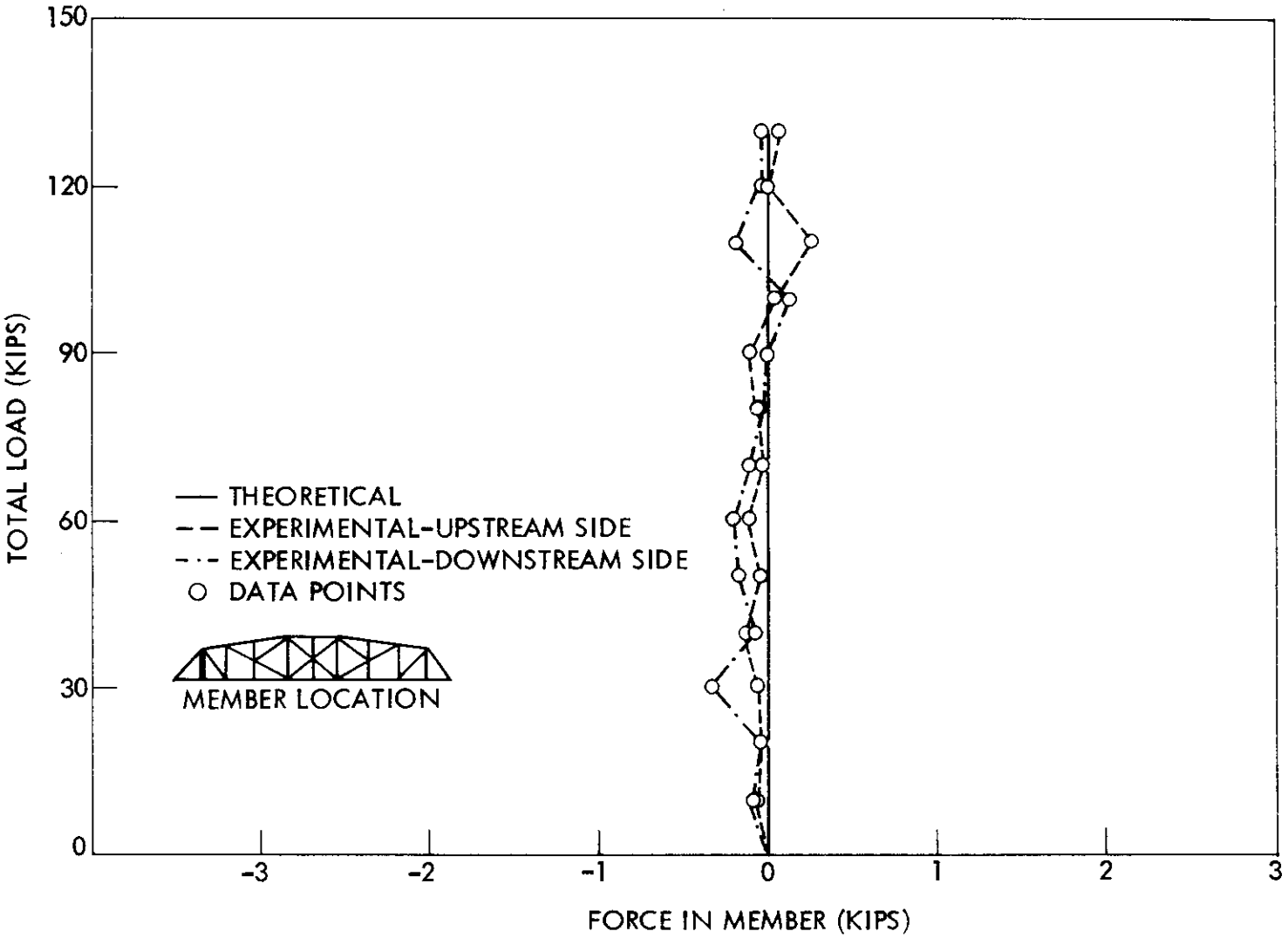

Fig. 62. Total load-force in member L_1U_1.

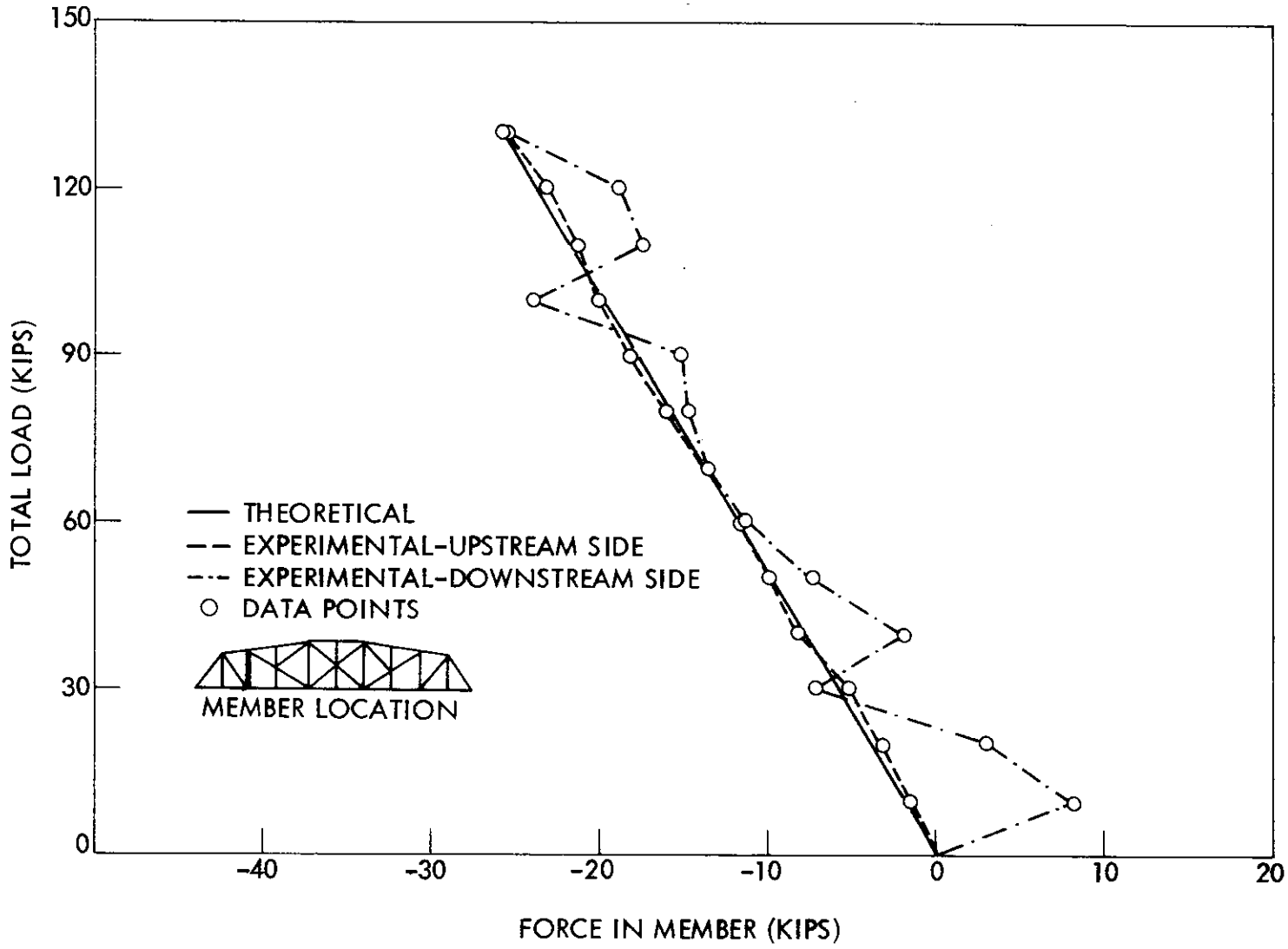

Fig. 63. Total load-force in member L_2U_2.

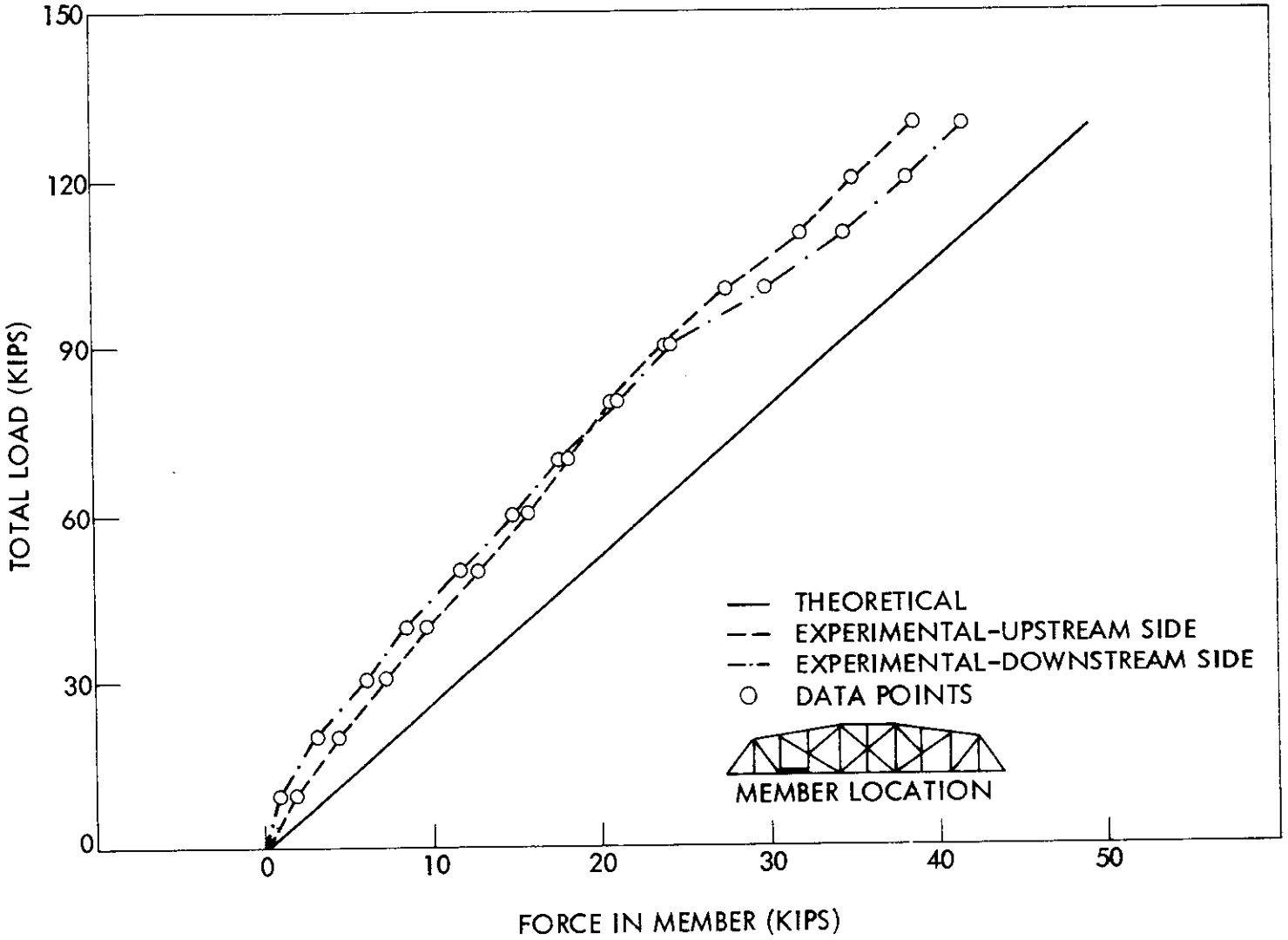

Fig. 64. Total load-force in member L_2L_3.

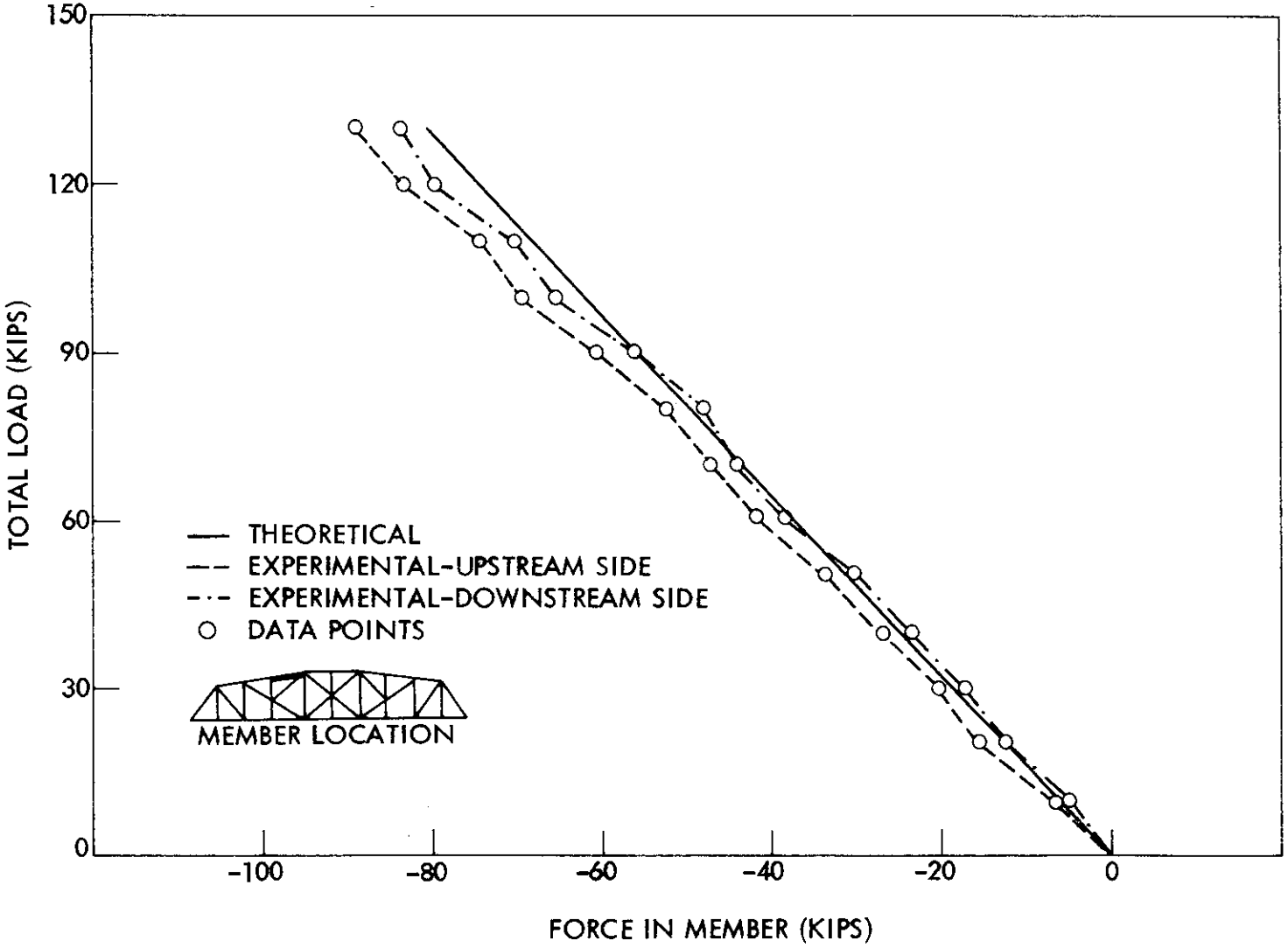

Fig. 65. Total load-force in member U_3U_4.

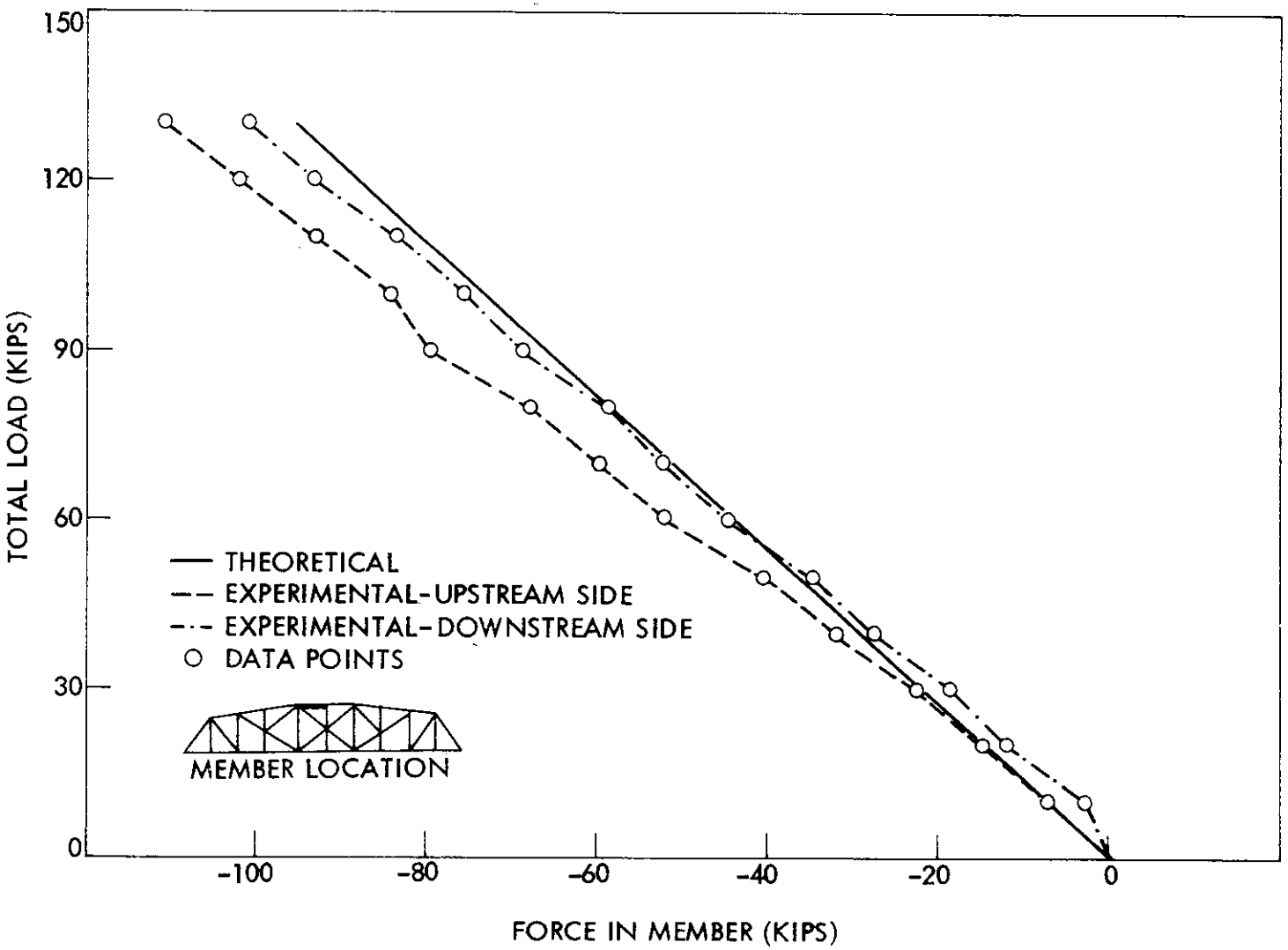

Fig. 66. Total load-force in member U_4U_5.

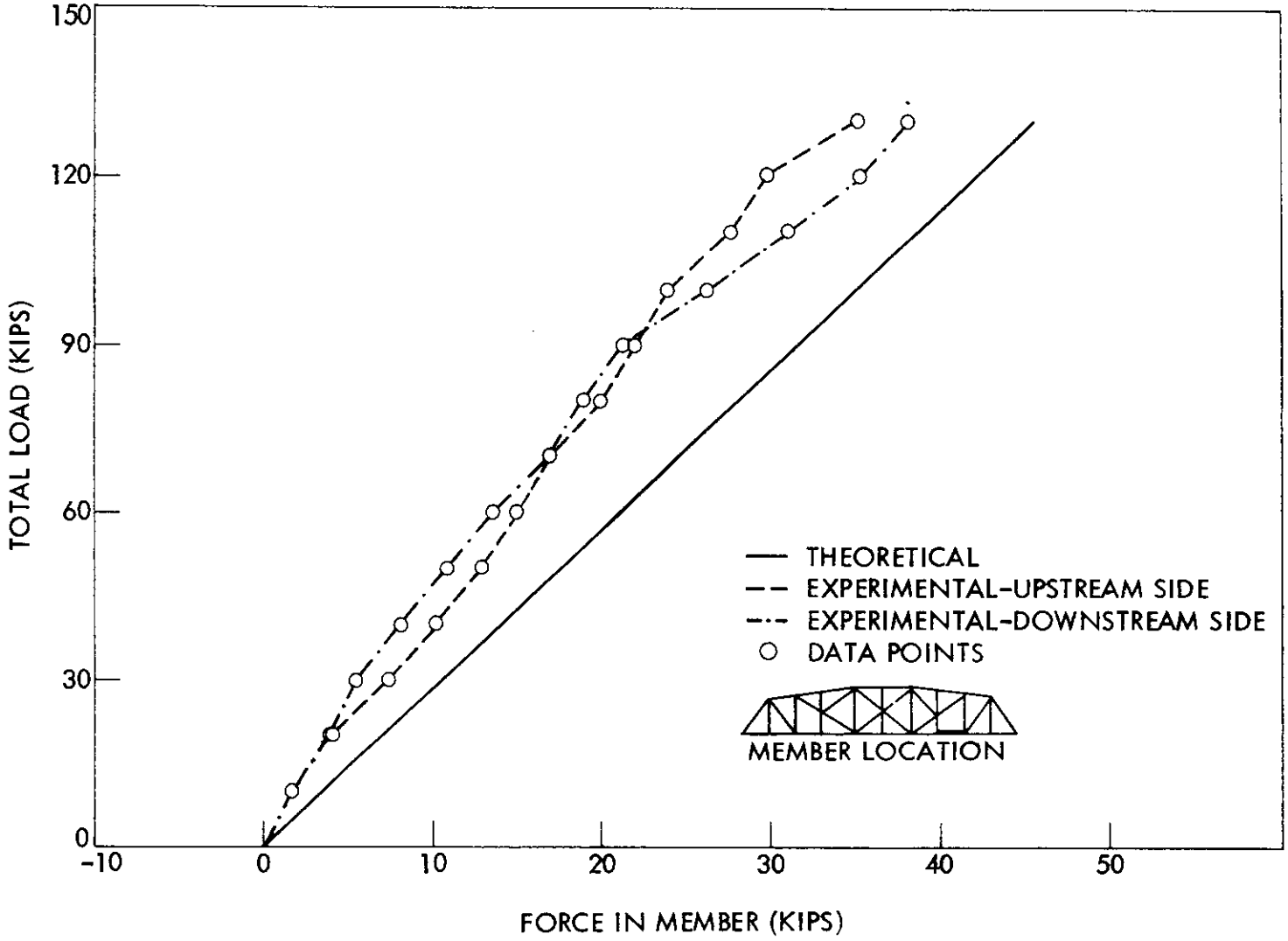

Fig. 67. Total load-force in member L_7L_8.

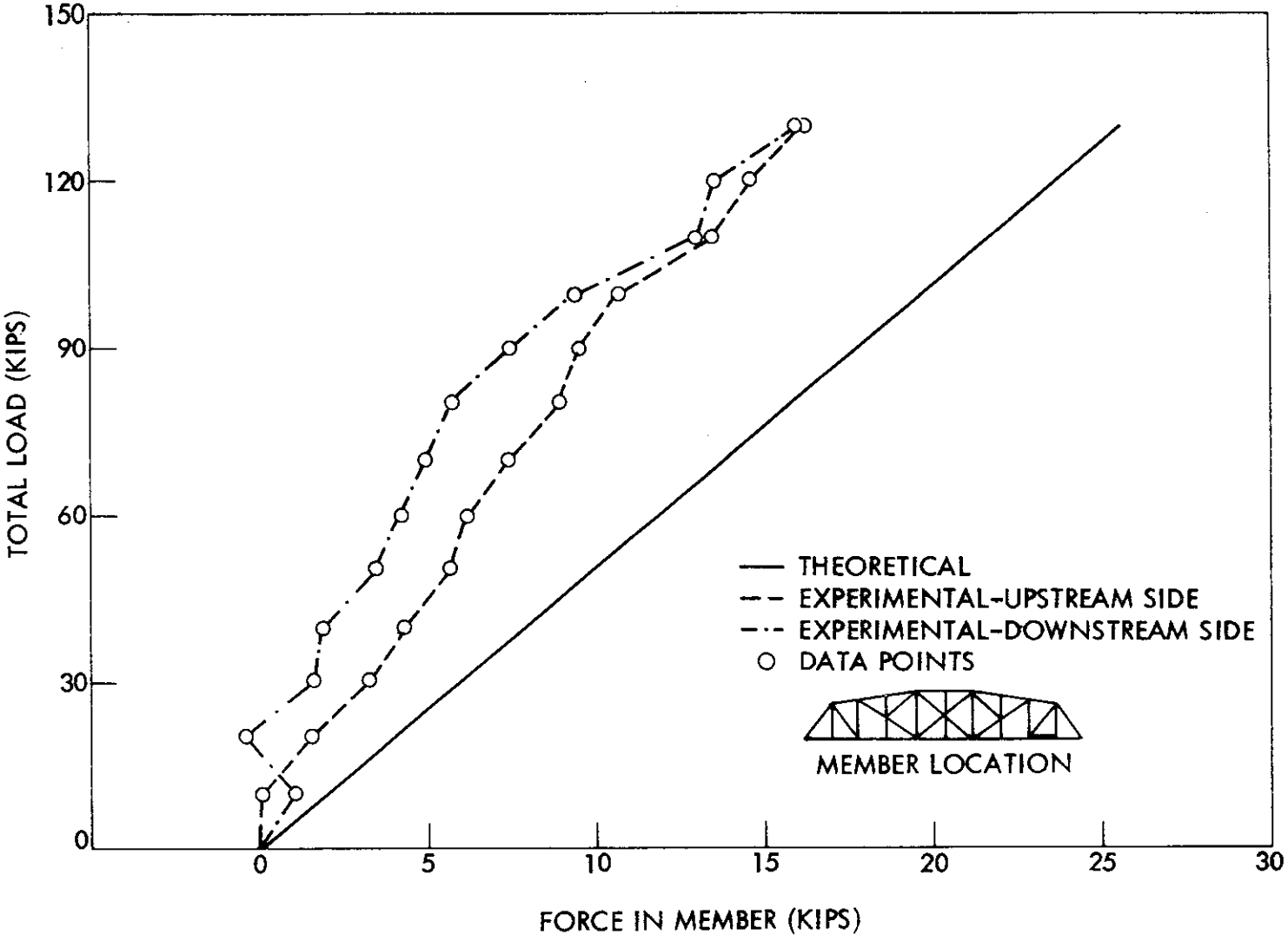

Fig. 68. Total load-force in member L_8L_9.

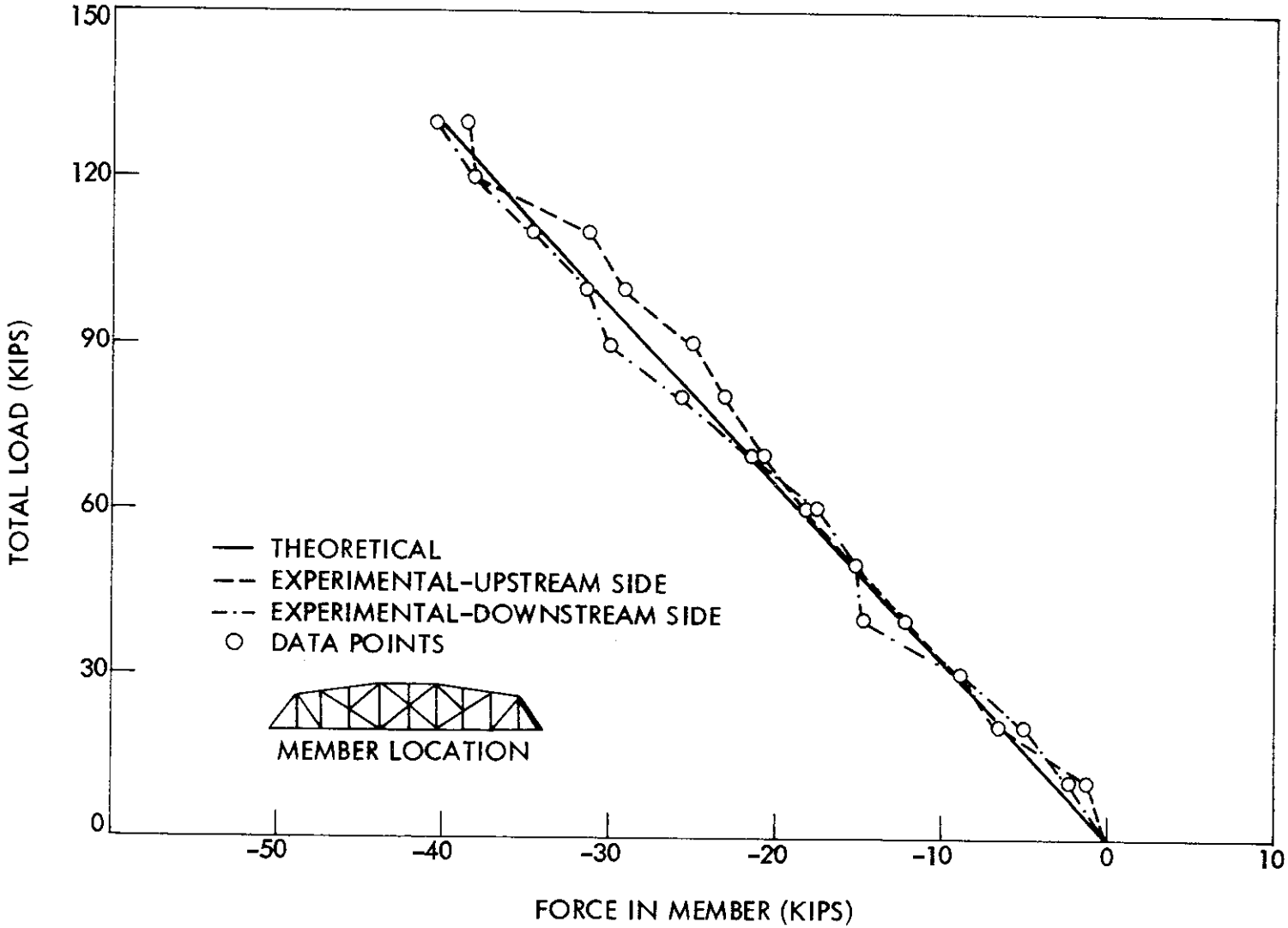

Fig. 69. Total load-force in member $L_{10}U_9$ (upper gages).

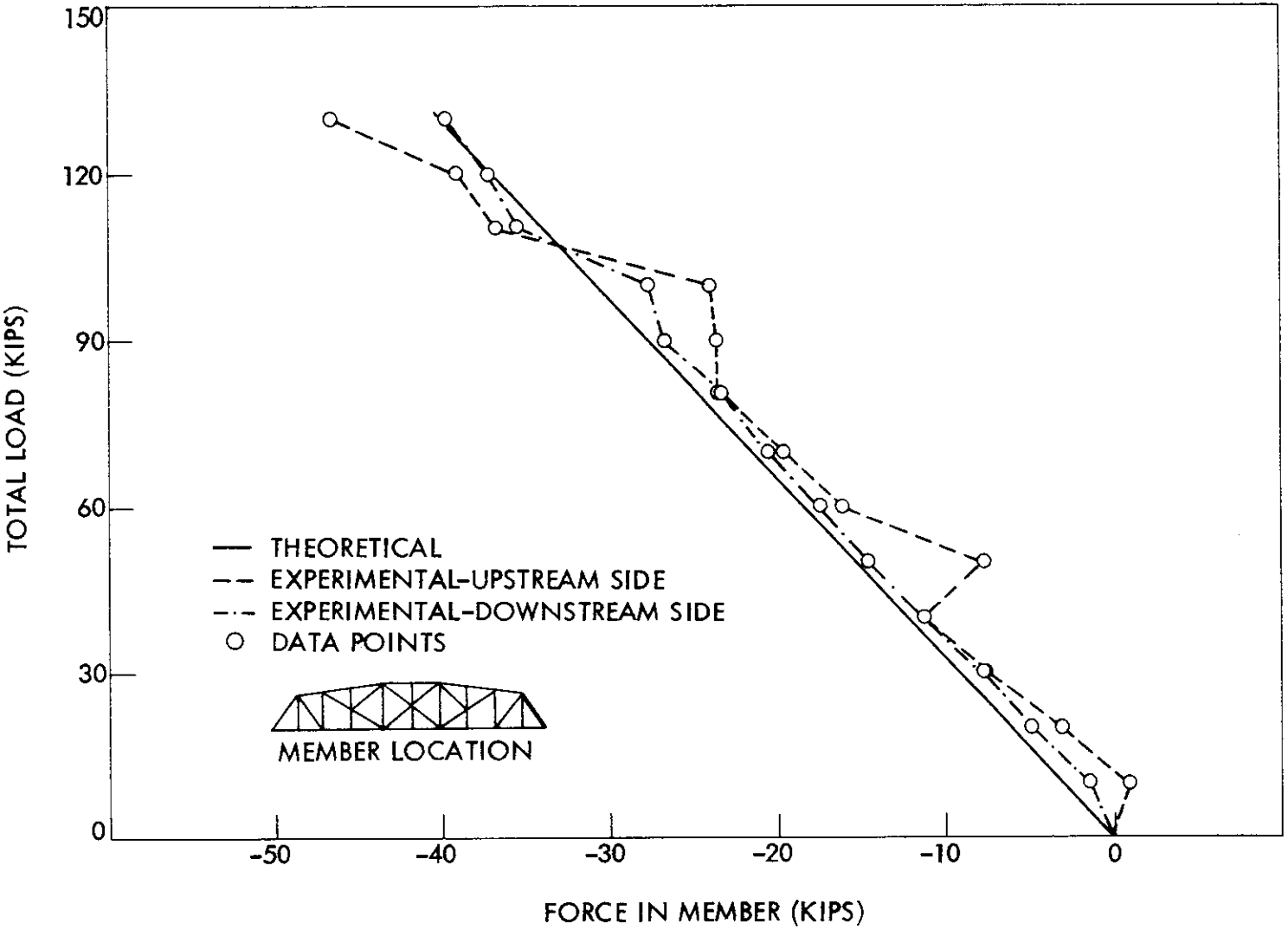

Fig. 70. Total load-force in member $L_{10}U_9$ (lower gages).

forces as indicated by Figs. 60, 61, 65, 66, 69, and 70 agree closely with the theoretical calculated forces. Good agreement was also found between the two sides of the truss.

Thus, although the actual conditions in the joints are unknown, considering the truss to be pin-connected does provide a realistic method of truss analysis for this old bridge. The tremendous flexibility of the members that allows accommodation of any joint restraint contributes to this conclusion.

The capacity of the hangers at L_5 as calculated using data from coupon tests was 110 kips. This was just a few kips greater than the load that actually caused the fracture of one of those hangers. The actual stress at fracture was 47.4 kips per square inch. This indicates that the "lap," near where the fracture occurred, was about 97% effective. An examination of the fracture (Fig. 35) indicates also that only a very small portion of the section was not fused. The current practice is to assume the "lap" only 40% effective, which is much lower than the actual capacity of the member.

The final configuration of the truss shows a noticeable sag in the lower chord of the truss between L_4 and L_6. This configuration is due mainly to the large amount yielding of the hanger, L_5M_5. Those hangers at L_5 that remained unfailed buckled out of line when the load was removed from the truss.

Floorbeam Test

The maximum load applied to the floorbeam at L_4, which was originally straight (within allowable tolerances) was 66.0 kips. The maximum load applied to the floorbeam at L_5 was only 50.0 kips, but this floorbeam had an initial crookedness of approximately 13/16 in.

The primary behavioral indicators for the floorbeam tests were the vertical deflections of the floorbeam along its length and the moments on the floorbeam as computed from strain gage data. These results are summarized in Figs. 71-74.

The load-deflection curves for the floorbeam test at L_4 are shown in Fig. 71. Both the experimental and theoretical deflections are indicated. This figure indicates that a departure from linearity occurs at a load of about 40 kips (H 24 truck). At this same load the observation was made that the floorbeam was beginning to buckle laterally. The lateral buckling of the floorbeam is indicated by the departure from linearity of the experimental load-deflection curves in this figure. This indicates that the natural dapping of the stringers provides sufficient lateral support of the floorbeam up to about 60% of the ultimate load. Beyond 60% of the ultimate load the floorbeam buckled laterally between the load points and deflected away from the stringers between the load points because there was no positive tie between the stringers and the floorbeam. Figure 71c also shows that between 50 and 60 kips of load the curve again becomes linear, indicating that the lateral buckling proceeds at a constant rate between these two loads.

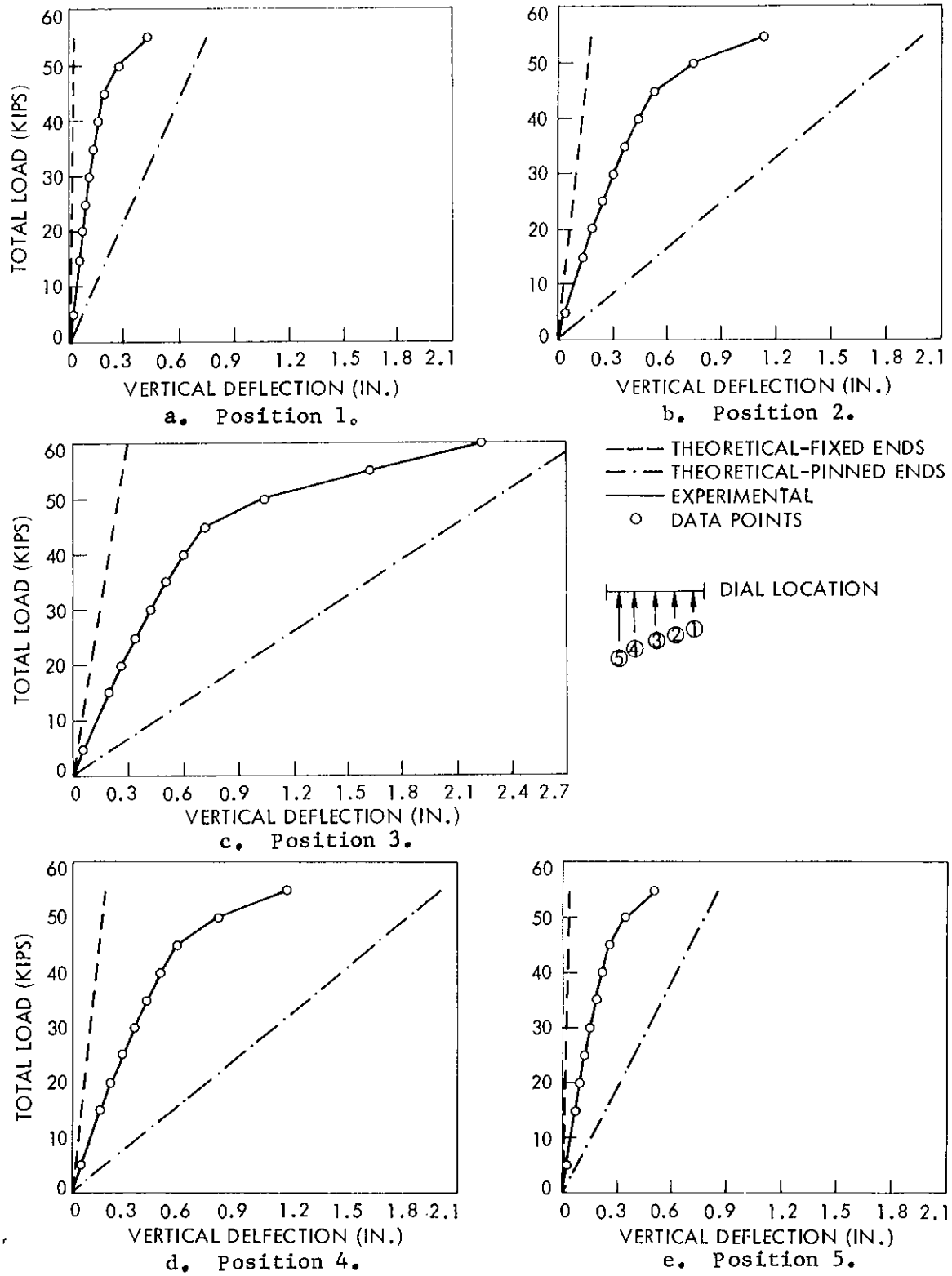

Fig. 71. Load-deflection for floorbeam test at L_4.

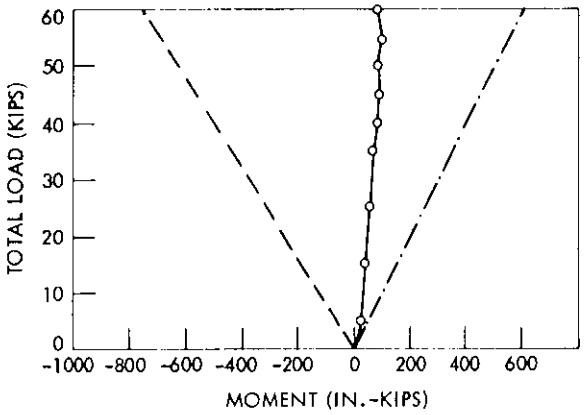

a. Position 1.

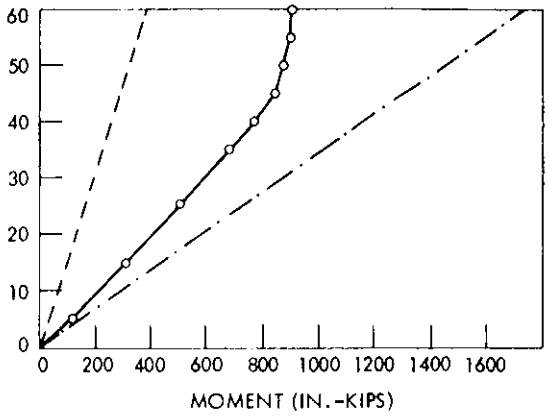

b. Position 2.

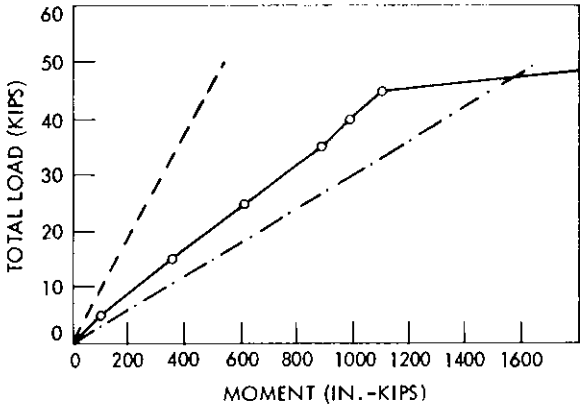

c. Position 3.

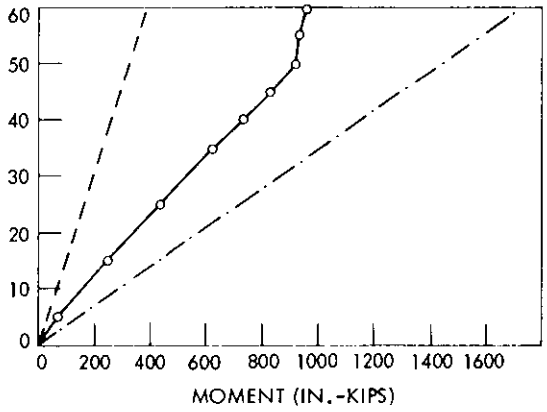

d. Position 4.

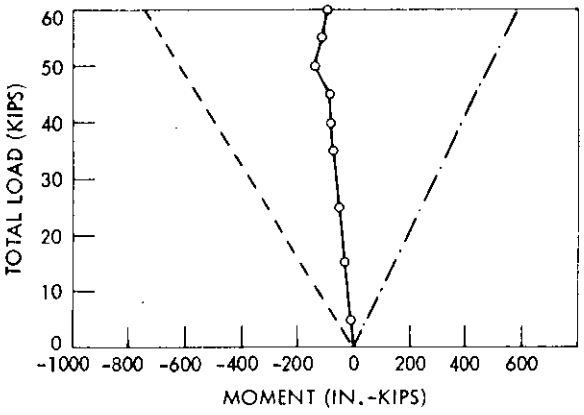

e. Position 5.

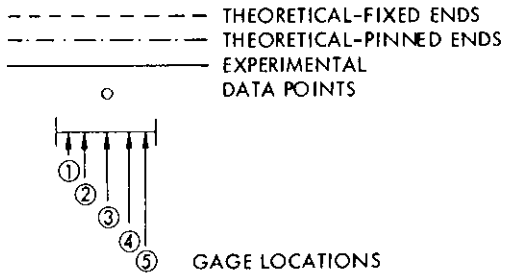

Fig. 72. Load-moment for floorbeam test at L_4.

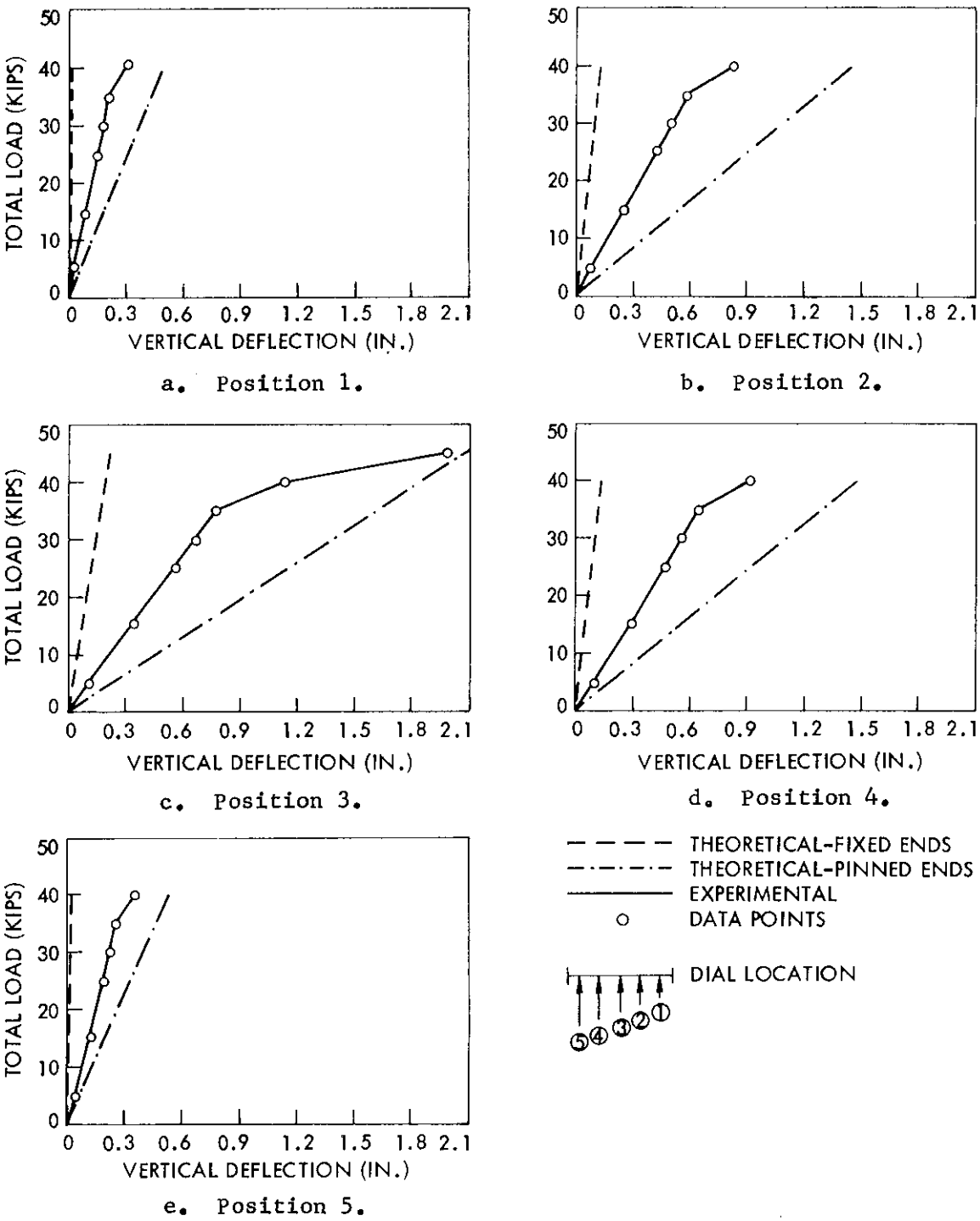

Fig. 73. Load-deflection for floorbeam test at L_5.

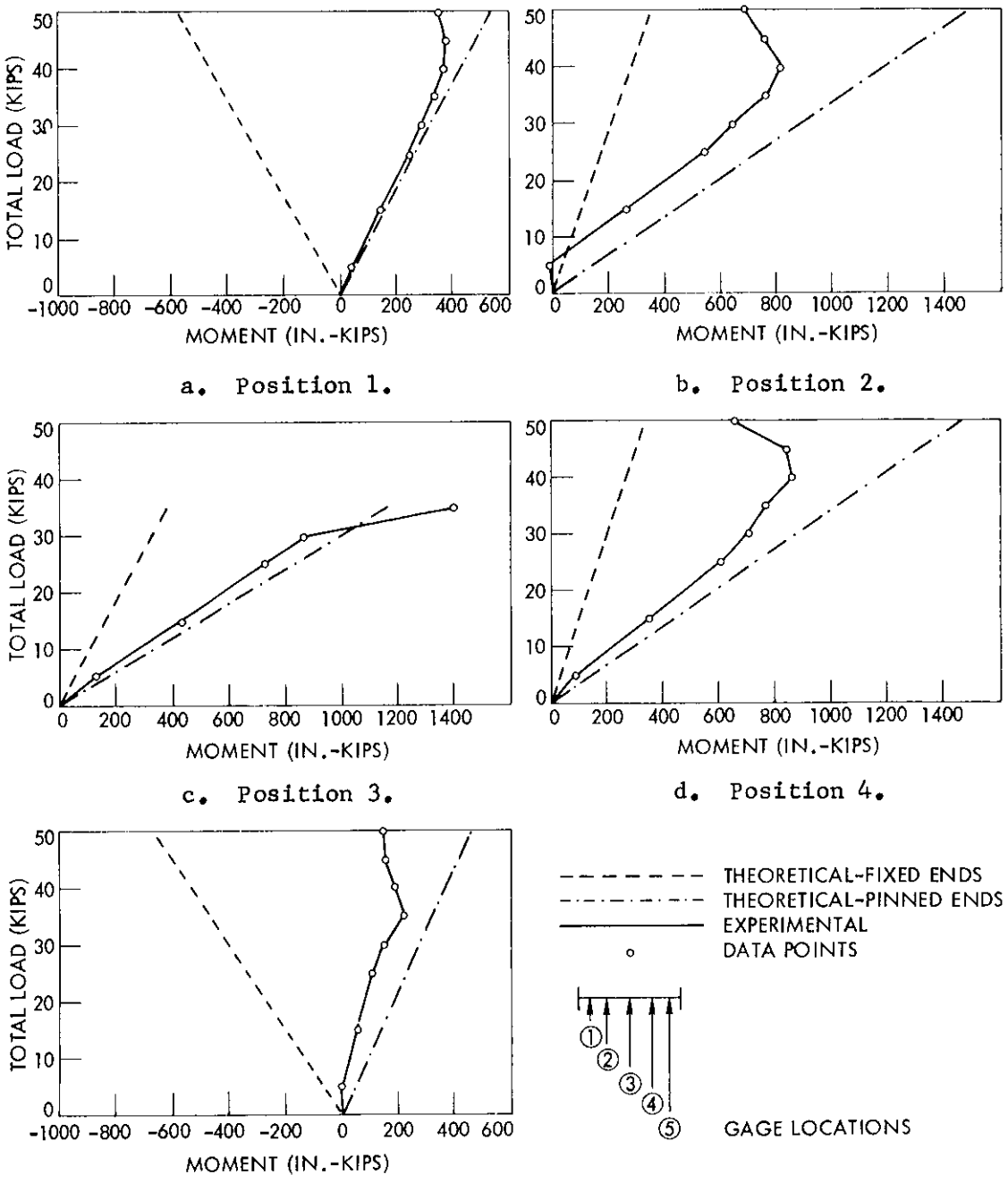

Fig. 74. Load-moment for floorbeam test at L_5.

The load-moment curves for the floorbeam test at L_4 are shown in Fig. 72. These experimental moments were computed from strain readings from strain gages on the top and bottom flanges of the floorbeam. The strain readings were first converted to stresses, using the same procedure as for the truss members, and these stresses were then transformed into moments on the floorbeam. From these moments it was not possible to determine if any composite action had taken place between the deck and floorbeam. Figures 72b and 72d indicate a departure from linearity at 40 and 50 kips, respectively, indicating the lateral buckling of the beam and a corresponding reduction in the load carrying capacity of the beam. No conclusions can be drawn from Figs. 72a and 72e, because the moments are so small in the end portions of the floorbeam. Figure 72c indicates a trend opposite to that shown in Figs. 72b and 72d. However, this trend is questionable because the strain gages near the center of floorbeam are beyond the yield stress for the steel beam.

The load-deflection curves for the floorbeam test at L_5 are shown in Fig. 73. This figure indicates a departure from linearity at a load of about 35 kips (H 21 truck). At about the same load the observation was made that the floorbeam was beginning to buckle laterally. This departure from linearity thus gave an indication of the initiation of lateral buckling in the floorbeam. This indicates that the natural dapping of the stringers provides sufficient lateral support of the floorbeam up to about 70% of the ultimate load. Beyond 70% of the ultimate load the floorbeam buckled laterally between the load points and deflected away from the stringers between the load points because

there was no positive tie between the stringers and the floorbeam. Figure 73c shows that between 40 and 45 kips of load the curve again becomes linear, indicating that the lateral buckling proceeds at a constant rate between these two loads.

The load-moment curves for the floorbeam test at L_5 are shown in Fig. 74. Figures 74a, 74b, and 74d indicate a departure from linearity at about 35 kips, indicating the lateral buckling of the beam and a corresponding reduction in the load carrying capacity of the beam. Figure 74e indicates a behavior which contradicts that seen in Fig. 74a. This contradictory behavior is due to the restraint of the rotation of that end of the floorbeam by a vertical channel on that end of the floorbeam resting against one of the hangers. Figure 74c indicates a behavior similar to that in Fig. 72c, and the same explanation applies for this figure.

The theoretical deflections and moments for the floorbeam were calculated by simulating the end support conditions of the floorbeam as either pinned or fixed. The actual experimental values for these deflections and moments should fall somewhere in between these two extremes.

Figure 71 shows that the experimental deflections for the floorbeam test at L_5 do fall between limits of fixed and pinned end supports. The experimental deflection curve is closer to the theoretical curve based on fixed ends, thus indicating a fairly stiff end condition. At higher loads the experimental deflection does move closer to the theoretical deflection based on pinned ends, indicating a loss of stiffness at the ends at higher loads. Figure 73 indicates that the

experimental deflections for the floorbeam test at L_5 also fall within the limits based on fixed and pinned end support. However, the experimental deflection curves for the floorbeam test at L_5 fall closer to the theoretical curve based on pinned ends, indicating an end condition that is not as stiff as that of the floorbeam at L_4 as can easily be seen in Figs. 4 and 5. Figure 4 is typical of the connections at L_5 and Fig. 5 is typical of the connections at L_4.

Figure 72 indicates that the experimental moments calculated from the strain readings for the floorbeam test at L_4 do fall between the limits of fixed and pinned end supports. The experimental moment curve falls closer to the theoretical curve based on pinned ends, indicating that the load-moment curves show a more flexible end condition than do the load-deflection curves for the floorbeam test at L_4. Figure 74 indicates the same trend as Fig. 72. However, the trend is even more pronounced than in the earlier figure. The figure indicates that the load-moment curves show a more flexible end condition than do the load-deflection curves for the floorbeam test at L_5. This is consistent with the actual end conditions.

Strain gages were also placed on the truss members for the floorbeam tests in a manner similar to the way in which it was done for the truss test. The same type of conversion from strain to forces was done. However, none of the plots of load-force in truss member indicate behavior anywhere close to that which was obtained from the truss test because of the erratic behavior of some of the strain gages. For this reason these plots are not included here. The erratic behavior of these strain gages may have occurred because of the long period of time

that the strain gages had been on these truss members. During the period from the time the gages were applied until they were used, heavy rains and high humidities occurred. The strain gage adhesive may have taken on moisture, and thus some of the bond between the strain gages and the truss member may have been lost.

The theoretical capacity of the floorbeam (initially straight) was calculated at 62.4 kips. This was based on the assumption that the load was uniformly distributed to the floorbeam and that the ends were partially fixed. This agrees quite closely with the actual capacity of the floorbeam that was initially straight (within allowable tolerances). The theoretical capacity of the floorbeam (initially crooked) will be somewhat less than that of the initially straight floorbeam. Thus the actual capacity of the initially crooked floorbeam will agree quite closely with its theoretical capacity.

The final configuration of each of the floorbeams was evidenced by a large amount of lateral buckling of the floorbeam, as was anticipated. The compression flanges of each floorbeam were tilted and severely deformed (Figs. 48 and 51). The floorbeam had also pulled away from the timber stringers above it.

Rating

One of the significant portions of this study was the rating of the test span (span 2) and the comparison of that rating with the actual capacity.

The field inspection used as the basis for the rating calculations was made by the Maintenance Department of the Iowa State Highway Commission. This information was forwarded to the agencies cooperating in this phase of the study. These agencies were the Corps of Engineers, the Iowa State Highway Commission, and Iowa State University. Using this data as a base, each agency computed the rating of the bridge using the AASHO Maintenance Manual[3].

Ratings were requested for each of the three separate portions of the truss tested, i.e., the deck, the floorbeams, and the trusses. The results of the ratings are shown in Table 6.

Table 6. Bridge ratings (operating)

Bridge portion	Agency 1	Agency 2	Agency 3	Test capacity (Table 3)
Deck	H 13.1	H 8.2	H 9.4	H 32
Floorbeam	H 2.4[a]	H 7.4	H 6.7	H 30
Truss	H 11.4	H 12.7	H 11.9	H 66.5[b]

[a]Did not consider beam laterally supported.

[b]Initial fracture of L_5M_5.

It can be seen that the ratings are quite consistent for the truss. However, there is a variation in the ratings for the floor system. In the case of the floorbeams, the assumptions related to lateral support of the compression flange are critical. Table 6 shows the effect of this assumption in the rating of the floorbeam.

Also shown in Table 6 are the capacities as determined from the field tests. The critical member as determined by the ratings (floorbeam) is also the critical member as found from the tests.

The relationship of the ratings at operating levels to the ultimate capacity range from ratings of only 7% of ultimate capacity for the floorbeam (assuming no lateral support) to about 40% for the deck. Except for the one floorbeam rating, the ratings are about 25% of capacity. Since the ratings do consider dynamic effects and are at the higher level (operating), the ratings appear to be quite conservative.

The results do, however, emphasize the need to accurately determine the real lateral support conditions for the beam and the realistic load distribution in the deck. Although, in this case, there were no positive supports, the natural dapping of the stringers did provide this lateral support.

CHAPTER 5. SUMMARY AND CONCLUSIONS

Summary

As a result of the construction of the Saylorville Dam and Reservoir on the Des Moines River, six highway bridges crossing the river were scheduled for removal. One of these, an old high-truss single-lane bridge, was selected for a testing program which included ultimate load tests.

The purpose of the ultimate load tests was to relate design and rating procedures presently used in bridge design to the field behavior of this type of truss bridge. The general objective of the test program is to provide data on the behavior of this bridge type in the overload range up to collapse.

The information available on overload and ultimate behavior of actual bridges is limited mainly to beam-and-slab type bridges. No information is available on the behavior of the old high-truss bridges typical of those found in Iowa and throughout other parts of the country. This load test program is intended to provide that information on the ultimate load carrying capability through the testing of a typical old truss bridge.

The test program consisted of ultimate load testing of one span of the bridge, ultimate load testing of two I-shaped floorbeams, and ultimate load testing of two panels of the timber deck. The truss span was tested in an "as is" condition with loads simulating actual truck loading. After initial failure the truss was damaged and retested in this condition. The floorbeams were tested with loads to simulate

an axle loading. One of the floorbeams had some initial crookedness, while the other was essentially straight. One of the timber deck tests was performed with loads simulating a truck centered on the deck panel and the other with loads placed 3 feet off center to simulate a truck on the edge of the deck panel.

The total ultimate load for deck test 1 (load centered on roadway) was 101.5 kips and for deck test 2 (load placed eccentrically) it was 77.4 kips. For deck test 1 this is equivalent to a load of 25.4 kips at each of the load points, with the corresponding maximum moment on the total deck panel at 279.4 ft-kips or 17.5 ft-kips per foot of width of the deck panel. For deck test 2 the equivalent load and moments are 19.4 kips, 212.8 ft-kips, and 13.3 ft-kips per foot of width, respectively. Although the loads were applied transversely at 6-foot centers (wheel track spacing), there were two equal loads spaced longitudinally at the third-points. The loads, however, can be related to other behavior by determining the equivalent AASHO H truck. For deck test 1 (centered load) failure occurred at an equivalent H 42 truck and for test 2 (eccentric load) at an H 32 truck.

The behavior of the deck at loads up to failure of one of the stringers compared quite well with that predicted by the AASHO Specifications[2]. The current load distribution criteria indicate that each stringer should be designed for about 14% of the total load on the bridge. The test results gave only about 10% for a centered load, but for the eccentric severe loading, the most heavily loaded stringer carried about 15% of the total load.

The initial failure of the truss took place at a load of 133 kips. This failure was the breaking of one of the hangers which made up member L_5M_5. The applied loading was 106 kips and 27 kips at L_5 and L_4, respectively. Additional load was applied in an attempt to get additional members to fail. A large distortion of the lower chord of the truss near the load at L_5 occurred under this higher loading without any failure. The maximum load under this general loading was 140 kips (H 70 truck) (112 kips at L_5 and 28 kips at L_4). The maximum vertical deflection at L_5 at this time was 15 in.

The fracture load for the hanger failure was 97% of the calculated load based on the full section. The fracture section confirmed that the section was nearly fully fused. This compares to the "40% effective" used by many designers in evaluating structures of this type.

After adjustment of the loading system, all load was applied at L_4 with the maximum load being 78.5 kips. The test program then included damaging a member. After member L_2U_2 was cut completely through, a load of 39 kips produced failure of the truss. This resulted in a vertical displacement of the member at the cut location.

The maximum load applied to the floorbeam at L_4 was 66.0 kips. The compression flange of this floorbeam was originally straight (within allowable tolerances). This load was approximately equal to that determined from theory.

The maximum load applied to the floorbeam at L_5 was 50.0 kips. This floorbeam had an initial crookedness of approximately 13/16 in.

Conclusions

As a result of the ultimate load tests performed on this truss bridge, the following conclusions were reached:

1. The behavior of the timber deck was linear up to about one-half of the ultimate load for each deck test.

2. For deck test 1 (centered load) the design percentage of the total load distributed to the most heavily loaded stringer, based on the AASHO Specifications, was greater than the experimental percentage of the load distributed to the most heavily loaded stringer based on the deck deflection at all load levels for which this is valid.

3. The theoretical capacity of the deck for deck test 1 was approximately equal to the experimentally determined capacity of the deck.

4. For deck test 2 (eccentric load) the design percentage of the total load distributed to the most heavily loaded stringer, based on the AASHO Specifications, was equal to or less than the experimental percentage of the load distributed to the most heavily loaded stringer based on the deck deflection at all load levels for which this is valid.

5. The theoretical capacity of the deck for deck test 2 was approximately equal to the experimentally determined capacity of the deck.

6. The deflections of the timber deck for both tests generally lay within the theoretical bounds.

7. The experimentally determined forces and the forces from analysis for the truss members were in close agreement. This indicated that the assumption of pinned end members is valid for this particular truss.

8. The theoretical capacity of the hangers agreed quite closely with the load that actually caused the fracture of one of these hangers.

9. The current practice of assuming the "lap" of an eye-bar to be only 40% effective is quite conservative. (Additional tests are required before any recommendation on changing this assumption is warranted.)

10. The natural dapping of the stringers provided sufficient lateral support of the floorbeam up to approximately 60% of the ultimate load.

11. The theoretical capacity of each floorbeam was approximately equal to the actual experimental capacity of each floorbeam.

12. The ratings of the bridge and its components averaged about 25% of capacity. The ratings were fairly consistent except for the floorbeams where the assumption on lateral support conditions for the compression flange caused considerable variation.

CHAPTER 6. REFERENCES

1. Sanders, W. W., Jr., and H. A. Elleby. "Feasibility Study of Dynamic Overload and Ultimate Load Tests of Full-Scale Highway Bridges." Final report to Iowa State Highway Commission, Engineering Research Institute, Iowa State University, Ames, January 1973.

2. American Association of State Highway Officials. Standard Specifications for Highway Bridges – Eleventh Edition. Washington, D.C.: American Association of State Highway Officials, 1973.

3. American Association of State Highway Officials. Manual for Maintenance Inspection of Bridges. Washington, D.C.: American Association of State Highway Officials, 1970.

4. Heins, C. P., Jr., and C. F. Galambos. "Highway Bridge Field Tests in the United States, 1948-70." Public Roads, 36, No. 12 (February, 1972), 271-291.

5. Vincent, G. S. "Tentative Criteria for Load Factor Design of Steel Highway Bridges." American Iron and Steel Institute Bulletin No. 15, March 1969.

6. Highway Research Board. Dynamic Studies of Bridges on the AASHO Road Tests. Highway Research Board Special Report 71, June 1972.

7. Highway Research Board. The AASHO Road Test – Report 4, Bridge Research. Highway Research Board Special Report 61D, 1962.

8. Rosli, A., and H. Hofacker. "Tests on the Glatt Bridge at Opfikon." Cement and Concrete Association Translation No. 106, London, August 1973.

9. Burdette, E. G., and D. W. Goodpasture. "Final Report on Full-Scale Bridge Testing – An Evaluation of Bridge Design Criteria." Department of Civil Engineering, University of Tennessee, December 31, 1971.

10. Doyle, S. K., and E. G. Burdette. "A Comparison of Measured and Computed Load-Deflection Relationships for Four Highway Bridges." Department of Civil Engineering Research Series No. 13, University of Tennessee, March 1972.

11. Burdette, E. G., and D. W. Goodpasture. "A Comparison of Measured and Computed Ultimate Strengths of Four Highway Bridges." Highway Research Record No. 387, 1972.

12. Varney, R. F. "Preliminary Research Reports of a Highway Bridge Loading Study with the HET-70 Main Battle Tank Transporter." Bureau of Public Roads, Washington, D.C., 1969-1970.

13. Salane, H., R. Duffield, R. McBean, and J. Baldwin. "An Investigation of the Behavior of a Three-Span Composite Highway Bridge." Missouri Cooperative Highway Research Program Report 71-5, University of Missouri, Columbia, 1972.

14. Sanders, W. W., Jr., H. A. Elleby, and F. W. Klaiber. "Field Test Details for Research Study HR-169 on Ultimate Load Behavior of Full-Scale Highway Truss Bridges." Informal Interim Report to Iowa State Highway Commission, Engineering Research Institute, Iowa State University, May 1974.

15. Hetenyi, M. I. Beams on Elastic Foundation; Theory with Applications in the Fields of Civil and Mechanical Engineering. Ann Arbor: The University of Michigan Press, 1946.

CHAPTER 7. ACKNOWLEDGMENTS

The research reported herein was conducted by the Engineering Research Institute of Iowa State University under a contract funded by the Iowa State Highway Commission and the Federal Highway Administration. Supplemental funding was also provided by the Engineering Research Institute.

The author wishes to express his appreciation to his major professor, Dr. F. W. Klaiber, for support and guidance throughout the duration of this investigation. Appreciation is also expressed to Dr. W. W. Sanders, Jr., Dr. H. A. Elleby, Dr. M. L. Porter, Dr. L. F. Greimann and Professor D. D. Girton for their assistance in the conduct of this investigation.

Appreciation is also expressed to the Advisory Committee formed to assist and guide the investigation. The Committee consisted of representatives of Iowa State University, the Iowa State Highway Commission, the U.S. Army Corps of Engineers, the Federal Highway Administration, and the Boone, Dallas and Polk County Engineers. Special appreciation is expressed to Carl Schnoor, Boone County Engineer, and his staff for their many efforts in making this investigation a success.

A special thanks is given to the undergraduate students, M. D. Reeves, T. C. Wilson and J. P. Sorenson for their assistance with the Summer Field Testing Program. Appreciation is also expressed to Mrs. Janet R. Peterson, Secretary, for her help and assistance.

An extra special thanks to my wife, Faith, for her continued understanding, encouragement, and love throughout the investigation.